ASSESSMENT OF CEREBELLAR AND HIPPOCAMPAL MORPHOLOGY AND BIOCHEMICAL PARAMETERS IN THE COMPOUND HETEROZYGOUS, TOTTERING/LEANER MOUSE

A Thesis

by

EMILY MARY MURAWSKI

Submitted to the Office of Graduate Studies of
Texas A&M University
in partial fulfillment of the requirements for the degree of

MASTER OF SCIENCE

December 2009

Major Subject: Biomedical Sciences

ASSESSMENT OF CEREBELLAR AND HIPPOCAMPAL MORPHOLOGY AND BIOCHEMICAL PARAMETERS IN THE COMPOUND HETEROZYGOUS, TOTTERING/LEANER MOUSE

A Thesis

by

EMILY MARY MURAWSKI

Submitted to the Office of Graduate Studies of
Texas A&M University
in partial fulfillment of the requirements for the degree of

MASTER OF SCIENCE

Approved by:

Chair of Committee,	Louise C. Abbott
Committee Members,	C. Jane Welsh
	George Stoica
Head of Department,	Evelyn Tiffany-Castiglioni

December 2009

Major Subject: Biomedical Sciences

ABSTRACT

Assessment of Cerebellar and Hippocampal Morphology and Biochemical Parameters in the Compound Heterozygous, Tottering/leaner Mouse. (December 2009)

Emily Mary Murawski, B.S., Texas A&M University

Chair of Advisory Committee: Dr. Louise C. Abbott

Due to two different mutations in the gene that encodes the α_{1A} subunit of voltage-activated CaV 2.1 calcium ion channels, the compound heterozygous tottering/leaner (*tg*/*tg*^{la}) mouse exhibits numerous neurological deficits. Human disorders that arise from mutations in this voltage dependent calcium channel are familial hemiplegic migraine, episodic ataxia-2, and spinocerebellar ataxia 6. The *tg*/*tg*^{la} mouse exhibits ataxia, movement disorders and memory impairment, suggesting that both the cerebellum and hippocampus are affected. To gain greater understanding of the many neurological abnormalities that are exhibited by the 90-120 day old *tg*/*tg*^{la} mouse the following aspects were investigated: 1) the morphology of the cerebellum and hippocampus, 2) proliferation and death in cells of the hippocampal dentate gyrus and 3) changes in basic biochemical parameters in granule cells of the cerebellum and hippocampus.

This study revealed no volume abnormalities within the hippocampus of the mutant mice, but a decrease in cell density with the pyramidal layer of CA3 and the hilus of the dentate gyrus. Cell size in the CA3 region was unaffected, but cell size in the

hilus of the dentate gyrus did not exhibit the gender difference seen in the wild type mouse. The cerebellum showed a decrease in volume without any decrease in cerebellar cellular density. Cell proliferation and differentiation in the subgranular zone of the hippocampal dentate gyrus remained normal. This region also revealed a decrease in cell death in the *tg*/*tg*^{la} mice.

Basal intracellular calcium levels in granule cells show no difference within the hippocampus, but an increase in the *tg*/*tg*^{la} male cerebellum compared to the wild type male cerebellum. There was no significant difference in granule cell mitochondrial membrane potential within the wild type and mutant animals in either the hippocampus or cerebellum. The rate of reactive oxygen species (ROS) production in granule cells revealed no variation within the hippocampus or cerebellum. The amount of ROS was decreased in cerebellar granule cells, but not granule cells of the hippocampus. Inducing ROS showed no alteration in production or amount of ROS produced in the hippocampus, but did show a ceiling in the amount of ROS produced, but not rate of production, in the cerebellum.

ACKNOWLEDGEMENTS

I would first like to thank my committee chair, Dr. Louise Abbott, for her unwavering support and guidance. She has inspired my academic career through her perseverance and knowledge. I cannot express how appreciative I am of her kindness and patience. I would also like to thank my committee members Drs. Welsh and Stoica for their guidance and feedback. Thank you to the Texas A&M University Department of Veterinary Integrative Biosciences for financial support.

I am grateful to Dr. Pine, Dr. Ruoff and my fellow anatomy lab teaching assistants. They have showed me what a wonderful experience teaching can be. Thank you to the members of Abbott lab, Dr. Nigussie, Dr. Thuett, Dr. Huang and Dr. Hassan. I have thoroughly enjoyed working with each of you.

Thank you to the undergraduate research assistants with who are credited to countless hours of research. My gratitude extends to Ransom Wyse, Joseph Hicks, Devang Gandhi, Asher Schusterman, Alex Thomas, Travis Berry, Brittany Kopecky, Ying Duan and Caleb Hunter.

To my parents, thank you for your unconditional love and encouragement throughout the years, especially as I pursued this degree. A special thank you to my sister Catherine for her willingness to listen and for always brightening my day. Thank you all for being my biggest fans. Lastly, I would like to thank John for his love and understanding. You have often been the gentle encouragement that I have needed to take the next step in my work.

NOMENCLATURE

Ca^{2+}	Calcium ion
CGC	Cerebellar granule cell
$Cacna1a^{rok}$	Rocker
$Cacna1a^{rol}$	Nagoya rolling
EA-2	Episodic ataxia type-2
FHM	Familial hemiplegic migraine
HVA	High voltage activated
LVA	Low voltage activated
NOS	Nitric oxide synthase
tg	Tottering
tg^{la}	Leaner
tg/tg^{la}	Compound heterozygous tottering/leaner
TH	Tyrosine hydroxylase
TRH	Thyrotropin releasing hormone
SCA-6	Spinocerebellar ataxia type-6
VDCC	Voltage dependent calcium channel

TABLE OF CONTENTS

LIST OF FIGURES

FIGURE Page

CHAPTER I

INTRODUCTION

CALCIUM CHANNEL MUTANT MICE

Mutation Characterization

A number of spontaneously occurring mutations and genetically engineered alleles of the α_{1A} subunit of P/Q type voltage dependent calcium channels (VDCC) has allowed for greater understanding of this complex structure. The CaV 2.1 channel is highly expressed throughout the mouse cerebral cortex, hippocampus, olfactory bulb, tectum, and hindbrain (Fletcher et al., 1996). The pore-forming subunit of the Cav2.1 voltage gated calcium channel (VGCC), alternatively known as the P/Q-type VGCC, is highly expressed in cerebellar granule and Purkinje cells (Westenbroek et al., 1995).

Both the tottering (*tg*) and leaner (tg^{la}) allelic mutations reside in chromosome 8 (Green and Sidman, 1962) and in the gene that encodes the alpha1A subunit of the voltage-activated CaV 2.1 calcium ion channels (Fletcher et al., 1996). This tg gene is prevalent throughout the mouse central nervous system in areas such as the cerebral cortex, hippocampus, olfactory bulb, tectum, hindbrain and cerebellar granule and Purkinje cells (Fletcher et al., 1996). Several mouse mutants that display different calcium channel mutations are of great interest because of their relationship to a variety of devastating human neurological disorders. Extensive research into autosomal

---

This thesis follows the style of Brain Research.

recessive mutations at the tg locus, including the leaner and homozygous tottering mutations, has proven valuable in understanding human diseases such as familial hemiplegic migraine (FHM), episodic ataxia-2(EA-2) (Ophoff et al., 1996), and spinocerebellar ataxia 6.

Human Disorders

FHM, an autosomal dominant mutation on chromosome 19 (Joutel et al., 1993), is an inherited form of migraine with some rare sporadic, noninherited, cases. FHM is characterized by visual perceptual disturbances, weakness in half of the body, motor and sensory losses (Blau and Whitty, 1955; Whitty, 1953) and in some cases, ocular motor defecit (Elliott et al., 1996), cerebellar atrophy (Terwindt et al., 1996), ataxia, nausea, vomiting (Blau and Whitty, 1955), acute paranoid psychosis with anxiety and visual hallucinations (Spranger et al., 1999). Rare documented cases have experienced fever, seizures and coma (Ducros, 2000). These preliminary aura symptoms are known to occur for 10 minutes to hours before onset of migraine headache which can last anywhere from two hours to seven days (Ahmed et al., 1996; Ducros, 2000). Within affected families and even within each patient, symptoms and severity of aura and migraine can vary (Ducros, 2000). This, in addition with incomplete penetrance within families, suggest that the symptoms of FHM could be a combination of genetic and environmental factors (Ducros, 2000).

Onset of symptoms occur in most often in youth, but can commonly begin in those between the ages of 4 and 30 (Ahmed et al., 1996). FHM is relatively rare, with

only over 47 families affected worldwide (Ahmed et al., 1996). Both stress and minor head trauma are known triggers of this migraine in roughly 2/3 of patients (Ophoff et al., 1996; Terwindt et al., 1996). Because this is an allelic mutation, patient treatment is often aimed at the symptoms of migraine and promising treatments include acetazolamide as a preventative (Battistini et al., 1999) and intranasal ketamine to shorten length of attacks (Kaube et al., 2000).

There is much clinical overlap with FHM and episodic ataxia type 2 (EA 2). EA 2, an autosomal dominant paroxysmal cerebral disorder, lies on the same chromosome and interval as the FHM locus (Kramer et al., 1995; Teh et al., 1995) and is also responsive to acetazolamide. Characteristics of EA 2 include vertigo, visual disturbances, dysarthria, ataxia and in some cases nyastagnus and other cerebellar dysfunctions much less severe than those of patients with SCA 6 (Jodice et al., 1997).

Many argue that SCA 6 and EA 2 are the same disorder with great phenotypic variability (Frontali, 2001; Geschwind et al., 1997; Jodice et al., 1997), while others stand by their belief that these as genetically and phenotypically distinct disorders (Zhuchenko et al., 1997). Predominant hallmarks that distinguish these mutations phenotypically are the presence of extracerebellar signs and a larger proportion of those with ataxia in those with SCA 6 (Frontali, 2001). It is possible that this discrepancy could be derived from different ages of examination or pathological differences between the disorders (Frontali, 2001).

SCA 6 results from a polyglutamine track created by small expansions in the CAG repeat in the coding region of CACNA1A gene(Zhuchenko et al., 1997). Typical

symptoms of SCA 6 include gait disturbances, slurred speech, eye movement disorder, paroxysmal vertigo and migraine (Craig et al., 2004). The characteristic cerebellar atrophy and functional deficit progress in severity over time and in some cases lead to permanent ataxia (Calandriello et al., 1997; Geschwind et al., 1997).

It is interesting to note that this mutation appears to increase calcium channel current and increased expression of α_{1a} at the cell surface, which could allow calcium ions (Ca^{2+}) to enter the cell at toxic levels (Piedras-Renteria et al., 2001). This discovery contradicts other α_{1A} mutations in which there is a decrease of P/Q type calcium channel current (Dove et al., 1998; Lorenzon et al., 1998; Wakamori et al., 1998).

Like FHM and EA 2, in some reported cases, SCA 6 episodes are responsive to treatment with acetazolamide (Calandriello et al., 1997). In addition, it is proposed that the drugs gabapentin and pregabalin help to decrease ataxia in patients with SCA 6 (Gazulla and Benavente, 2007; Gazulla and Tintore, 2007). SCA 6 is more prevalent in populations than the previously presented human disorders, with an estimated 1 in 19,210 people with SCA 6 or at risk for SCA 6 in the northeast of England alone (Craig et al., 2004).

Leaner Mutation

Of these mutations, the leaner mutation (tg^{la}) is considered the most severe. Homozygous leaner mice experience early onset of disorders, at postnatal days (P)8-10, which include debilitating ataxia, absence epilepsy and paroxysmal dyskinesia (Herrup and Wilczynski, 1982). These disorders in tg^{la} mice result from a splice site mutation in

the 5' end of the α_{1A} gene that truncates the carboxy terminus of the α_{1A} protein, which likely creates two α_{1A} splice variants (Doyle et al., 1997; Fletcher et al., 1996).

The *tg*^{la} mouse is known to exhibit cerebellar granule cell (CGC) loss that begins soon after P10, with the greatest amount of death at P20. These mice still P40 still experience a marked CGC loss as compared to age matched wild type mice at P30 and P40 (Lau et al., 2004). More specifically, there was an increase in CGC death in the anterior lobe as compared to the posterior lobe of the leaner cerebellum (Frank et al., 2003; Lau et al., 2004). This increase in CGC death is by way of apoptosis and continues into adulthood (Bawa and Abbott, 2008). In addition, the pattern of CGC death follows the same spatial pattern in adulthood (Bawa and Abbott, 2008) as initially expressed during postnatal development (Lau et al., 2004).

While there is no apparent change in basal intracellular calcium homeostasis in leaner Purkinje cells (Dove et al., 2000), there is an absolute decrease in the levels of calretinin expression in leaner CGC (Nahm et al., 2002) as well as a marked decrease in the number of CGCs (Bawa and Abbott, 2008). Mitochondrial membrane potential is also decreased in CGCs of the adult leaner mouse as compared to both wild type and tottering mice (Bawa and Abbott, 2008). Interestingly, there is no significant alteration in generation of reactive oxygen species in CGCs of leaner mice as compared to wild type or tottering mice (Bawa and Abbott, 2008). It is hypothesized that CGC death in the leaner mouse may be more dependent upon an apparent mitochondrial dysfunction rather than decreased basal intracellular calcium levels (Bawa and Abbott, 2008).

The complexity of calcium homeostasis in leaner Purkinje cells has been revealed as investigations have ventured into calcium buffering mechanisms within the cell. An additional decrease in calcium current amplitude in the cerebellum possibly creates the noticeable decrease in calbindin and parvalbumin expression in Purkinje cells (Dove et al., 2000). Despite no alteration in leaner Purkinje cell resting somatic Ca^{2+} concentration, there is a reduction in Ca^{2+} buffering (Dove et al., 2000). There is not only diminished Ca^{2+} uptake by the endoplasmic reticulum in leaner mice, but reductions in mRNA levels of Ca^{2+} binding proteins which are a proposed result of the P/Q type mutation that creates this severely affected phenotype (Dove et al., 2000).

As a possible result of altered calcium homeostasis, the adult leaner mouse exhibits decreased neuronal nitric oxide synthase (NOS) mRNA expression and NADPH-diaphorase histochemical staining, with no alteration in levels of neuronal NOS protein as compared to age matched wild type mice (Rhyu et al., 2003). It has been proposed that these decreases may be attributed to their severe neuronal deficits in which nitric oxide acting as a trophic factor is unable to prevent granule and Purkinje cell death in the leaner mouse cerebellum (Rhyu et al., 2003).

Purkinje cells have been closely examined in the leaner mouse as these cells are now known to be highly concentrated in P/Q type VDCC and have a 60% reduction in P/Q type VDCC calcium current and one third the channel open probability of that in the wild type animal (Dove et al., 1998; Lorenzon et al., 1998; Wakamori et al., 1998). This reduction in Ca^{2+} current is not a result of α_{1A} abundance, as the amounts of mRNA and protein for α_{1A} subunits are unaltered (Lau et al., 1998). The leaner cerebellar cortex

and inferior olive are marked with neuronal loss (Heckroth and Abbott, 1994). Purkinje cell death in the cerebellum is increased in the leaner mouse compared to wild type mice where it begins at P25, peaks in the vermis at P40, in the hemispheres at P50 and continues to show low levels of cell death at P80 (Frank et al., 2003). In addition, the leaner cerebellum expresses decreased serum and cerebellar insulin-like growth factor-I at P30 compared to age matched wild type mice (Nahm et al., 2003). Exogenous administration of insulin-like growth factor-I is shown to improve cerebellar function in leaner mice, but remains futile in arresting Purkinje cell death (Nahm et al., 2003).

The leaner mouse, in addition to tottering and compound heterozygous tottering/leaner, exhibits enlarged parallel fiber varicosities that synapse on multiple Purkinje cells dendritic spines in both juvenile and adult animals (Rhyu et al., 1999). With closer examination, the leaner mouse has a greater amount of these synapses to the Purkinje cells dendritic spines than the tottering and compound heterozygous tottering/leaner mouse which may indicate greater morphological abnormality linked to a more severe phenotype (Rhyu et al., 1999).

Because this malformation precedes the expression of the disorder in the tottering mouse, it is possible that it is not a result of the pathogenic change (Rhyu et al., 1999). On the other hand, Purkinje cell and parallel fiber synapse alterations are more apparent in the adult animal and this increase could be a result of prolonged interaction and compensation of this mutation (Rhyu et al., 1999). It is also noted that *tg*, tg^{la} and tg/tg^{la} juvenile and adult genotypes all display axonal swellings which allude to Purkinje cell

damage that could cause impaired axonal transport (Abbott et al., 1996; Rhyu et al., 1999).

Tottering Mutation

The tottering (*tg*) mutation remains less severe with a later phenotypic onset at P21-28, and clinical signs that include: mild ataxia, paroxysmal dyskinesia and absence seizures (Noebels and Sidman, 1979). The tottering deficits are a result of a point mutation residing in the extracellular region linking the IIS5 and IIS6 domains in the α_{1A} protein, which is responsible for a proline-to-leucine amino acid substitution (Fletcher et al., 1996).

Various cerebellar morphological deficits exist in the adult tottering mouse compared to age-matched wild type mice. Overall cerebellar volume is decreased in the mutant, along with a decrease in the volume of the Purkinje cells in the cerebellar molecular layer of 3-month-old tottering mice, with specific reduction in the posterior cerebellar region (Isaacs and Abbott, 1995). Molecular layer Purkinje cell density remains unchanged in the mutant cerebellum, without evidence of excessive Purkinje cell loss (Isaacs and Abbott, 1995). Forebrain, cerebellum and hindbrain weight are significantly less in the adult tottering mouse as compared to age matched wild type, although malnutrition is not thought to be responsible for this weight decrease (Isaacs and Abbott, 1995). The ratio of cerebellum to body weight remains greater in adult tottering mice than in age matched wild type mice which rules out the hypothesis that

smaller brain weight is merely a result of overall body weight loss (Isaacs and Abbott, 1995).

Early postnatal tottering mice do not exhibit the expected increase in P-Type VDCC current density in Purkinje cells and at P8 continue to show a 25% decrease as compared to age matched wild type mice (Erickson et al., 2007). Because tottering mice at P15 begin to display normal levels of Purkinje cell P-Type VDCC current density, it is believed that there is an obvious developmental delay that precedes any visible behavioral abnormalities (Erickson et al., 2007).

While the P/Q type VDCC are likely to be the primary responsibility for the observed neurological deficits, it is proposed that L-type VDCC may play a small role in episodes of paroxysmal dyskinesia (Campbell and Hess, 1999). L-Type VDCC blocking agents have shown to reduce this specific type of motor deficit in the tottering mouse by presumably acting on the central nervous system rather than skeletal or cardiac muscle (Campbell and Hess, 1999). In addition, tottering mouse Purkinje cells exhibit mRNA upregulation of the L-type VDCC α_{1C} subunit (Campbell and Hess, 1999), and experience a two fold increase in calcium current density at P15 through these channels as compared to wild type animals (Erickson et al., 2007). Such an increase would be consistent with an upregulation of this VDCC in response to P-type VDCC dysfunction (Erickson et al., 2007). Further analyses indicate compensation of Cav1 channels in basal forebrain neurons (Etheredge et al., 2007) and N-type channels in the Schaffer collateral cells neurotransmitter release (Qian and Noebels, 2000) in response to the Cav2.1 channel mutation.

Tottering Purkinje cells show axonal damage beginning at 3 to 5 weeks of age and persist through adulthood, encouraging the interpretation that postsynaptic activities may be altered in cerebellar nuclei and help to create their ataxic phenotype (Hoebeek et al., 2008).

The tottering mutation is likely the culprit for an observed decrease in CGC basal intracellular calcium homeostasis (Bawa and Abbott, 2008). In addition, there is a noticeable decrease in the tottering CGC mRNA expression of calretinin, calcium binding protein, which could be correlated with impaired calcium homeostasis and motor coordination (Cicale et al., 2002). The tottering Purkinje cell layer in the cerebellar flocculus has shown a decrease in the mRNA expression of ryanodine receptor type 1, a calcium channel in the endoplasmic reticulum, which may alter synaptic plasticity and be attributed to their ataxic phenotype (Cicale et al., 2002).

Tyrosine hydroxylase (TH) expression in the tottering and compound heterozygous tottering/leaner cerebellum also is altered (Abbott et al., 1996; Austin et al., 1992; Hess and Wilson, 1991), while expression of Zebrin II remains like that of normal mice and exhibits areas positive for TH immunoreactive for Zebrin II and those negative for TH displaying no immunoreactivity for Zebrin II (Abbott et al., 1996).

In contrast to the leaner mouse, there is a significant increase in NOS mRNA and protein in the cerebellum and NADPH-diaphorase histochemical stain in the cerebellar molecular and granule cell layer of adult tottering and rolling Nagoya mice as compared to age-matched wild type mice (Rhyu et al., 2003). This is presumed to be a result of

their VDCC malformation and could be a potential byproduct of some mechanism that prevents their cell death (Rhyu et al., 2003).

Epileptic seizures of the tottering mouse are postulated to be correlated with excitability defects in the CA3 region of the hippocampus (Helekar and Noebels, 1991). Closer examination reveals prolonged paroxysmal depolarizing shifts in hippocampal CA3 pyramidal neurons after exposure to high potassium levels in vitro during the developmental stage of the tottering mouse (Helekar and Noebels, 1992). As this abnormality is most prominent in young tottering mice, it appears to possibly be a part of a genetically signaled neuronal synchronization mutation rather than an effect of a life of seizures (Helekar and Noebels, 1992).

Compound Heterozygous, Tottering/Leaner Mutation

The compound heterozygous, tottering/leaner (tg/tg^{la}) mouse carries one tottering allele and one leaner allele. Much less is known about the tg/tg^{la} mouse, which also exhibits several neurological deficits to a lesser degree than the leaner mouse, but to a greater degree than the tottering mouse. The characteristic phenotype of tg/tg^{la} mutant mice is noticeable around P20-22 with a moderate ataxia (Green and Sidman, 1962; Herrup and Wilczynski, 1982).

While the tg/tg^{la} mouse appears to be a "compromise" between the leaner and tottering mutations, the morphological and biochemical characteristics remain unique, seemingly mimicking neither mouse. The tottering and leaner mutations result in ataxia and movement disorders, suggesting that the cerebellum is affected. Previous studies of

cerebellar structure in mice carrying these mutations show atypical functioning of Purkinje cells that are likely related to the ataxic phenotype (Rhyu et al., 1999). It is understood that the leaner mouse but not tottering mice, experience significant cerebellar granule, Golgi and Purkinje cell death, but little is known regarding potential excessive neuron cell death the *tg/tg*^{la} genotype (Herrup and Wilczynski, 1982; Isaacs and Abbott, 1995). In addition, because some mice that carry mutations in this gene exhibit atypical spatial and memory learning, the hippocampus is also a possible site of abnormality.

Preliminary investigation of *tg/tg*^{la} mice has revealed that the weight of the forebrain, cerebellum and hindbrain are significantly decreased in the adult *tg/tg*^{la} mouse as compared to age matched wild type mice (Isaacs and Abbott, 1995). Malnutrition is not thought to be responsible for the significant decrease in brain weights (Isaacs and Abbott, 1995). Like the tottering mouse, overall cerebellar volume is decreased in the *tg/tg*^{la} mouse, along with a decrease in the volume of the Purkinje cells in the molecular layer of the 3 month old tottering cerebellum (Isaacs and Abbott, 1995). Purkinje cell density per unit of cerebellar molecular layer remains unchanged in the *tg/tg*^{la} cerebellum, without evidence of excessive Purkinje cell loss (Isaacs and Abbott, 1995). Adult *tg/tg*^{la} mice show a ratio of cerebellum to body weight that is greater than that of age-matched wild type mice, which rules out the hypothesis that smaller brain weight is merely a result of overall body weight loss (Isaacs and Abbott, 1995).

As reported previously, the *tg/tg*^{la} mouse exhibits enlarged parallel fiber variscosities that synapse on multiple Purkinje cells dendritic spines in both juvenile and adult animals (Rhyu et al., 1999). Purkinje cells in the *tg/tg*^{la} cerebellum show

significantly higher mRNA expression of tyrosine hydroxylase in both juvenile and adult pre seizure animals as compare to age matched wild type controls, indicating that the occurrence of these neurological abnormalities is likely to be independent of seizure onset (Austin et al., 1992).

Additional mutations affecting the α_{1A} subunit include the Nagoya rolling ($Cacna1a^{rol}$) and rocker ($Cacna1a^{rkr}$) mutations. The Nagoya (rolling) mouse, which is a Cacan1a mutant that originated from Nagoya University in Japan, has an autosomal recessive mutation, (tg^{rol}) on chromosome 8 that demonstrates an ataxic phenotype with α motor disturbances in its hind legs, much like the tottering and leaner mouse in which this mutation shares a locus (Oda, 1981; Tsuji and Meier, 1971). An ataxic gait and difficulty balancing beginning at P10-14 is a characteristic phenotype of these mice (Oda, 1981). Similarities with the leaner or tottering mutant mouse include loss of granule cells in the anterior cerebellum (Nishimura, 1975; Suh et al., 2002) presumably by way of apoptosis (Suh et al., 2002), altered Purkinje cell synapses (Rhyu et al., 1999), altered ryanodine receptor expression (Sawada et al., 2008) and persistent tyrosine hydroxylase expression in the cerebellum (Muramoto et al., 1981). Cerebellar tyrosine hydroxylase expression in Nagoya rolling mice is also correlated with increased numbers of corticotrophin-releasing factor-positive climbing fibers, but not mossy fibers, which could alter the function of connecting Purkinje cells (Sawada et al., 2001).

The cerebellum, parietal cortex, ventral tegmental area and basal ganglia of the rolling mouse is understood to have low levels of local cerebral glucose utilization (Kato et al., 1982; Kinoshita et al., 1995; Yamaguchi et al., 1992), a neuronal metabolic index

for neuronal activity (Sokoloff et al., 1977; Sokoloff, 1981). Dysfunction in the basal ganglia is thought to lie predominantly in the striatal projection neurons (Taniwaki et al., 1996). Thyrotropin-releasing hormone (TRH: L-pyroglutamyl-L-histidyl-L-prolinamide) and its analog TA-0910 ((-)-N-[(S)-hexahydro-l-methyl-2,6-dioxo-4-pyrimidinylcarbonyl]-L-histidyl-L-prolinamide tetrahydrate) are observed to reduce ataxia in the rolling mouse (Kinoshita et al., 1995) possibly by way of activating thryotrophin-releasing hormone receptors in the ventral tegmental field directly and through receptors in the cuneiform nucleus indirectly (Kinoshita et al., 1997).

A more recent discovery of a Cacna1a allelic mutant mouse is rocker ($Cacna1a^{rkr}$), which stems from the fourth generation offspring of a male mouse mutagenized with ethylnitrosourea (Bode, 1984). A proline to leucine substitution at position 1310 on chromosome 8 affects the alteration of polarity of the extracellular membrane near the pore-forming region of P/Q type VDCC (Zwingman et al., 2001).

Characteristics of the rocker mouse appear very similar to that of the tottering mouse (Figure 1.1), with an ataxic gait initiated by an action tremor (Zwingman et al., 2001). Onset of behavioral conditions is around P21-28 (Zwingman et al., 2001). Although the rocker mouse is phenotypically reminiscent of the tottering mouse, its brain shows quite different patterns of neurological abnormalities. Cerebellar morphology and cytoarchitecture remains normal along with no Purkinje cell loss or abnormal staining patterns with various neuronal or non-neuronal antibodies (Zwingman et al., 2001). There are abnormalities in dendritic structure in cerebellar Purkinje cells as rocker mice age, with normal appearance in 6-month-old rocker mice, but reduced

dendritic mass and secondary growth of distal dendrite tips in 1-year-old rocker mice (Zwingman et al., 2001). In addition, Purkinje cells exhibited no axonal swellings, ectopic spines on distal branches or aberrant TH expression in adult rocker mice (Zwingman et al., 2001).

Rocker mice show identical morphological and temporal patterns of cortical burst activity and behavioral seizure arrest to that observed for tottering mice (Zwingman et al., 2001). Rocker mice display moderately reduced calcium current density in cerebellar Purkinje cells with normal gating and voltage dependence (Kodama et al., 2006). While presynaptic parallel fibers to Purkinje cell synapses appear normal, postsynaptic function is impaired (Kodama et al., 2006). Decreased number and density of postsynaptic a-amino-3-hydroxy-5-methyl-4-isoxazolepropionic acid (AMPA) receptors may suggest that even a mild calcium mutation, such as rocker, can have profound neurological effects (Kodama et al., 2006).

	tottering	**tottering/leaner**	**leaner**
Cerebellar ataxia	Mild ~P20	Moderate ~P16	Severe ~P10
Absence epilepsy	Present (1-3 sec.) ~P24	Present (2-5 sec.) ~P20	Present (4-7 sec.) ~P14
Paroxysmal dyskinesia	Present (20-30min.) ~P25	Present (20-40+ min.) ~P22	Present (short) ~P16 Disappear after ~P40-60

Figure 1.1
Comparison of phenotypic onset and severity of mutant genotype disorders.

VOLTAGE DEPENDENT CALCIUM CHANNELS

Calcium homeostasis and neuronal calcium ions in neurotransmission are critical components for cell function and survival. Many experts in the field hypothesized that multiple types of VDCC existed, but not until the late 1980's was clear progress made to actually describe them (Bean, 1989). VDCC are classified into two distinct groups based on the principal of voltage-activation threshold. These two groups or categories are high-voltage (HVA) channels and low-voltage activated (LVA) channels (Carbone and Lux, 1984; Fedulova et al., 1985). LVA, or T type channels, exhibit a voltage activation threshold of less than -50mV and inactivate quickly in contrast to HVA, that function at a voltage activation threshold of less than -20mV and inactivate more slowly (Carbone and Lux, 1984; Nowycky et al., 1985).

HVA channels are further divided into several different channels (L, N, P, Q, O and R types), based upon specific properties of each channel with respect to physiological and pharmacological parameters (Bean, 1989; Hess, 1990; Tsien et al., 1988). Of the HVA channels, the L type is sensitive to dihydropyridine (DHP) and several peptide toxins, while N, P, Q, O and R are all insensitive DHP. Second to be discovered was the N type channel, which is a class of calcium ion channel with greater heterogeneity and therefore is best characterized by its blockage by ω-conotoxin GVIA (McCleskey et al., 1987; Nowycky et al., 1985; Tsien et al., 1988). Further analysis of peptide toxins revealed the R type channel, which is believed to have multiple subtypes (Tottene et al., 1996) and whose complete blockage is still to be elucidated (Randall and Tsien, 1995) .

Of greatest importance for this study are the P and Q type channels. The P type channels exhibit similar conductance as L and T type channels and voltage dependence between N and T type channels. P type channels were first discovered in Purkinje cells (Llinas et al., 1989; Regan, 1991) and were noted for their resistance to L and T type channel blocking agents such as DHP and w-conotoxin. One particular toxin has proven to block P type channels is the venom of the funnel-web spider, *agelenopsis aperta* and more specifically, its toxic peptide component, ω-Aga IVA (Llinas et al., 1992; Mintz et al., 1992; Takahashi and Momiyama, 1993). Another toxin, ω-CgTx MVIIC, derived from the marine cone snail, *Conus magus*, similarly inhibits P type channels in addition to Q- and O- channel conductance and N- type channels (Hillyard et al., 1992; Takahashi and Momiyama, 1993). The P type channel persists throughout the mammalian nervous system, with particularly high expression in cerebellar granule cells, (Randall and Tsien, 1995) neuroendocrine cells and the cell soma and dendrites of Purkinje cells (Usowicz et al., 1992), and P type channels are thought to have critical function in neuronal integration and death (Llinas et al., 1992).

While the Q type channel is fully blocked by ω-CgTx MVIIC (Hillyard et al., 1992), it's partial resistance to ω-Aga IVA at concentrations known to block that of the P type channel is its novel characteristic (Randall and Tsien, 1995; Zhang et al., 1993). The Q type is the most highly represented of the channels in cerebellar granule cells (Randall and Tsien, 1995). Because Q type channel malformation that is so highly present in CGCs, this type of cell begs for closer examination regarding its role in the tg/tg^{la} phenotype.

VDCC consist of a complex structure that allows for specific channel functions. There are four to five subunits, β, γ, α2-δ and α1, involved in forming the complete channel. The β subunit is intracellular with α helices (Ruth et al., 1989). The γ subunit is a glycosylated hydrophobic protein with four transmembrane domains and two N-linked glycosylation sites (Jay et al., 1990). A single gene for the α2-δ subunit is post-translationally cleaved to allow for a disulfide link between α2 and δ proteins (De Jongh et al., 1990; Ellis et al., 1988; Jay et al., 1991). The α2-δ subunit is a transmembrane domain which mediates subunit interactions and is attached to a glycosylated extracellular domain that enhances current amplitude (Gurnett et al., 1996).

While each subunit plays an integral part, the diversity of calcium channels is owed to the α1 subunit (Hofmann et al., 1994). The α1 subunit was discovered to act in all voltage dependent calcium channels and is understood to act as the conduction pore, voltage sensor and gating apparatus and a common site of second messenger, drugs and toxins channel regulation (Sather et al., 1993; Smith et al., 1996; Stea et al., 1994). In mammals, the α1 subunit is controlled by at least ten genes. It consists of four homologous mostly hydrophobic domains I, II, III and IV and is believed to have six membrane spanning subunits (S1-6) within each domain. In the α1 subunit, the S4 subunit is believed to act as specifically as part of the voltage-sensing mechanism for the channel whereas the channel pore proper is formed between the hydrophobic domains of S5 and S6.

Using cDNA analysis and Northern blotting, the P/Q type calcium channel was found to have the α_{1A} subunit, also referred to as Cav2.1. This subunit is prevalent

throughout the nervous system, heart and pituitary, with high concentration in the cerebellum. It accounts for the largest number of VDCC subunits within the entire nervous system (Mori et al., 1991) and can be found in cell bodies, dendrites and presynaptic terminals (Westenbroek et al., 1995). It is noted that CaV 2.1 channels account for about 45% of calcium channels in cerebellar granule cells and over 90% of calcium channels on the Purkinje cell somata of mammals (McDonough et al., 1997; Mintz et al., 1995; Randall and Tsien, 1995).

The α_{1A} subunit (Figure 1.2) is thought to express various electrophysiological properties according to the type of β subunit coexpressed (Stea et al., 1994). The coexpression of α_{1A} with a β2α subunit appears more similar to the P type VDCC current waveform, while β1b or β3 lend themselves to mimic the Q type VDCC current waveform (Stea et al., 1994). The α_{1A} subunit is most convincingly present in the P type VDCC because of the high localization of α1α transcripts and common immunoreactivity between the two (Westenbroek et al., 1995).

Recent discoveries highlight the important role of signal transducing molecules on modulating Cav2.1 channels. In the mouse Purkinje cells, immunohistochemical and electrophysiological evidence has shown that this subunit is also responsible for GABAergic inhibitory transmission (Stephens et al., 2001). It also colocalizes tightly with GAD, indicating that GABA is likely produced in this region thought to comprise mostly of basket cell terminals (Stephens et al., 2001).

Calcium modulating protein, calmodulin (CaM) is known to mediate Ca^{2+} dependent facilitation and inactivation as it binds to local calcium after a voltage-gated

calcium influx through Cav2.1 channels and induces conformational changes (DeMaria et al., 2001; Lee et al., 2003). An intricate mechanism allows for positive regulation of Cav2.1 channels in the instances of local Ca^{2+} increases and negative regulation in instances of global Ca^{2+} increases (Lee et al., 2003). CaM is also believed to interact with neuronal Ca^{2+}-binding protein 1 (CaBP1) in Cav2.1 channels to inhibit neuronal calcium influx (Lee et al., 2002). Additional calcium sensors such as neuronal calcium sensor 1 (NCS-1) are recently hypothesized to alter P/Q-type VDCC presynaptic calcium channel current (Tsujimoto et al., 2002).

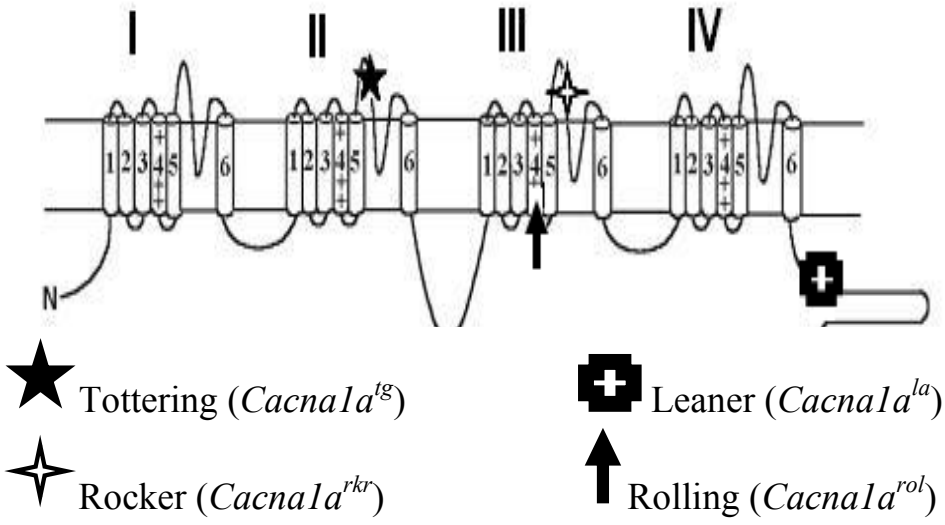

Figure 1.2
Diagram of α1A VDCC subunit. Spontaneous mutations responsible for the tottering, leaner, rocker and rolling phenotypes indicated.
(Adapted from Pietroban 2002)

CEREBELLUM

The cerebellum is a brain region marked with diverse postulations regarding its complicated and intriguing functions. It is linked to roles in motor coordination (Bastian, 2006; Thach et al., 1992), processing in cognition (Booth et al., 2007; Gordon, 2007; Thach, 2007), sensation (Andreasen et al., 1998; Gao et al., 1996), emotion (Schmahmann and Sherman, 1998; Schmahmann, 2004; Schmahmann and Caplan, 2006), and behavioral learning (Cheron, 1990; Miles and Lisberger, 1981; Raymond et al., 1996).

The cerebellum is divided into 10 distinct lobules (I-X), which can be combined or further divided into sublobules depending on the species (Larsell, 1970). Layers of the cerebellum include an inner white matter core composed of axons surrounded by a granule cell layer. The granule cell layer, in addition to numerous granule cells is also populated with Golgi cell somata, Lugaro cell interneurons and unipolar brush cells (Mugnaini et al., 1997). The Purkinje cell layer lies on top of the granule cell layer and is composed primarily of Purkinje cell somata with a sparse scattering of Bergmann glia cell bodies (Voogd and Glickstein, 1998) and candelabrum cells throughout (Laine and Axelrad, 1994). The outermost layer, called the molecular layer, is comprised of Purkinje cell dendrites, climbing fibers from inferior olive neurons and granule cell axons along with a thinly dispersed number of stellate, basket cell interneurons, as well as rows of Bergmann glia fibers (Voogd and Glickstein, 1998).

Sensory nerves innervating the cerebellum include mossy fibers that synapse in the granule cells layer and climbing fibers that synapse in the molecular cell layer.

Mossy fibers originate from many areas, but primarily innervate the cerebellum from their origin of the basilar pontine nuclei, external cuneate nucleus, vestibular nuclei and lateral reticular nuclei (Harvey and Napper, 1991). They also are known to project from all levels of the spinal cord in rodents and along with projections from the brain, end in the cerebellum by entering through the superior, middle and inferior cerebellar peduncles.

Each climbing fiber emanates from a neuronal cell body found in the inferior olive and forms multiple synapses with one Purkinje cell dendritic tree in the cerebellar molecular layer (Eccles et al., 1966; Thach, 1968). In addition, climbing fibers are also able to make multiple synaptic contacts with NG2-immunoreactive glia cells (Lin et al., 2005).

Noradrenergic neurons originating from the locus coeruleus project to the cerebral cortex, cerebellum, brain stem and spinal cord (Abbott and Sotelo, 2000) and this pathway allows one to respond and avoid dangerous situations brought upon by unexpected environmental stimuli. Serotonergic neurons also project to many areas in the brain, including the cerebellar cortex and cerebellar nuclei from their origin in the raphe nuclei (Strahlendorf and Hubbard, 1983). Cholinergic neurons extending from the pedunculopontine tegmental nucleus to the cerebellum, lateral paragigantocellular nucleus and various raphe nuclei to the cerebellum (Jaarsma et al., 1997) and are thought to possibly aid in regulation of sleep and arousal (McCormick, 1989).

The cerebellum can be further divided into interwoven transverse zones in the cerebellar vermis and hemispheres: anterior zone, posterior zone and nodular zone (Ahn

et al., 1994; Hawkes and Eisenman, 1997). These zones are revealed with patterns of zebrin II expression in Purkinje cells (Brochu et al., 1990; Ozol et al., 1999) a transgene expression in Purkinje cells such as L7/pcp2-LacZ transgene 4 and an olfactory marker protein (OMP)-LacZ transgene (Nunzi et al., 1999), and even some types of cerebellar neurodegeneration (Sarna and Hawkes, 2003). Cerebellar long term depression at the cerebellar parallel fiber-Purkinje cell synapse may also be contained within this striping pattern as many proteins involved with glutamatergic neurotransmission display parasagittal stripes in cerebellar Purkinje cells (Ekerot and Kano, 1985; Ito and Kano, 1982; Ito et al., 1982).

HIPPOCAMPUS AND NEUROGENESIS

The hippocampus is a well-studied brain region responsible for various aspects of memory storage. The circuitry of the hippocampus includes stellate cells from the entorhinal cortex giving input through the perforant pathway to synapse on granule cells. Mossy fibers, granule cell axons, then synapse onto CA3 pyramidal cells that synapse on CA1 pyramidal cells, ending with their axons leaving the hippocampus proper. It is now understood that neurogenesis occurs in the adult hippocampus (Altman, 1963; Altman and Das, 1965b) and olfactory system (Altman and Das, 1965a; Altman, 1969). As hippocampal neurogenesis is most pertinent to these studies, it will be given greater attention.

The role of hippocampal neurogenesis is still relatively unclear, but various studies using techniques to halt neurogenesis are proving promising in elucidating this

mystery. Hippocampal neurogenesis is thought to possibly play a role in timing or task difficulty in learning such as trace eye blink conditioning (Bruel-Jungerman et al., 2007; Shors et al., 2001). Adult hippocampal neurogenesis may also be responsible for long term spatial memory storage (Snyder et al., 2005) and spatial memory, but no alteration in contextual fear conditioning (Dupret et al., 2008). It is possible that neurogenesis improves these tasks because of the activity-dependent plasticity of newly formed neurons in the DG (Bruel-Jungerman et al., 2007). Hippocampal dependent learning is believed to increase the amount of survival (Gould et al., 1999; Leuner et al., 2007) and possibly proliferation (Dobrossy et al., 2003; Lemaire et al., 2000) in adult hippocampal neurogenesis. In addition, exercise and environmental enrichment may affect neurogenesis (Brown et al., 2003; Bruel-Jungerman et al., 2007; van Praag et al., 1999).

The path of neurogenesis migration in the hippocampus begins with the proliferation of the precursor cells, quiescent progenitor cells, in the sub granular zone (SGZ) of the dentate gyrus. Precursor cells are composed of both horizontal astrocytes and radial astrocytes, multipotent cells resembling radial glia (Seri et al., 2004). These cells express various markers such as nestin, precursor cell marker protein and glial fibrillary acidic protein (GFAP).

Daughter cells of quiescent progenitor cells become the amplifying neural progenitors (Encinas et al., 2006). These cells express nestin and Sox2, but not GFAP, can be labeled with BrdU and predominantly cluster along the SGZ (Encinas et al., 2006). Amplifying neural progenitor cells gives rise to the intermediate precursors, D2 which then mature to D3 cells (Seri et al., 2004) and express a variety of different

markers not found in its parent cells (Encinas and Enikolopov, 2008; Rao and Shetty, 2004; Seki and Arai, 1993; Seri et al., 2004). D3 cells look more like immature granule cells rather than glia and extend processes through the granule cell layer and hilus of the dentate gyrus (Seri et al., 2004).

Once D3 cells are in the dentate gyrus they begin to mature and make neuronal connections with mature granule cells and transiently express doublecortin, calretinin, and neuronal markers NeuN and calbindin (Kempermann, 2005). Within 4-10 days of differentiation, the maturing cells are able to make axonal connections to neurons in CA3 (Markakis and Gage, 1999). These cells continue to send axons called mossy fibers that project to the CA3 region to synapse with pyramidal cells and the polymorphic layer (Patestas, 2006). Polymorphic-layer neurons send fiber projections and are able to modify information by with synapses to the dendrites and cell bodies of granule cells (Patestas, 2006). Pyramidal cells of the CA3 region (Figure 1.3) are able to emit Schaefer collaterals that project within itself, the CA1 region and septal nuclei (Patestas, 2006). CA3 axons are also able to join the band of white matter in the medial hippocamous, the fimbria (Patestas, 2006). At seven weeks, these neurons are fully functional and posses the ability to produce action potentials and complete integration within the hippocampal network (van Praag et al., 1999). There is an excess of newly proliferated cells and a portion of them will die in an apoptotic manner before reaching maturity (Biebl et al., 2000).

Figure 1.3
Representative photo of the mouse hippocampus. The following pecific regions are labeled: pyramidal cell layer of CA3 (CA3) and CA1 (CA1), oriens layer (OL), lacunosum molecular layer (LML), hilus (H) and granular cell layer (G) of the dentate gyrus.

CELLULAR ENVIRONMENT

The dynamics related to mitochondrial responses to Ca^{2+} are physiologically important. Mitochondria are primarily involved in the production of ATP by oxidative phosphorylation, but also are linked to cellular functions such as buffering cytosolic [Ca^{2+}], apoptosis (Kroemer et al., 1997; Kroemer, 1999), the urea cycle (Lehninger, 1970), beta oxidation of fatty acids (Lehninger, 1970) and metabolic synthesis.

Mitochondria employ methods of efflux and influx as well as mitochondrial permeability transition to control calcium ion transport. Calcium influx in mitochondria is mediated by the mitochondrial calcium uniporter located in the organelles inner membrane (Deluca and Engstrom, 1961; Kirichok et al., 2004). Other methods of Ca^{2+} influx are driven by rapid mode or RaM and the mitochondrial ryanodine receptor (Beutner et al., 2001). Methods regulating Ca^{2+} efflux include the Na+ dependent and Na+ independent mechanisms (Puskin et al., 1976).

While mitochondria have the highest Ca^{2+} capacity of all cellular components, the endoplasmic reticulum and nuclear envelope are also known sources.

Reactive oxygen species (ROS) are byproducts of the mitochondrial respiration chain in the inner mitochondrial membrane that creates ATP. There are multiple forms of ROS such as hydrogen peroxide (H_20_2), superoxide anions (O_2-), hypochlorous acid (HOCL), singlet oxygen (O_2) and hydroxyl radical (OH). O_2- is the most prevalent form of ROS that is primarily produced by complex I and II of the electron transport chain. While ROS is believed to play a role in normal cell signaling (Brookes et al., 2002), an overabundance of ROS in a cell can overwhelm antioxidant machinery and prove

deadly. These deadly levels of ROS, oxidative stress, are believed to play a role in various neurodegenerative diseases, cancer and aging (Cross et al., 1987; Halliwell et al., 1992) .

There are several antioxidant enzymes in the cell that act to degrade ROS such as superoxide dismutase (SOD), catalase and glutathione peroxidase. As mentioned previously, oxidative stress can arise because of an overabundance of ROS, but can also be a response to a lack of sufficient antioxidants. Mechanisms in the cellular matrix work to detoxify superoxide anions in the cell through reactions of manganese superoxide dismutase (MnSOD) that create the much less deleterious H_20_2 (Melov, 2000). The most abundant form of SOD, inter-membrane space copper zinc superoxide dismutase (CuZn-SOD), creates H_20_2 and oxygen forms superoxide anions within the intramembrane. In addition to mitochondria, ROS is produced in other cellular compartments such as the nuclear membrane.

OBJECTIVE OF THIS THESIS

In light of knowing that the cerebellum is responsible for many of the deficits associated with several mutations at the tottering locus and the strong possibility that the hippocampus also could be affected, it becomes interesting to investigate these regions in the tg/tg^{la} mouse. Interesting differences observed in the cellular environment, and neuronal proliferation in the leaner and tottering mouse are cause for more detailed study of the less known tg/tg^{la} mouse. This thesis seeks to determine if and how the tg/tg^{la} mouse is morphologically and biochemically different from wild type mice with respect

to the cerebellum and hippocampus. In this thesis, cerebellar and hippocampal morphology and cellular biochemistry of neurons in those two brain regions in adult male and female tottering/leaner mice that are 90-120 days of age have been assessed.

Overall Hypothesis

The cerebellum and hippocampus of adult tottering/leaner mice are morphologically and biochemically different from age- and sex-matched wild type mice.

This hypothesis has been tested through completion of three experimental aims: 1) examination of the morphology of the cerebellum and hippocampus of tottering/leaner mice 2) assessment of proliferation and death in the dentate gyrus of tottering/leaner hippocampus 3) investigation of changes in basic biochemical parameters in granule cells of the cerebellum and hippocampus in tottring/leaner mice.

Experimental Protocols

I examined both male and female mice. All experiments examined adult mice at ages 90-120 days. Six animals of each genotype and gender were used in each experiment, except when including fewer animals in each group resulted in observing significant differences. For histological analyses both frozen, unfixed brains and fixed brains were used. For volume analyses all mice will be anesthetized with isoflurane (Abbott Laboratories, North Chicago, IL, USA) and decapitated. To obtain fixed tissue, mice were deeply anesthetized with intraperitoneal injections of xylazine (Vedco, St.

Joseph, MO, USA) and ketamine (Vedco, St. Joseph, MO, USA; 0.5mg xylazine plus 3.0 mg ketamine per 20 gm body weight) and then perfused.

CHAPTER II

MORPHOLOGY OF THE CEREBELLUM AND HIPPOCAMPUS OF TOTTERING/LEANER MICE

INTRODUCTION

Determine Hippocampal and Cerebellar Morphology

Previous work from this lab has revealed decreased forebrain and hindbrain weights in mice that are homozygous for the tottering and leaner mutations as well as the compound heterozygous tottering/leaner mice, but the volume of the cerebellum and hippocampus has not been previously published (Huang et al., 2007). To gain greater understanding of the brain regions potentially responsible for the many neurological abnormalities exhibited by these mice, volumes of both the hippocampus and cerebellum of *tg*/*tg*^{la} and age- and gender-matched wild type mice have been measured.

It was hypothesized that cerebellar volume of *tg*/*tg*^{la} mice would be significantly less than that of age-matched wild type mice, as it is an area that is known to be affected by both the tottering and leaner mutations. Another hypothesis was that there would be no significant difference in the hippocampal volume of the *tg*/*tg*^{la} mouse, as this brain region does not exhibit as many overt alterations as those seen in the cerebella of leaner and tottering mice.

Potential differences in volume of these structures could result from a change in cell density in either region. For these experiments, density is referred to as numbers of cells per unit area. Any potential change in cell density could reveal further deficit in

terms of altered neuronal death or proliferation. An absence of density change could imply synapse loss without significant loss of neuronal cell bodies or processes or increased numbers of glial cells.

In the assessment of cell density, the original hypothesis was that granule cell density in the cerebellum would be decreased in all lobules investigated, while the hippocampus will have fewer cells per unit area in the *tg*/*tg*^{la} mouse as compared to age- and gender-matched wild type mice.

Volume or density differences could also be the result of a change in the size of neurons in various brain regions within the hippocampus. Various diseases such as Alzheimer's disease (van de Nes et al., 2008) and epilepsy (Andres et al., 2005; Bothwell et al., 2001) show abnormalities in neuronal size in some brain regions of affected patients. The hypothesis regarding neuronal size was that average cell size in specific regions of the hippocampus of the *tg/tg*^{la} mouse would be significantly smaller when compared to the same specific regions in age- and gender-matched wild type mice.

EXPERIMENTAL PROCEDURES

Hippocampal and Cerebellar Volume

For volume studies, every fifth, coronal, 25 micrometer thick frozen section of unfixed mouse brain was thaw-mounted onto microscope slides, stained with 0.1% thionin (Thermo Fisher Scientific Inc., Fair Lawn, NJ, USA) in 0.1M acetate buffer, dried and coverslipped using Permount (Thermo Fisher Scientific Inc.). The slides were coded to blind the investigator as to sex and genotype during measurements. A 2X

objective on a Nikon E400 microscope with a Nikon DXM1200 video camera and ACT1 software was used to capture images for measurement. After outlining the images of sections of the cerebellum and hippocampus with Image J software (Rasband, 1997-2008), the area was computed and then multiplied by section thickness and number of sections skipped to determine total volume.

Cell Density in the Hippocampus and Cerebellum

Cellular density in six different regions of the hippocampus was examined: pyramidal cell layer of CA1 and CA3, oriens layer, lacunosum molecular layer, granule cell layer of the dentate gyrus, and hilus of the dentate gyrus. In the cerebellar vermis, rostral lobe II and caudal lobes VI and X were examined for density of cells in the granule layer, Purkinje cell layer and molecular layer.

Coronal, 5 μm thick paraffin sections of each region were stained with hematoxylin (Sigma Aldrich, Milwaukee, WI, USA) and eosin (Sigma Aldrich, Milwaukee, WI, USA), coverslipped and coded to blind the investigator as to sex and genotype during scoring. Two sections were counted for each brain region for each animal. A 40X objective on a Nikon E400 microscope with a Nikon DXM1200 video camera and ACT1 software was used to capture images for counting. A uniform area of 100 x 50 μm was randomly selected twice for each region to count numbers of cells in each area. Only cells completely within the specified area that contained an obvious nucleus were counted.

Hippocampal Cell Size

Coronal sections through the rostral hippocampus from sections that were stained with Thionin were used to assess cell density were used to assess neuronal area. In regions where significant differences in density were observed, 10 cells were randomly chosen and images captured with a 40X objective on a Nikon E400 microscope with a DXM1200 video camera and ACT1 software. After outlining individual neurons with Image J software, the areas were measured. To ensure that neuronal area was measured in similar planes through each cell, each measured cell was required to fulfill the criteria of having a nucleus present, a nucleolus visible within the nucleus and a distinct plasma membrane.

Data were analyzed using SPSS Version 12.0.1 Multivariate Analysis of Variance (ANOVA) at $\alpha = 0.05$ to test gender differences. A Univariate Analysis of Variance (ANOVA) at $\alpha = 0.05$ two way ANOVA was used if the Multivariate ANOVA showed that genders could be combined. Tukey's honest significant difference (HSD) post hoc test was used when significant differences within region and genotypes were assessed.

RESULTS

Hippocampal and Cerebellar Volume

Hippocampal volume showed no significant difference between gender or genotype ($P = 0.841$). This implies that although the forebrain weight in the mutant mouse is significantly less than that of the wild type mouse, there is no apparent volume

variation that is observed in the hippocampus. It is possible that other affected forebrain regions could account for the observed forebrain weight differences.

There was a significant difference in cerebellar volume (Figure 2.1) in the mutant mice compared to age-matched wild type mice ($P = 0.021$). It is logical to believe that the decreased cerebellar volume in the tottering/leaner mouse could be partially responsible for their decrease in hindbrain weight. As the cerebellum is an area known to be severely affected in mice with similar mutations and noting the gravity of the movement disorders of the tottering/leaner mouse, it is no surprise that the cerebellum exhibits such abnormal architecture.

Cellular Density in the Hippocampus and Cerebellum

Even though the hippocampus showed no change in hippocampal volume when the two genotypes were compared, there was a variation in cellular density within some regions of the tottering/leaner hippocampus. The pyramidal cell layer of CA3 ($P = 0.001$) and the hilus of the dentate gyrus showed a significant decrease in cellular density ($P = 0.009$). It is possible that there are increases in cellular processes or glial cells that might compensate for the decrease in cellular density loss that allows for no alteration in hippocampal volume.

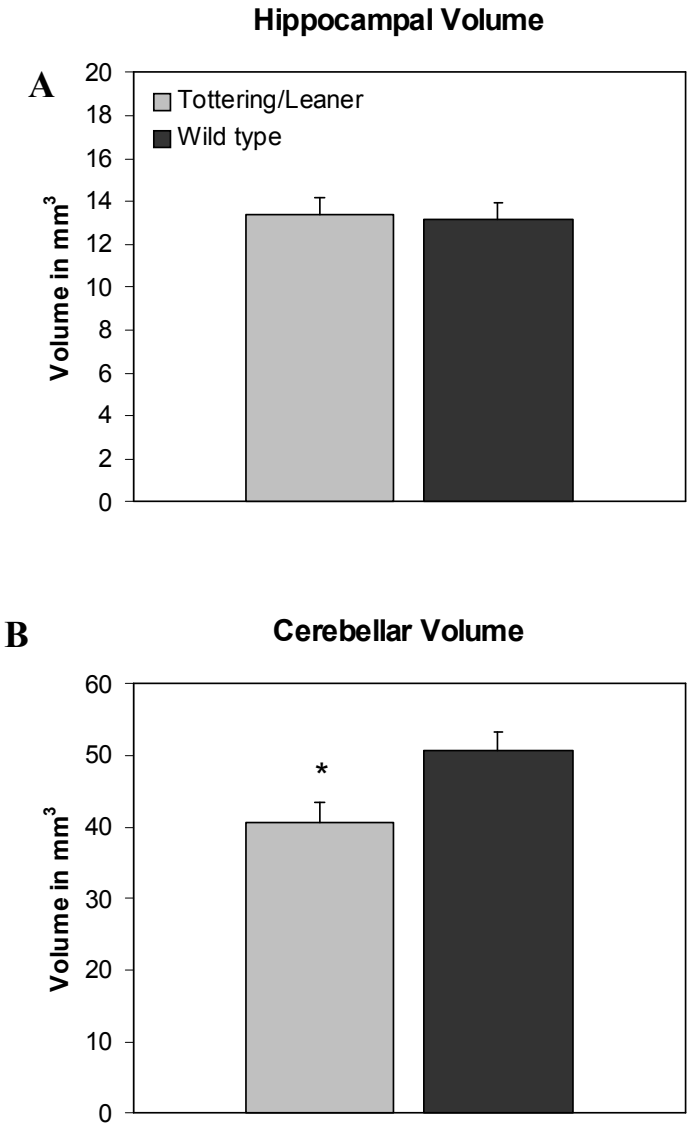

Figure 2.1: Quantitative comparison of volume within brain regions. Volume of tottering/leaner and wild type mice at 90-120 days of age is determined by measuring area of region in every fifth section, multiplied by section thickness and sections skipped. Comparison of hippocampal volume (A) and cerebellar volume (B). **A)** No significant difference between gender or genotypes observed. **B)** Significant difference between genotypes denoted by single asterisk (*), where tottering leaner cerebellar volume is significantly less than wild type cerebellar volume ($P = 0.021$).

One explanation for the decrease in cellular density (Figure 2.2) of the CA3 region in the *tg*/*tg*^{la} mouse may be explained by the defects the homozygous tottering mouse shows in this region. Epileptic seizures exhibited by the tottering mouse are postulated to be correlated with excitability defects in the CA3 region of the hippocampus (Helekar and Noebels, 1991). Closer examination reveal prolonged paroxysmal depolarizing shifts in hippocampal CA3 pyramidal neurons after exposure to high potassium levels in vitro during the developmental stage of the tottering mouse (Helekar and Noebels, 1992). As this abnormality appears most prominently in young tottering mice, it appears that this is possibly a genetically signaled neuronal synchronization mutation rather than an effect of a life of seizures (Helekar and Noebels, 1992).

The *tg*/*tg*^{la} mouse similarly exhibits seizures like the homozygous tottering mouse and could perhaps also have this abnormal CA3 excitability defect. There could be less neurons in the *tg/tg*^{la} mouse hippocampal CA3 region because the abnormal neuronal synchronization may cause them to die. It could also be hypothesized that the decrease in cell density in this region is partly responsible for any abnormal excitability in this region with some underlying cause of neuronal loss waiting to be elucidated.

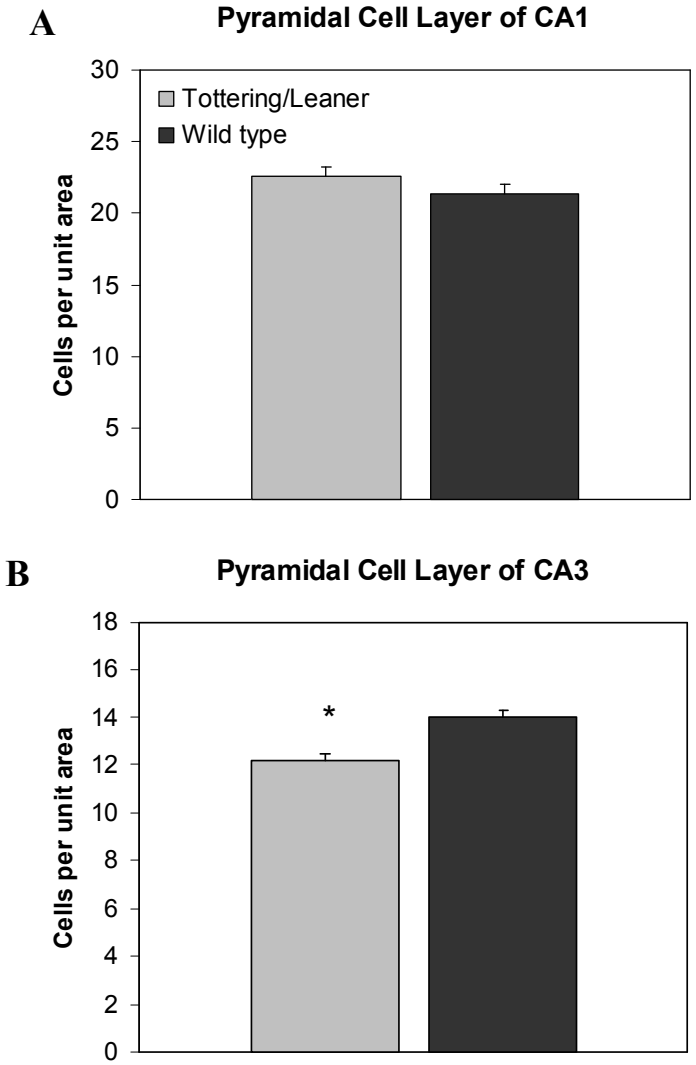

Figure 2.2: Cellular density in the hippocampus. Cellular density of 90-120 day old tottering/leaner and wild type mice defined as cells per unit area. Six regions of the hippocampus are examined: pyramidal cell layer of CA1 (A) and CA3 (B), granule cell layer of the dentate gyrus (C), and hilus of the dentate gyrus (D), lacunosum molecular layer (E) and oriens layer (F). **A), C), E), F)** No significant difference between genotypes observed. **B)** Single asterisk (*) indicates significantly decreased cellular density significantly tottering/leaner mice as compared to wild type (P = .001). **D)** Double asterisk (**) indicates significantly decreased cellular density in tottering/leaner mice as compared to wild type (P = .009).

C

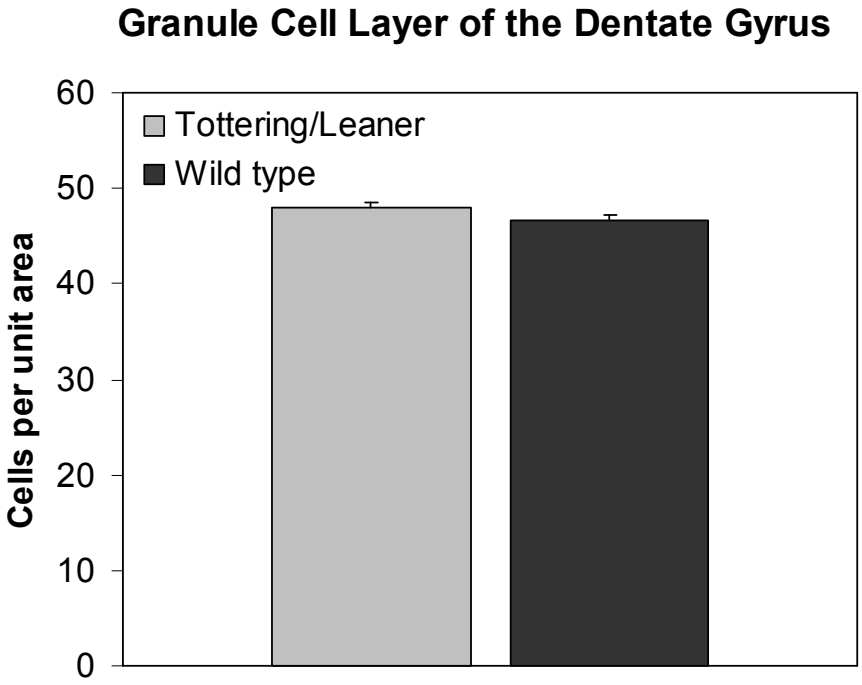

D

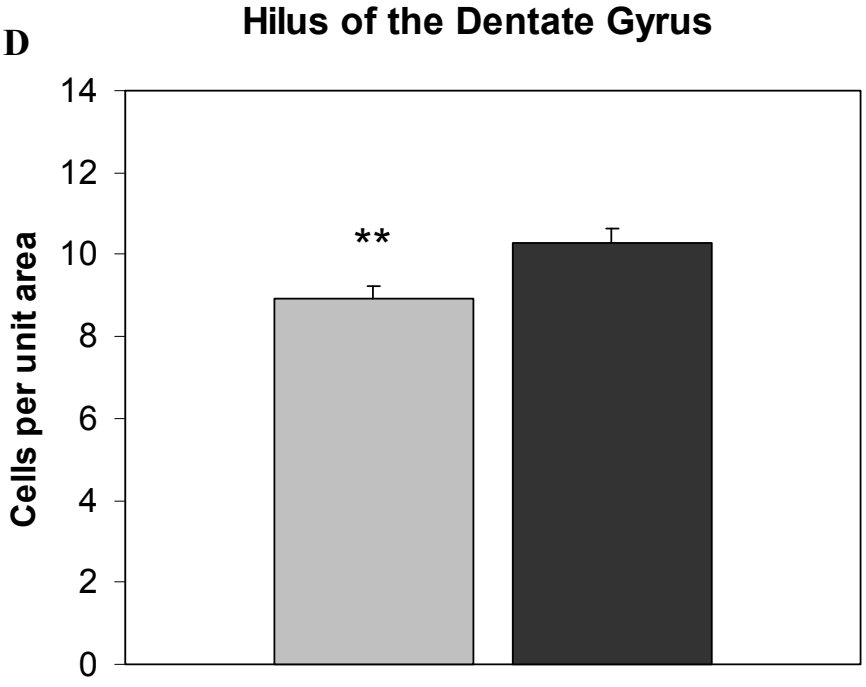

Figure 2.2 continued

E

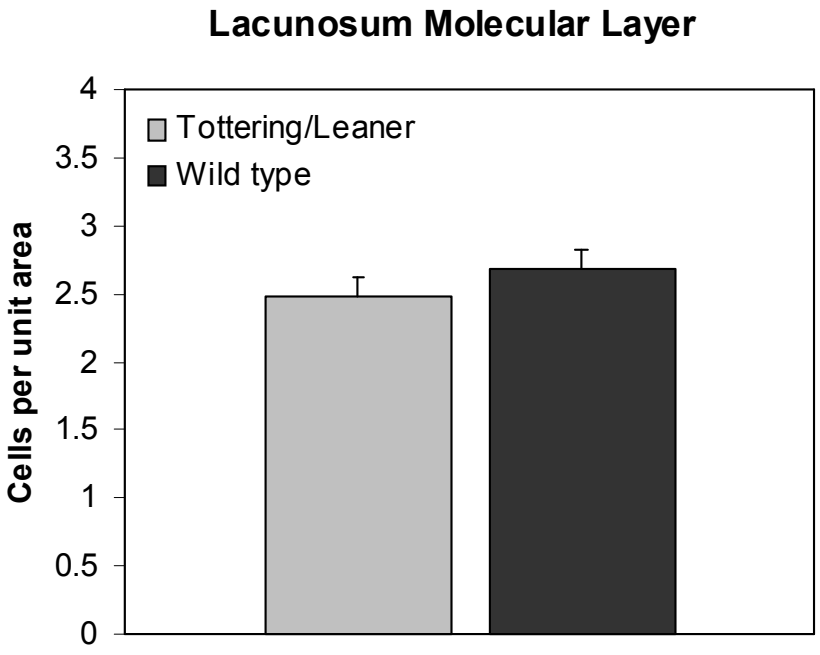

F

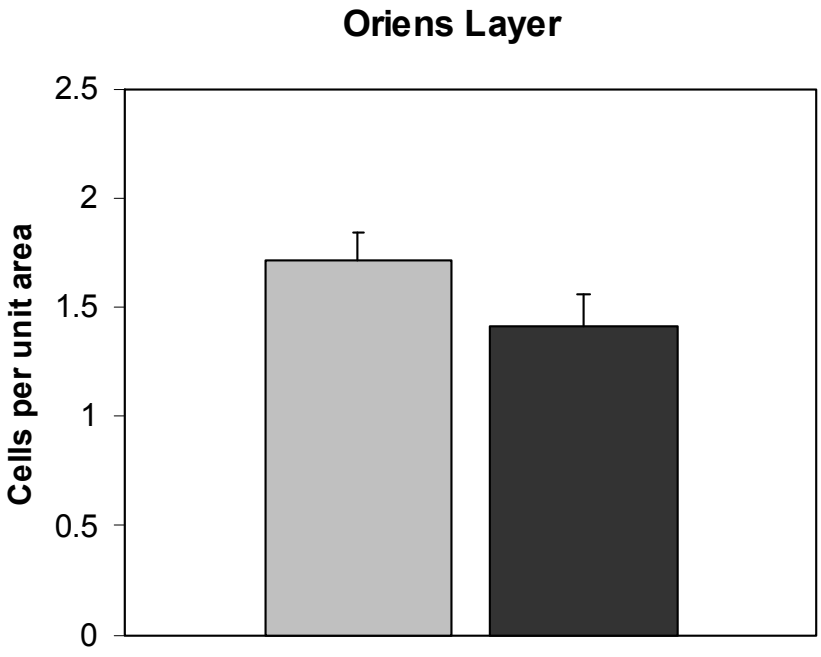

Figure 2.2 continued

In the investigation of cerebellar density (Figure 2.3), there was an observed trend towards decreased density in the anterior and posterior lobes combined in the cerebellum of the *tg/tg*^{la} mouse in comparison to the wild type mouse (P = 0.053). On closer inspection, this discrepancy was found to be a result of a significant decrease specific to the anterior lobe of the tottering/leaner mouse as compared to the posterior lobe of the wild type mouse (P = 0.016). There was also a significant decrease in the *tg/tg*^{la} mouse cellular density in the granule cell layer anterior and posterior lobes combined as compared to the wild type mouse (P = 0.036). It appears that there is enough of a subtle difference, but not a significant difference, in that the anterior lobe is slightly decreased in comparison to the posterior lobe in the *tg/tg*^{la} mouse. The subtle increase in the posterior lobe of the wild type mouse and slight decrease in the anterior lobe of the *tg/tg*^{la} mouse presumably leads to an overall significance between the wild type mouse posterior lobe and *tg/tg*^{la} mouse anterior lobe. It is likely that this decrease in cellular density in the *tg/tg*^{la} mouse comes from the cerebellar granule cell layer.

There was no significant difference within genotypes when comparing lobule 10 or the layers of lobule 10. In addition, there were no other significant differences in the anterior or posterior lobules other than that previously stated. The decrease in cerebellar volume, but no decrease in cerebellar density leads one to believe that there possibly is a decrease in cellular processes.

A

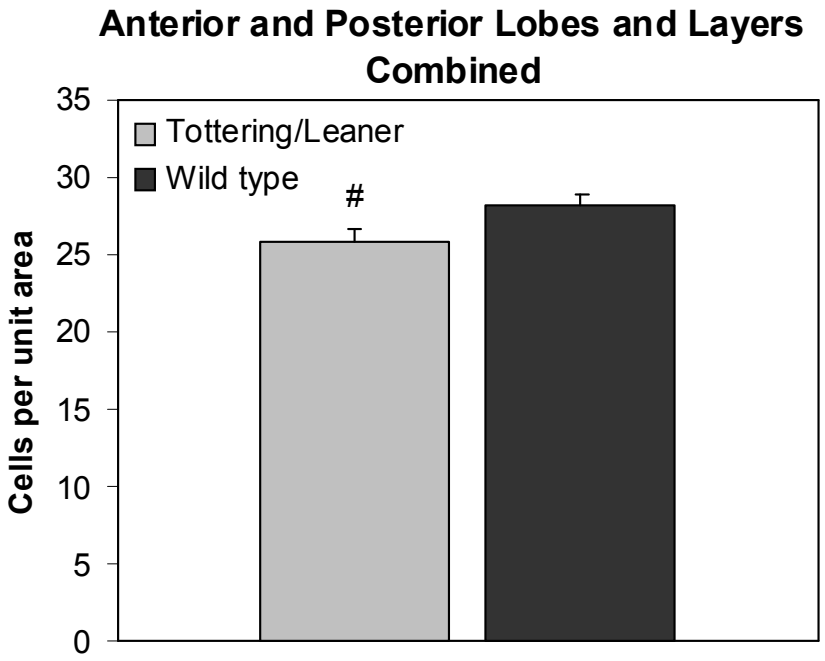

Figure 2.3: Cellular density in the cerebellum. Graphs depict anterior (lobule 2) and posterior (lobule 6) lobes combined (A) of 90-120 day old *tg/tg*^{la} and wild type mice and the examination distinct layers in the combined anterior and posterior lobes combined: molecular layer (B), granule layer (C) and Purkinje cell layer (D). Further analyses includes granule cell layer of anterior lobe compared to posterior lobe (E). Lobule 10 is described separately with layers combined (F) and in distinct layers: molecular layer (G), Purkinje cell layer (H) and granule cell layer (I). **B), D), F) -I)** No significant difference between genotypes observed. **B)** Number sign (#) indicates no significant difference, but a trend (P=0.053) where tottering/leaner is cellular density is decreased in anterior and posterior lobes combined as compared to wild type anterior and posterior lobes combined. **C)** Single asterisk (*) indicates significant decrease in *tg/tg*^{la} cellular density in anterior and posterior lobes combined in granule cell layer as compared to wild type cellular density in corresponding regions (P=0.036) **E)** Ampersand symbol (&) indicates significant decrease in tottering/leaner anterior lobe as compared to wild type posterior lobe in the granule cell layer (P = 0.016).

B

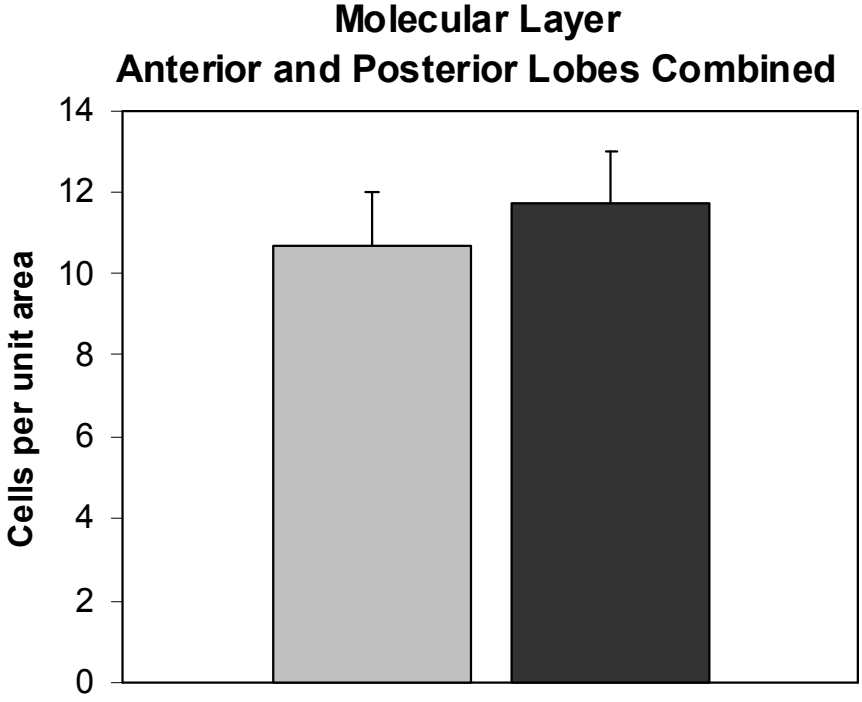

C

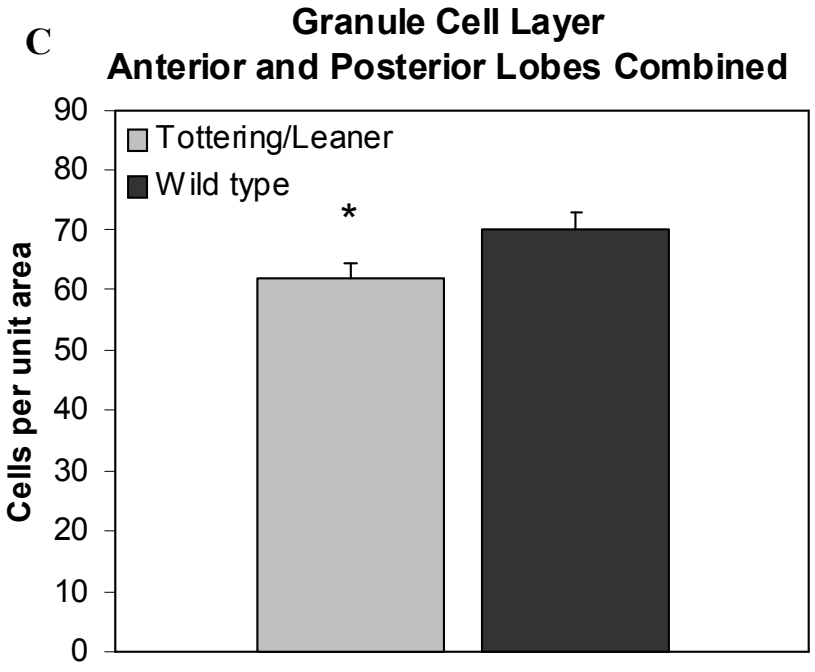

Figure 2.3 continued

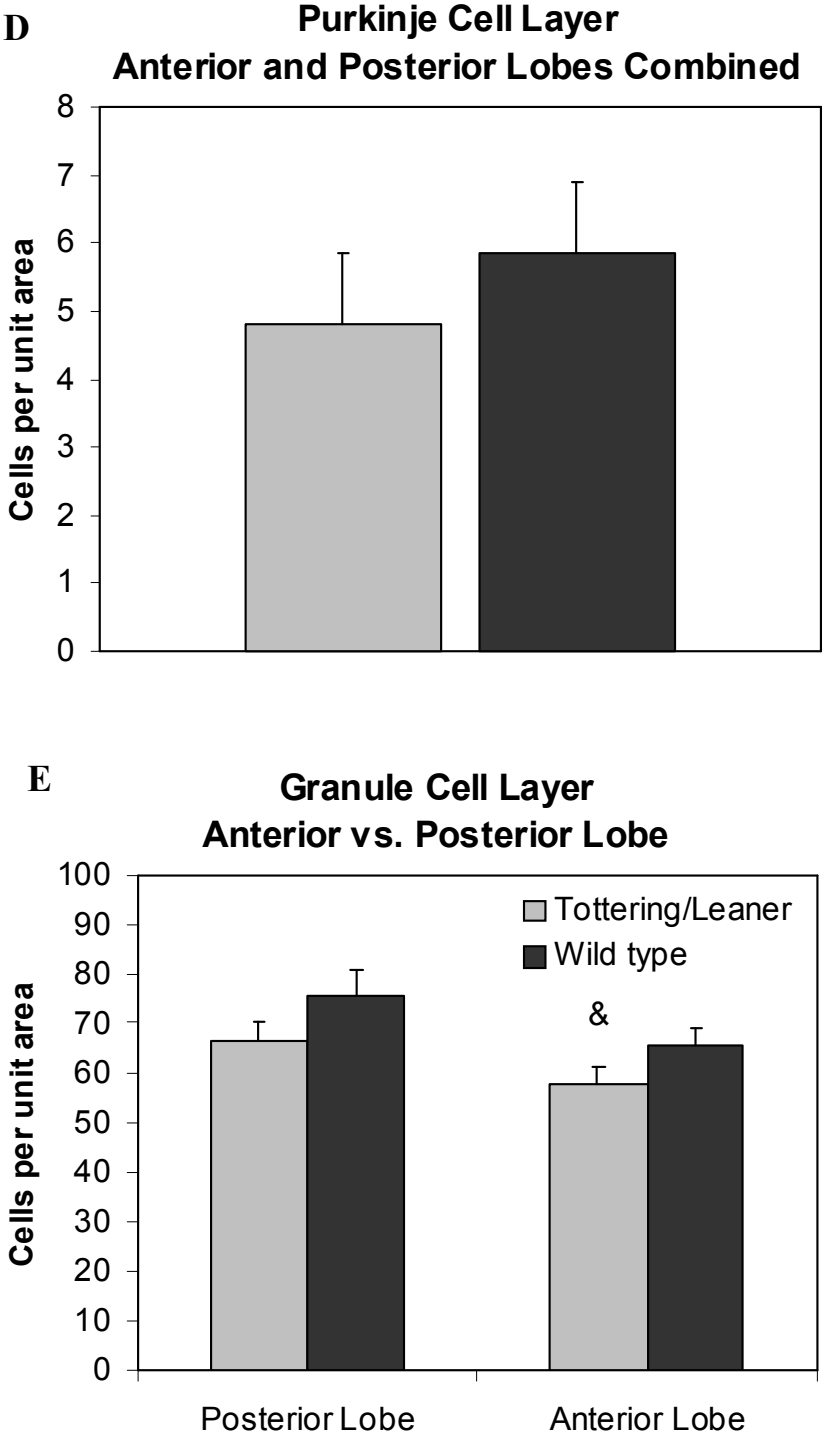

Figure 2.3 continued

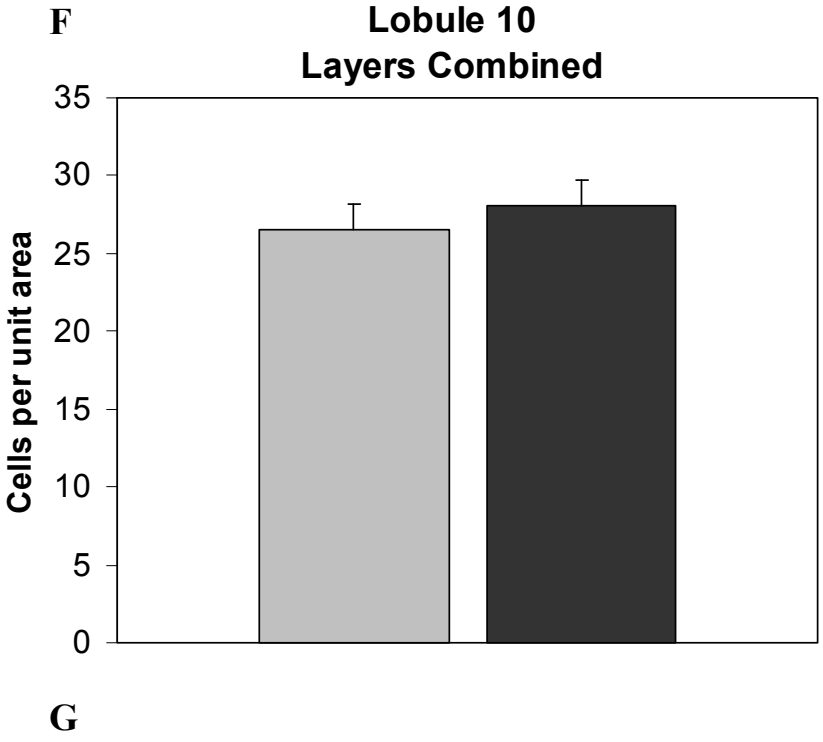

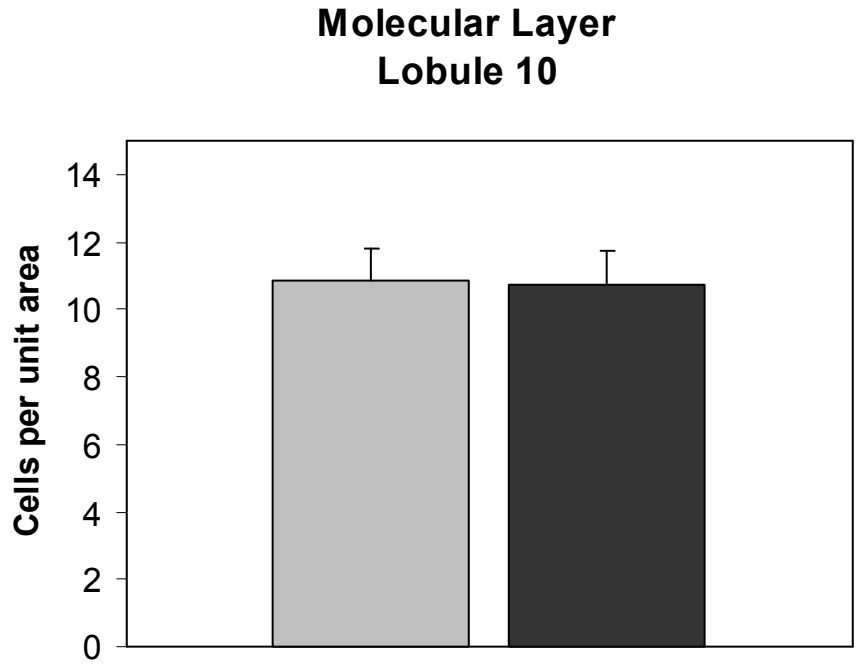

Figure 2.3 continued

H

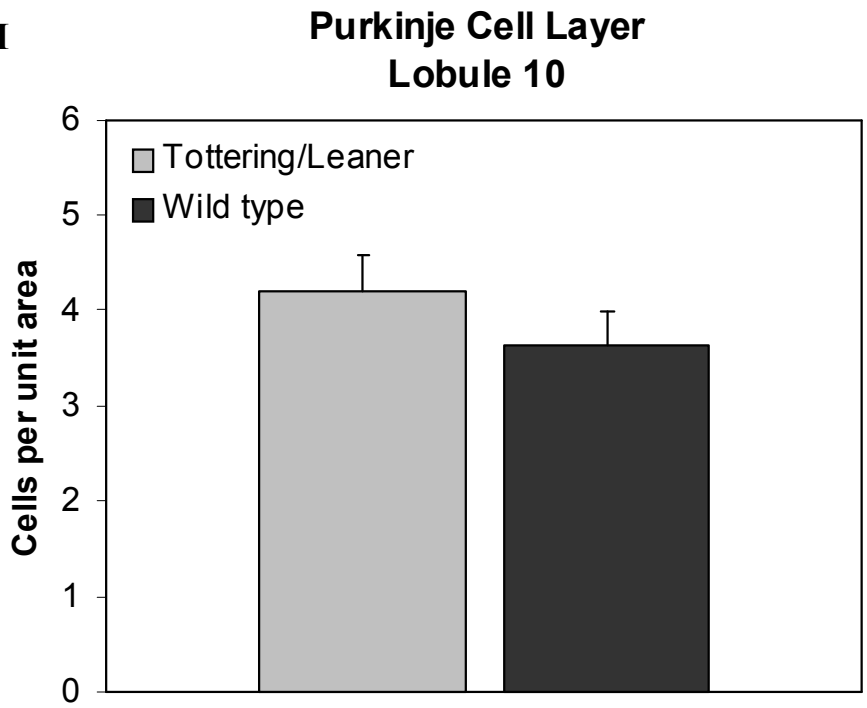

I

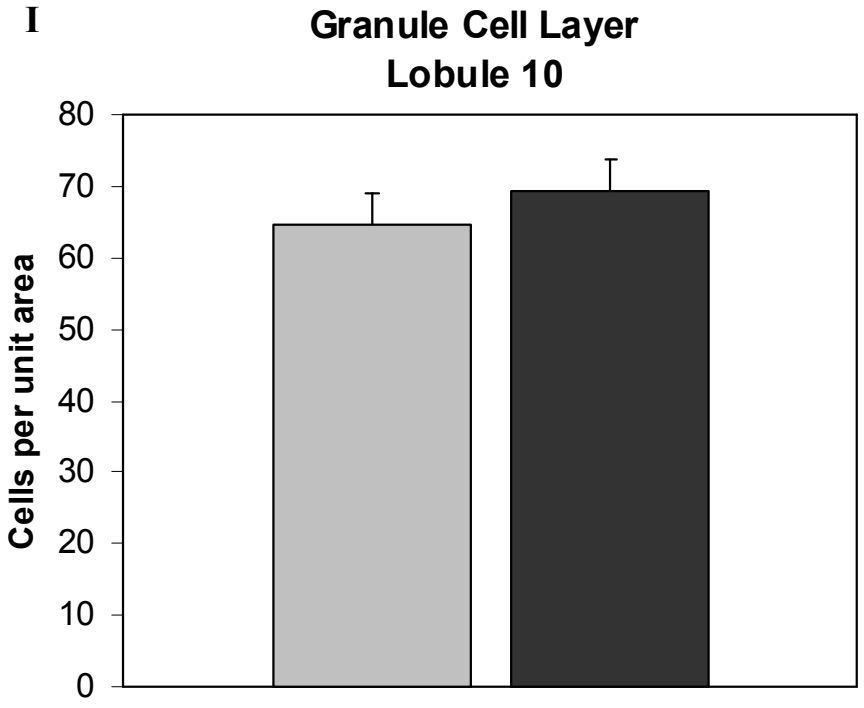

Figure 2.3 continued

Hippocampal Cell Size

As there was a significant difference in cellular density in the hippocampus in the hilus of the dentate gyrus and in the pyramidal cell layer of CA3, it was necessary to investigate the neuronal size as indicated by area within these two regions. Results showed that there was no difference in the pyramidal cell layer of CA3 between *tg*/*tg*^{la} mice and wild type mice (Figure 2.4). There was a significant difference within the hilus of the dentate gyrus with the female wild type cell size being larger than the cell size of all other genders and genotypes (P = .000 to .001). This shows that the *tg/tg*^{la} mouse fails to exhibit the normal gender difference in cell size within hilus of the dentate gyrus when the wild type mouse displays this difference. Alterations in *tg/tg*^{la} hormonal expression may lie behind this discrepancy.

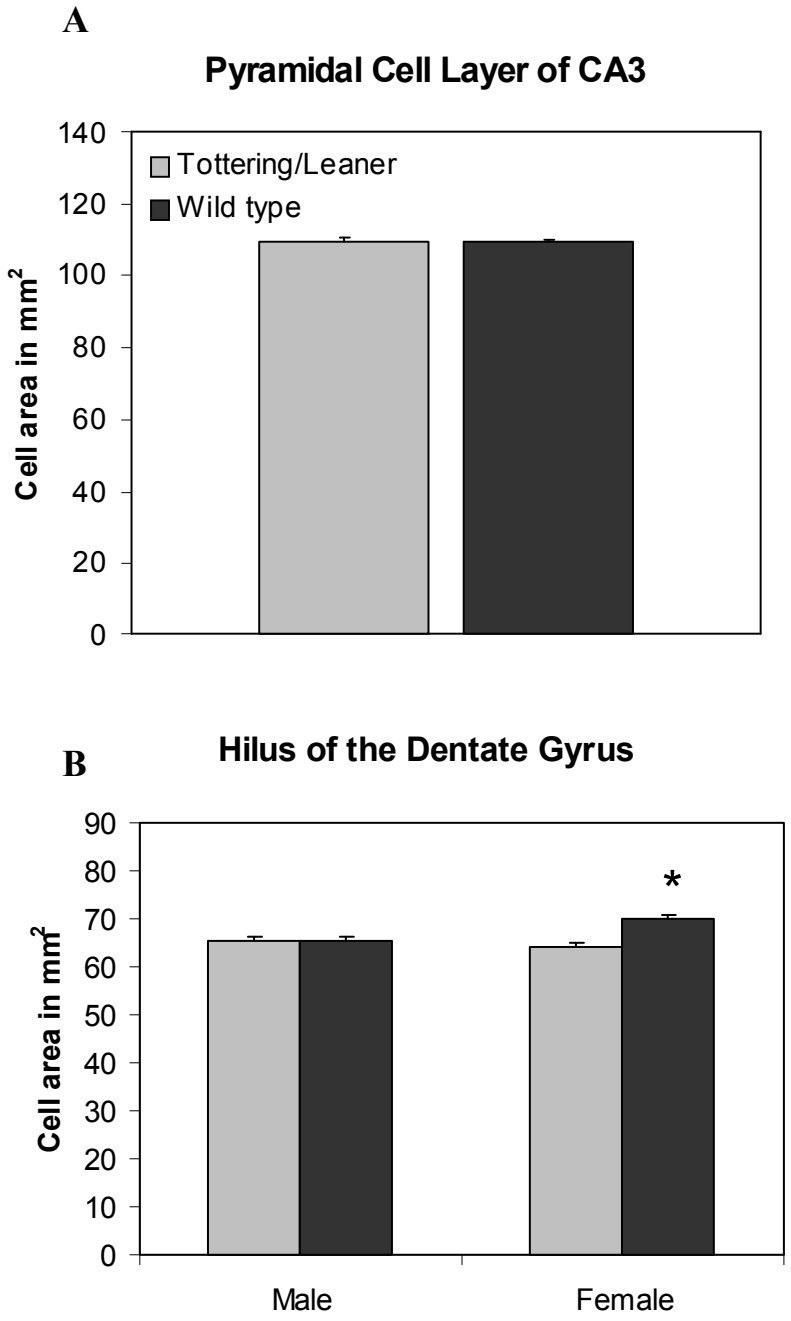

Figure 2.4: Cell size in hippocampal areas. This includes the pyramidal cell layer of CA3 (A) and the hilus of the dentate gyrus (B) in tottering/leaner and wild type mice at age 90-120 days. **A)** No significant difference observed within genotypes (P = 0.841). **B)** Single asterisk (*) indicates significant increase in female wild type cell size as compared to all other genders and genotypes (P = 0.000 to 0.001).

DISCUSSION

Results revealed no decrease in hippocampal volume in *tg/tg*^{la} mice while cellular density in the CA3 and hilus of the dentate gyrus was decreased and hippocampal cell size remained normal. This indicates that there could be a compensation of cellular processes in the CA3 and hilus of the dentate gyrus to account for the cellular density decrease in these regions as increased hippocampal cell size is ruled out as a possible mechanism.

The *tg/tg*^{la} cerebellum displayed a significant decrease in cerebellar volume, which confirms previous results from our lab that further describe a 24% decrease in the amount of cerebellar molecular layer per Purkinje cell layer without Purkinje cell loss as compared to the wild type mouse (Isaacs and Abbott, 1995). In line with previous assumptions, it is likely that the cerebellar volume loss in our study could be due to one or a combination of the following; glial cell loss, loss or shrinkage of parallel fibers, or a decrease in Purkinje cell dendritic arborizations in the cerebellar molecular layer (Isaacs and Abbott, 1995).

Alternatively, it could be suggested that the slight, but not significant decrease in the *tg*/*tg*^{la} anterior lobe as compared to the posterior lobe and the slight but not significant increase in the wild type posterior lobe as compared to the anterior lobe are suggestive of an actual biological difference. The homozygous leaner (*tg*^{la}/*tg*^{la}) mouse is known to exhibit a greater decrease in cerebellar granule cells in the anterior lobe when compared to the posterior lobe (Frank et al., 2003; Lau et al., 2004) by way of apoptosis (Bawa and Abbott, 2008), which leads to the possibility that the *tg*/*tg*^{la} mouse is

following a similar trend that is not as pronounced as that observed for the tg^{la}/tg^{la} mouse. It would be necessary to measure the volume of the granule cell layer in the tg/tg^{la} mouse and stain markers of cellular death such as fluoro-jade to investigate this aspect further.

CHAPTER III

PROLIFERATION AND DEATH IN THE DENTATE GYRUS OF TOTTERING/LEANER HIPPOCAMPUS

INTRODUCTION

It was necessary to determine whether changes in the number of neurons observed within the hippocampus as overall neuronal loss could result from increased cell death, decreased proliferation or interactions between these two processes.

Neuronal death has been examined in the subgranular zone of the dentate gyrus by means of Fluoro-Jade staining. Fluoro-Jade is an anionic tribasic fluorescein known to stain cell bodies, axons and axon terminals of degenerating neurons without staining healthy neurons, myelin, vascular elements or neuropil (Schmued et al., 1997). Fluoro-jade has proven successful for staining in a genetic model of cell death in the homozygous leaner mouse cerebellum (Frank et al., 2003). It is a fast and reliable method that does not have a clearly understood, but it is thought to function histologically based upon its chemical properties of high acidity that may attract a degenerating neurons strongly basic molecule (Schmued et al., 1997). As Fluoro-Jade has an emission peak of 550 nm and excitation peaks at 362 and 390 nm, appropriate fluorescence microscope visualization can be obtained with a FITC filter system.

The original hypothesis regarding this experiment was that the number of dying cells stained by Fluoro-jade in the *tg*/*tg*^{la} subgranular zone (SGZ) of the hippocampal dentate gyrus (DG) would be significantly higher than the number of Fluoro-jade positive cells observed in age- and gender-matched wild type mice.

In addition to characterizing cell death, cell proliferation and differentiation in the SGZ of the hippocampal DG must be examined using the immunohistochemical analyses. As early as 1965, postnatal neurogenesis in the SGZ of the DG in the hippocampus was characterized in rats using thymidine-H^3 to label S-phase cells (Altman and Das, 1965b). As research progressed, the immunohistochemical method of detecting of 5-bromo-2'-deoxyuridine (BrdU) incorporated into nuclear DNA was shown to appropriately label the nuclei of dividing cells that are in S-phase (Gratzner, 1982; Miller and Nowakowski, 1988; Miller and Nowakowski, 1991; Nowakowski et al., 1989). Leaner and tottering mice have been shown to exhibit decreased cell proliferation in the SGZ of the DG (Wills, 2006).

Proliferating cell nuclear antigen (PCNA) is an endogenous cell cycle protein that is localized within the cell nucleolus during the S phase of cell replication (Bravo and Celis, 1980; Bravo and Macdonald-Bravo, 1987; Takasaki et al., 1981). Using antibody to PCNA in conjunction with BrdU immunohistochemistry is a powerful tool to aid in cellular birth dating and cell cycle kinetics (Mandyam et al., 2007).

Prior to experimentation, it was hypothesized that there would be a decrease in cell proliferation in the dentate gyrus of *tg/tg*^{la} mice as compared to age- and gender-matched wild type mice as revealed using BrdU immunohistochemical staining. PCNA immunohistochemical staining would mirror the results of BrdU immunohistochemical staining and show a decrease in the amount of cell proliferation in the dentate gyrus of the *tg/tg*^{la} mice as compared to wild type mice.

While BrdU immunohistochemistry will show cell proliferation, it is not able to give information regarding differentiation of newly formed cells. It was necessary to determine the fate of these proliferating cells to have a more complete understanding of adult neurogenesis in *tg/tg*^{la} mice. To identify mature neurons, primary antibody to Neuronal nuclear protein (NeuN) was used to double label the sections along with BrdU. NeuN is neuronal cell-type specific protein that is expressed and will label neurons as early as one week after cell division and differentiation and peaks at four weeks (Mullen et al., 1992).

In addition to neurons, the proliferating cells are also capable of differentiating into astrocytes. Glial fibrillary acidic protein (GFAP) was used to characterize mature cells of astrocytic lineage (Bignami et al., 1972; Bignami and Dahl, 1973). Specifically, mature radial astrocytes and horizontal astrocytes are the two cell types that can be immunostained in the subgranular zone of the dentate gyrus (Seri et al., 2004).

Unpublished data from the Abbott lab has shown no significant difference in percent of cell differentiation of proliferating neurons as mature astrocytes or neurons between leaner, tottering and wild type mice. These previous findings lead to the hypothesis that the *tg/tg*^{la} mouse would reveal no significant difference in the percent of cell differentiation of proliferating neurons as mature neurons or astrocytes as compared to age- and gender-matched wild type mice.

EXPERIMENTAL PROCEDURES

Neuronal Death with Fluoro-Jade Stain

Fixed frozen 25µm thick coronal sections of the hippocampal DG were cut on a cryostat and thaw mounted onto gelatin-coated slides. Desired slides of the hippocampal DG were selected and taken through Fluoro-Jade staining according to a standard protocol (Schmued et al., 1997).

According to procedure, slides were thawed and dried for 3 hours in a 50°C incubator to assist adherence of sections to slides. An additional section of fixed frozen mouse testes were taken through this procedure to serve as a positive control. After cooling to room temperature, slides were taken through a series of alcohol immersions; 3 minutes in 100% ethyl alcohol, 1 minute in 70% ethyl alcohol and 1 minute in distilled water.

To help minimize background stain, slides were then placed in a 0.06% potassium permanganate solution (Thermo Fisher Scientific Inc., Fair Lawn, NJ, USA) for 15 minutes, while being gently agitated on a rotating platform. Two rinses in distilled water for 1 minute each is then followed by the immersion of slides into 0.001% fluoro-jade staining solution (Chemicon International, Temecula, CA, USA) while being gently agitated on a rotating platform for 30 minutes. One slide of mouse DG did not enter the fluorojade stain to serve as a negative control. Lastly, slides are rinsed in distilled water three times for 1 minute each, excess water is drained from slides and they are rapidly dried with a hot air gun. After slides are completely dry, they are

immersed in xylene for about 5 minutes, coverslipped with permount and allowed to dry for 24 hours prior to imaging.

Images of the fluoro jade stained SGZ of the DG will be captured using a FITC fluorescent filter on a Zeiss Axioplan Microscope with Zeiss Axiocam. Once coded to eliminate investigator bias, images will be scored according to their bright green fluorescence. Only positive fluorescing cells along the SGZ of the DG and those of appropriate cell size and shape will be counted to ensure proper scoring.

Degree of Cellular Proliferation Using BrdU Labeling and PCNA Immunohistochemistry

The first experiment examined neuronal proliferation in the SGZ using BrdU immunohistochemical detection. Mice were dosed with 100mg/mL BrdU (Sigma Aldrich, Milwaukee, WI, USA) given in sterile lactated Ringer's solution in volumes of 0.01mL/g body weight. Injections occurred twice daily with 8-12 hours between each injection for three days and one injection on the final fourth day, for a total of seven injections. One hour after the final injection, mice were perfused with Tyrode's saline (50mL; pH 7.2-7.4) and 4% phosphate buffered paraformaldehyde (J.T Baker Inc., Phillipsburg, NJ, USA). Brains were stored in 4% phosphate buffered paraformaldehyde for 12-24 hours followed by cryoprotection in 20% sucrose solution (EMD Chemicals Inc., Gibbstown, NJ, USA) in PBS after which they were rapidly frozen using powdered dry ice and stored at -70°C until used.

A cryostat coronally cut brains at 15μm throughout the desired brain regions and the sections were thaw-mounted onto gelatin coated microscope slides. Cut sections were stored at -70°C until they use. Sections containing the rostral DG were stained with a standard BrdU immunostaining protocol (Kempermann et al., 1997).

Slides were initially selected for desired sections of the DG and allowed to thaw and dry at room temperature for 15 minutes. After drying, slides were placed in HCl for 1 hour in a 40C incubator to open up the cell membrane. Three rinses of sodium borate (Fisher Scientific Co., Fair Lawn, NJ, USA) for 5 minutes neutralized the acid. Slides were then rinsed three times for 10 minutes each in NIH-PBS and then immersed in a detergent, Triton-X (Sigma Aldrich, St. Louis, MO, USA) for one hour. Another three rinses for 10 minutes each in NIH-PBS followed before slides were placed in 5% normal goat serum (Invitrogen, Eugene, OR, USA) for 1 hour at room temperature. Next, slides were immersed in a primary antiboby of 1:1000 anti-BrdU (Sigma, St. Louis, MO, USA) in 2% normal goat serum overnight in the refrigerator. One slide was not placed in the primary antibody and used as a negative control, instead, it set in 2% normal goat serum overnight in the refrigerator.

The following day, slides were removed from the primary antibody and rinsed three times in NIH-PBS for 10 minutes each. Slides were then are kept in a dark environment and placed in a solution of 1:1,000 Alexa-fluor 594 (Invitrogen, Eugene, OR, USA), a red fluorescence dye that binds to the anti-BrdU, in 1% bovine serum albumin (EMD Chemicals Inc., Gibbstown, NJ, USA) for six hours. Following this step, slides were rinsed three times for 10 minutes each in NIH-PBS. Moisture was carefully

wicked away from the slides with a kimwipe, avoiding any brain tissue, and then coverslipped in slo-fade gold (Invitrogen, Eugene, OR, USA). Coverslipped slides set for 24 hours and then were sealed along the edges with nail polish to prevent any dehydration. A period of atleast 30 minutes took place before slides were imaged.

A Zeiss Axioplan Microscope with Zeiss Axiocam was used to capture fluorescence images of at least four sections of the DG with a gap of at least 75um between sections so not to count the same nuclei more than once. The investigator counted the number of fluorescent nuclei along the SGZ of the coded images. Size and shape of fluorescent nuclei was examined to ensure that no background or other neuronal processes are counted.

Paraffin sections were used for PCNA staining. Immersion fixed brains in 4% phosphate buffered paraformaldehyde were paraffin embedded and cut coronally in 5 μm thick sections. Slides were heated for 30 minutes in a 40°C oven to ensure adhesion of the sections to the microscope slides. After cooling, the sections underwent deparaffinization in xylene and decreasing concentrations of alcohol. Slides then entered a basic immunohistochemistry procedure with peroxidase quenching (Mandyam et al., 2007). PCNA anti-mouse (Sigma, St. Louis, MO, USA) at a dilution of 1:10,000 in PBS served as the primary antibody. Diaminobenzedine (DAB; Curtin Matheson Scientific, Houston, TX, USA) stain labeled PCNA reactive cells for counting. The investigator counted the number of cells with DAB stained nuclei in the hilus, granular layer and along the SGZ of the DG. At least four sections each separated by at least 25 μm were counted from each animal. Sections of PCNA stained mouse intestines were

used as a positive control, while sections of hippocampus stained without primary antibody were used as a negative control. Positive cell counts per area were averaged for each gender and genotype.

Fate of Surviving New Cells Using NeuN and GFAP Immunohistochemistry

After injecting animals with BrdU as described previously, a period of four weeks passed before euthanasia. Sections were cut from paraformaldehyde fixed, cryoprotected brains sectioned at a thickness of 15 μm on a cryostat and thaw-mounted onto gelatin coated microscope slides. The protocol followed in the same manner as previously described for BrdU immunohistochemistry with the exception of adding a second label of immunostaining of NeuN (Chemicon International, Temecula, CA, USA) at concentrations of (1:1000) in bovine serum albumin and fluorescent marker Alexa-fluor 488 (Invitrogen, Eugene, OR, USA). Fluorescent nuclei labeled with BrdU were imaged as described previously, but those nuclei stained with Alexa-fluor 488 were captured with a FITC filter. Nuclei were counted in same manner as those stained with BrdU alone, but additional NeuN positive cells were counted in the event of evidence of staining overlap with BrdU labeled nuclei. This ensured that proliferating cells of neuronal lineage were counted.

Using an additional set of slides from the rostral DG, the immunohistochemical staining protocol followed in the same manner as in the BrdU / NeuN double labeling with the exception of the second label that will allow for immunostaining for GFAP (Sigma, St. Louis, MO, USA) at concentrations of (1:2000) and fluorescent marker

Alexa-fluor 488 (Invitrogen, Eugene, OR, USA). Fluorescent cells labeled with BrdU were imaged as described previously, but those cells stained with Alexa-fluor 488 were captured with a FITC filter. Sections of mouse intestine were stained as a positive control, while hippocampal sections were stained without a primary antibody for negative controls. Cells were counted in same manner as those stained with BrdU alone, but additional GFAP-positive cells were counted if there was evident staining overlap with BrdU labeled cells. This ensured only proliferating cells of astrocyte and radial glial cell lineage were counted.

All data were analyzed using SPSS Version 12.0.1 Multivariate Analysis of Variance (ANOVA) at $\alpha = 0.05$ to test gender differences. A Univariate Analysis of Variance (ANOVA) at $\alpha = 0.05$ two way ANOVA was used if the Multivariate ANOVA showed that genders could be combined. Tukey's honest significant difference (HSD) post hoc test was used when significant differences within region and genotypes were assessed.

RESULTS

Neuronal Death with Fluoro-Jade Stain

Fluoro-Jade staining with ANOVA analysis (Figure 3.1) revealed no significant gender difference, but a significant decrease in cell death within the tottering/leaner mouse hippocampus subgranular zone as compared to the wild type mouse ($P = 0.039$). Positive and negative controls both revealed that this procedure appropriately labels dying cells. An unexpected neuroprotective effect is revealed from this mutant mouse.

While some hippocampal regions experienced decreased density in the tottering/leaner mouse, the subgranular zone is not one believed to have an increase in neuronal loss. As cells in this area are continuing to proliferate, these results give reasonable belief that in the 3 month old tottering/leaner mouse a greater amount of newly formed cells remain viable than in the wild type animal.

Despite the results that there was a decrease in neuronal death in this area, it is yet to be determined whether the cells that are living are fully functional and integrated into the circuitry. It is possible those in the wild type subgranular zone a number of cells die for the benefit of this brain region and that the decrease in neuronal death in the mutant mouse proves unbeneficial and potentially harmful to hippocampal performance. Death signals may go unnoticed and not brought to completion in the cells of the subgranular zone of the DG in this unique mouse.

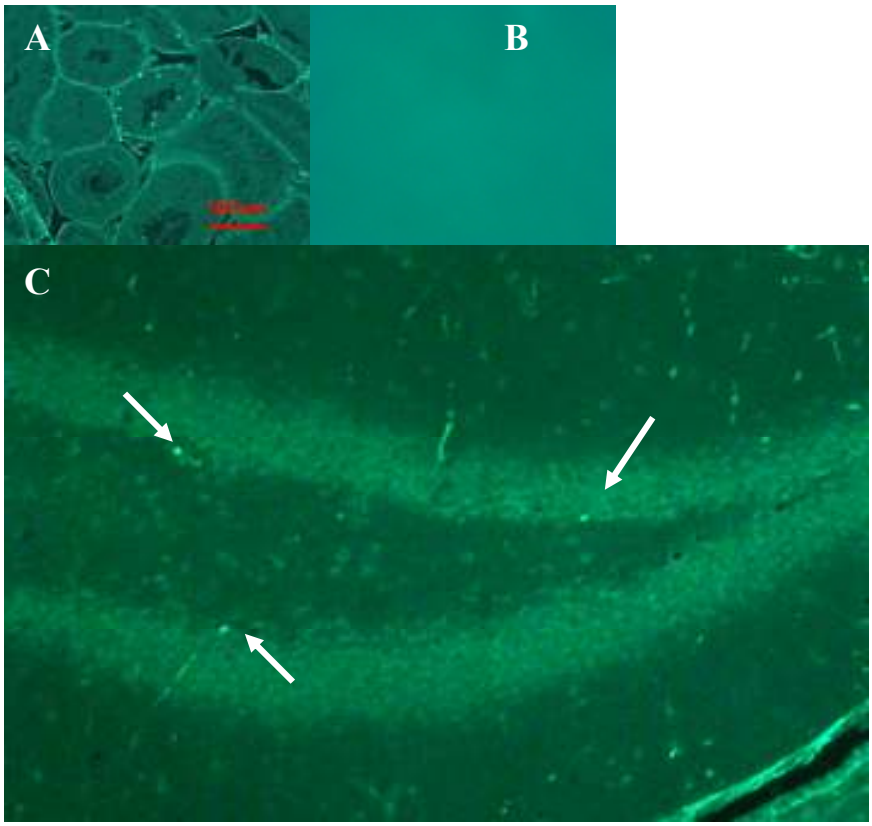

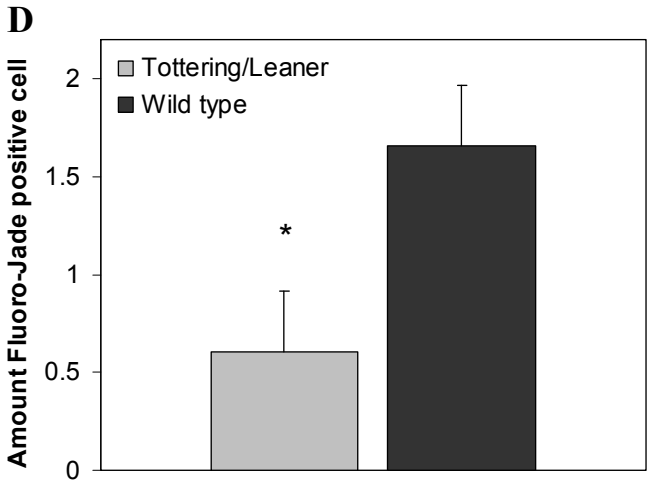

Figure 3.1 Representative image of neuronal death in the subgranular zone of the dentate gyrus as revealed by Fluoro-Jade stain. Positive control testes (A), negative control (B) and stained wild type male dentate gyrus (C). Arrows indicate positive cells. Graph depicts amount of fluoro-jade positive cells as averaged per section (D) A single asterisk (*) indicates no significant difference in gender, but a significant decrease in neuronal death in the tottering/leaner mouse as compared to the wild type mouse (P = 0.039).

Degree of Cellular Proliferation Using BrdU Labeling and PCNA Immunohistochemistry

BrdU labeling (Figure 3.2) revealed no significant difference between gender or genotypes regarding neuronal proliferation in the subgranular zone of the dentate gyrus ($P = 0.166$), conflicting with my previous hypothesis. This revealed that the decrease in cellular density in some regions of the hippocampus was not due to any changes in neuronal proliferation. It also helps to describe the interaction of proliferation and cell death in that the decrease in cell death is not a result of less new cells being formed.

PCNA further confirmed BrdU labeling results and revealed no significant difference in cell proliferation between genotypes (Figure 3.3; Figure 3.4). There was a slight trend of increased *tg/tg*^{la} PCNA labeling in the hilus of the dentate gyrus and the subgranular zone ($P = .081$ and .087 respectively).

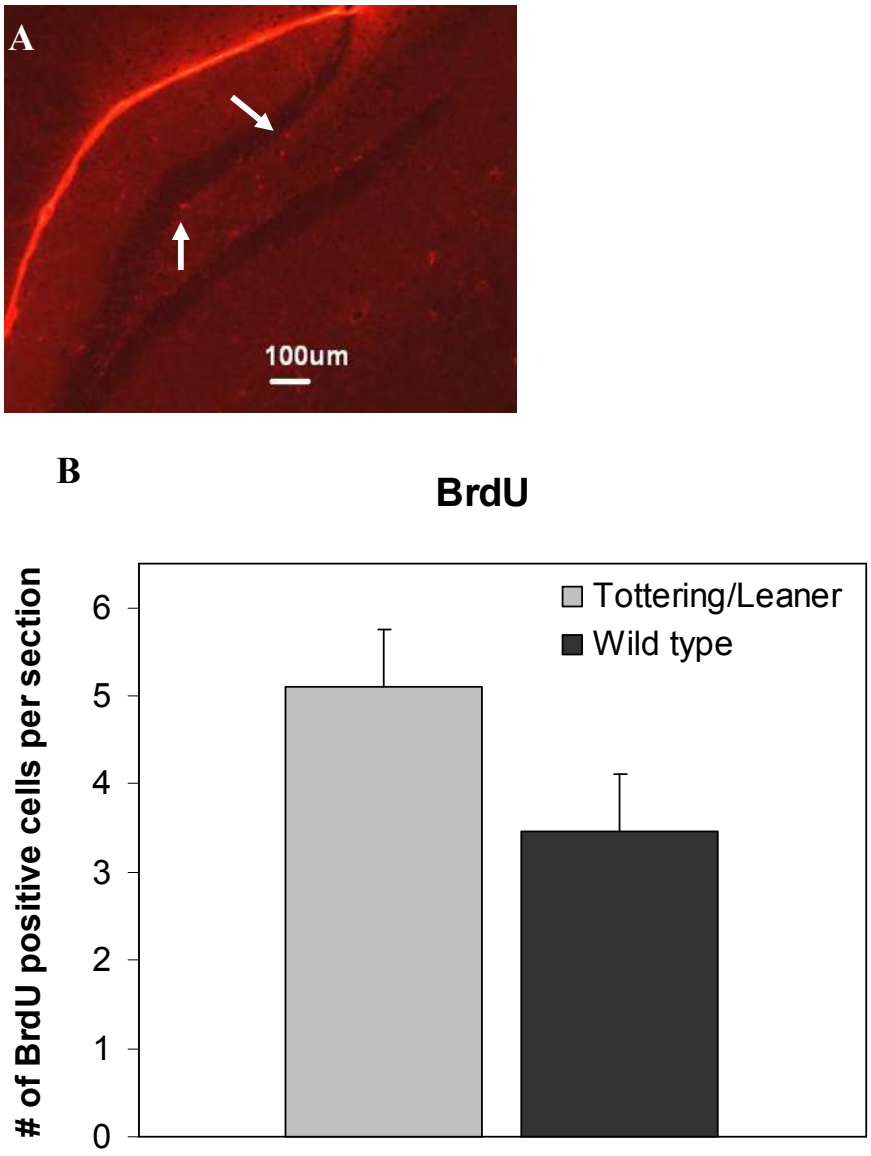

Figure 3.2 Image and graph of BrdU immunohistochemistry. Representative of BrdU labeled wild type 3-month-old dentate gyrus (A). Arrows indicate BrdU positive cells. Cellular proliferation in the subgranular zone of the hippocampal dentate gyrus in 3 month old animals as labeled by BrdU (B). BrdU labeled cells were averaged within each animal examined as number of positive cells per section. B) No significant difference in neuronal proliferation between gender or genotype.

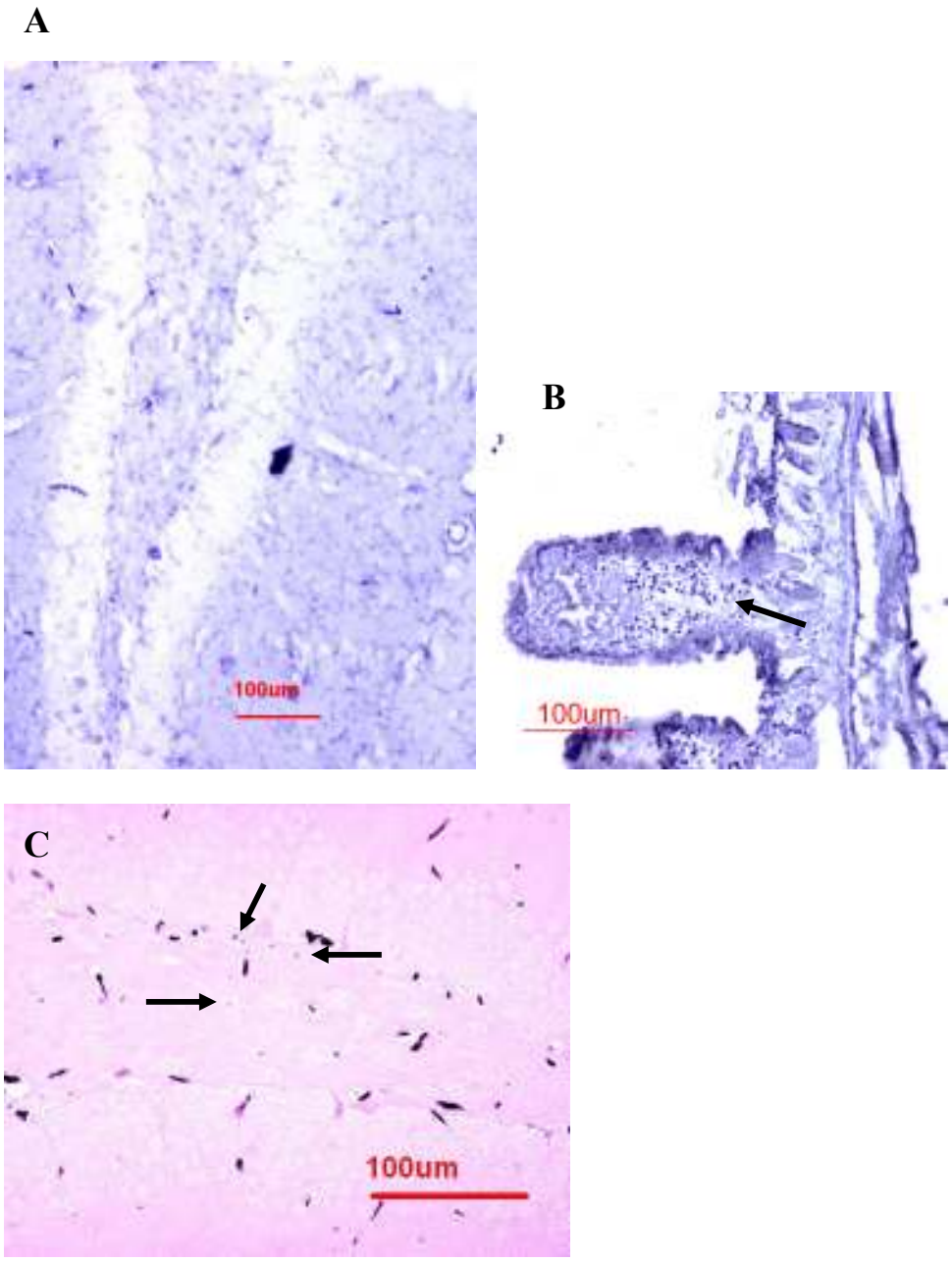

Figure 3.3 Representative images of PCNA immunohistochemistry. Negative control with non-specific staining (A), Positive intestine control (B) and PCNA labeled wild type hippocampus (C). Arrows indicate PCNA positive cells.

A

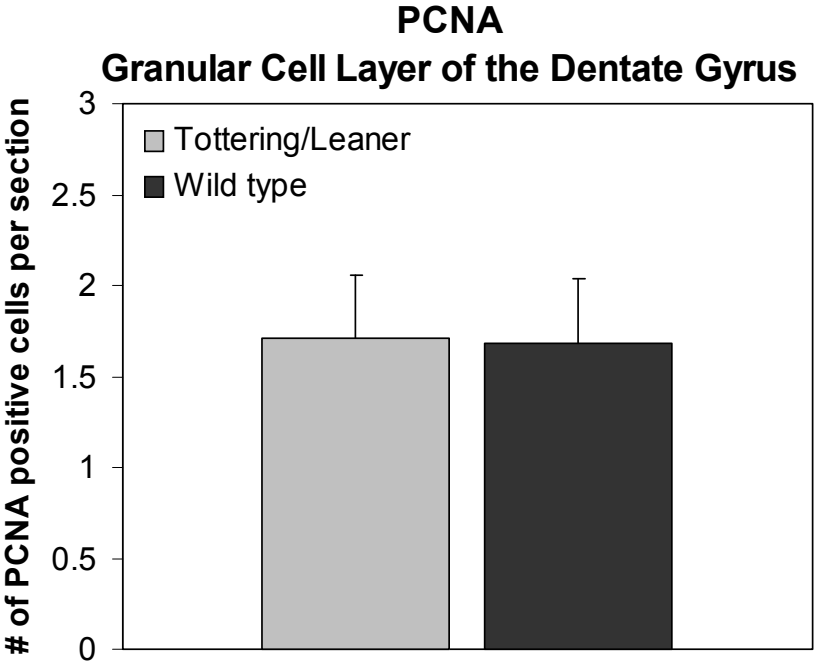

Figure 3.4
Graphs of comparison of 3-month-old *tg/tg*^{la} and wild type PCNA labeled regions. Granular cell layer of the dentate gyrus (A), hilus of the dentate gyrus (B), and sub granular zone of the dentate gyrus (C). PCNA labeled cells were averaged within each animal examined as number of positive cells per section. (A-C) No significant difference between genotypes. (B) Trend of increased tg/tg^{la} PCNA positive cells with (P = .081. (C) Trend of increased tg/tg^{la} PCNA positive cells with (P = 0.087).

B

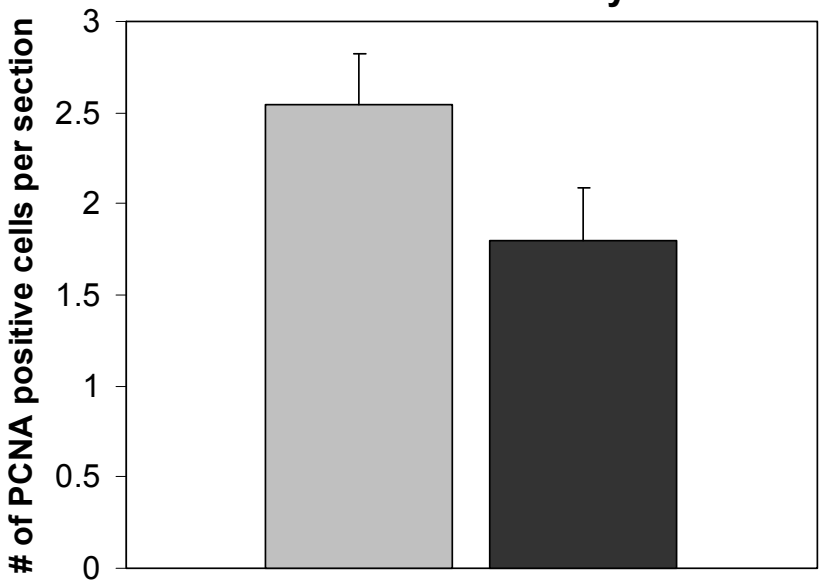

C

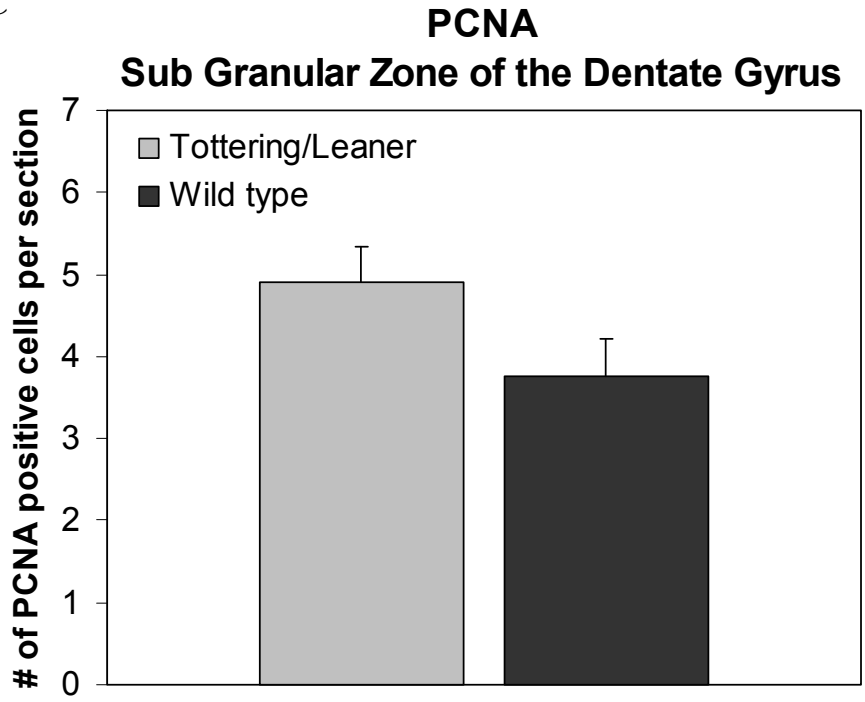

Figure 3.4 continued

Fate of Surviving New Cells Using NeuN and GFAP Immunohistochemistry

While basic cellular proliferation and death allow for a greater understanding of the process of new cell formation, the percent of cells in the subgranular zone of the dentate gyrus double labeled with BrdU and GFAP showed how many of the newly formed cells differentiated into astrocytes. The percentage of cells double labeled with BrdU and GFAP showed no significant difference between gender or genotype ($P = 0.706$). In line with the number of single labeled BrdU positive cells per section, double labeled cells showed no significant difference when gender or genotype were compared, giving more confidence to the results. The result of this experiment revealed that newly proliferated cells showed no abnormal differentiation to astrocytes (Figure 3.6).

When comparing gender and genotype ($P = 0.772$) of percent of BrdU/NeuN double labeled cells, no significant difference was found (Figure 3.5). Number of BrdU positive cells per section in BrdU/NeuN double labeled immunohistochemistry showed no significant difference in the same manner as single labeled BrdU results. While no significant difference was shown in percent of newly proliferating cells differentiating into neurons or astrocytes, these results remain in the expected range of normal cellular differentiation observed by our lab in this region (Wills, 2006).

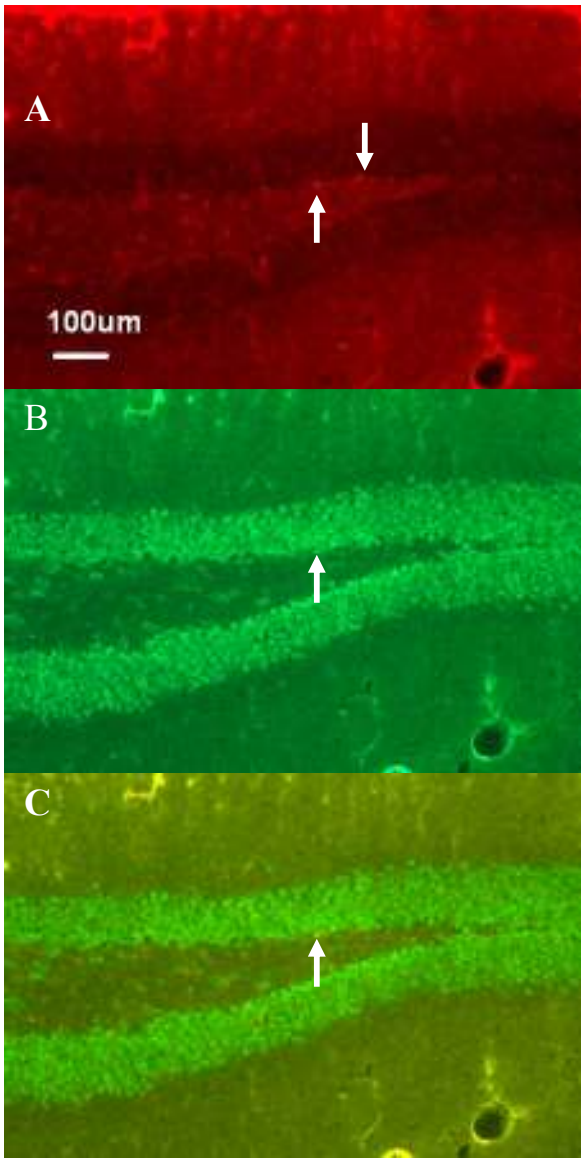

Figure 3.5 Images of NeuN/BrdU immunohistochemistry. Representative images of BrdU labeled (A), NeuN labeled (B) and BrdU/NeuN double labeled (C) 3 month old *tg/tg*^{la} subgranular zone of the dentate gyrus. Arrows indicate positive cells.

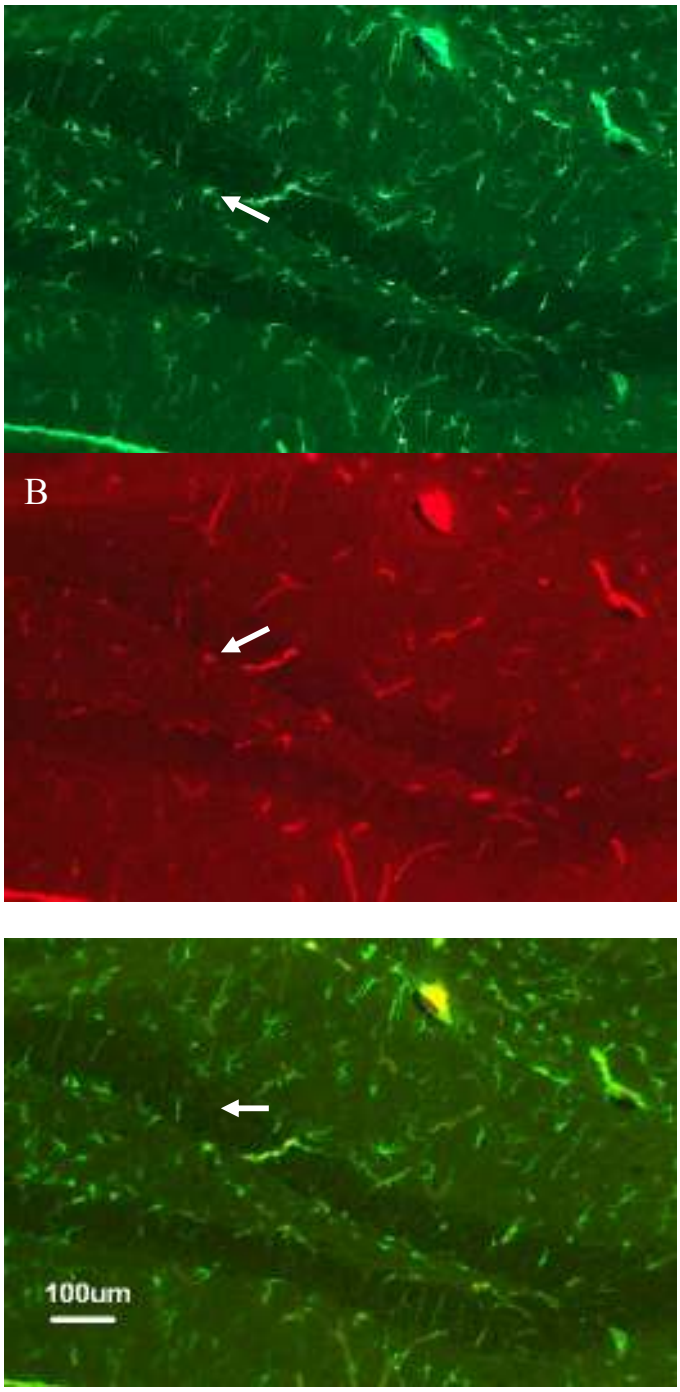

Figure 3.6 Images of GFAP/BrdU immunohistochemistry. Representative images of GFAP labeled (A), BrdU labeled (B) and BrdU/GFAP double labeled (C) 3 month old *tg/tg*^{la} subgranular zone of the dentate gyrus. Arrows indicate positive cells.

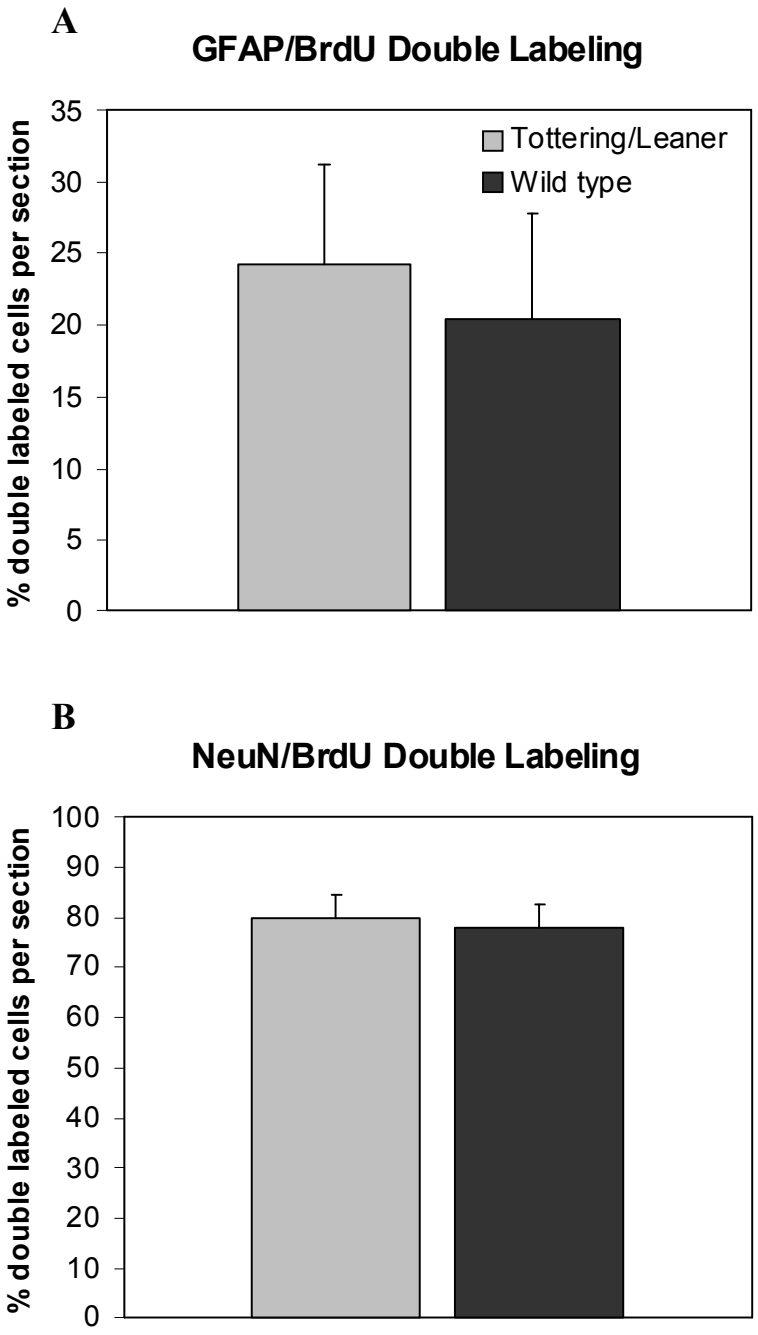

Figure 3.7 Graphs of percent cells labeled GFAP/BrdU and NeuN/GFAP. Graph comparing percent of 3-month-old *tg/tg*^{la} and wild type positive GFAP/BrdU (A) and NeuN/BrdU (B) double labeled cells per section of subgranular zone of the dentate gyrus. (A,B) No significant difference between genotypes.

DISCUSSION

The Fluoro-jade, BrdU and PCNA results indicated that the decrease in cell death in the *tg/tg*^{la} mouse was not due to an increase in cellular proliferation (Figure 3.7). In addition, newly proliferating cells differentiate into neurons and glia in the same percentages as wild type animals. Although the proliferating cells have differentiated into normal lineages, it is unknown whether they are fully functional or integrated into their environment. The *tg/tg*^{la} mutation appears to have deleterious effect to the brain region as cells that normally would die in a wild type animal are not allowed to enter normal cell death. It is possible that the cells that are not dying as intended, and are not properly functioning which could be adding to this dysfunction.

Unpublished research from our lab reports an increase in neuronal proliferation in the leaner mutant mouse at P42-50, but then a decrease in neuronal proliferation as compared to wild type mice at P100-150 (Wills, 2006). While the *tg/tg*^{la} mouse shows no variation at P90-120, it is possible that it may follow proliferation fluctuations as the leaner mouse displays. It cannot be ruled out that there are changes in proliferation in the dentate gyrus in *tg/tg*^{la} juvenile or adult mice aged above the age range this research investigated. As the leaner mutation is more phenotypically severe than the *tg/tg*^{la} mouse (Green and Sidman, 1962; Herrup and Wilczynski, 1982), it could be that neurogenesis is in fact never altered in these mice.

CHAPTER IV

CHANGES IN BASIC BIOCHEMICAL PARAMETERS IN GRANULE CELLS OF THE CEREBELLUM AND HIPPOCAMPUS IN TOTTRING/LEANER MICE

INTRODUCTION

Changes in several intracellular biochemical parameters have been observed in granule cells of homozygous leaner and tottering mice (Bawa and Abbott, 2008). Previously it was unknown whether any alterations in cellular physiology exist in granule cells from tg/tg^{la} mice.

As the characteristic mutation of these mice results in malformations of the Cav2.1 calcium channel, it is likely that calcium homeostasis may be altered. It has been shown that basal free intracellular calcium is reduced by 20% in cerebellar granule cells from the tottering and leaner mouse as compared to age- and gender-matched wild type mice (Bawa and Abbott, 2008).

It was previously hypothesized that basal intracellular calcium levels would be reduced in cerebellar and hippocampal granule cells in the tg/tg^{la} mouse as compared to age- and gender-matched wild type mice.

Calcium homeostasis along with cellular metabolism and bioenergetics are held in a delicate balance with mitochondrial activity being a critical component. Ca^{2+} accumulation by mitochondria can affect ATP synthesis along with alterations in ATP synthesis effecting the removal of Ca^{2+} from the cytoplasm by ion pumps. Alterations in mitochondrial membrane potential, an indicator of mitochondrial activity, may

ultimately result in a cascade of cellular events ending in cell death (Nicholls and Ward, 2000). Previous research revealed a reduction in the mitochondrial membrane potential in leaner mouse cerebellar granule cells as compared to wild type cerebellar granule cells, but no significant difference was observed between cerebellar granule cells from tottering and wild type mice (Bawa and Abbott, 2008).

As the *tg/tg*^{la} mouse appears to more closely resemble the tottering mouse rather than the leaner mouse with respect to several morphological and biochemical features, the initial hypothesis was based upon the plausibility that there will be no difference in mitochondrial membrane potential, and therefore, mitochondrial activity, in this mutant mouse as compared to the wild type mouse.

With the goal of further characterizing these mutations' possible effects on cell functioning and viability, examination of several aspects of reactive oxygen species (ROS) production in the cell took place. Reactive oxygen species refers to partially reduced metabolites of oxygen that are more reactive than molecular oxygen and include: superoxide anions, hydrogen peroxide, and hydroxyl radicals (Thannickal and Fanburg, 2000). ROS can result from a variety of processes, and are often found as an abundant byproduct in the mitochondrial respiratory chain. Fluctuations in ROS can serve the cell positively be aiding in intracellular signaling and regulatory functions, but an excess of ROS can cause serious damage to DNA, lipids and protein, possibly leading to cell death (Droge, 2002; Stadtman and Levine, 2000).

This experiment assessed the activity of ROS by using 5-(and-6)-chloromethyl-2',7'-dichlorodihydrofluorescein diacetate, acetyl ester (CM-H_2DCFDA). This dye

fluoresces in response to removal of acetate groups by intracellular esterases and oxidation within the cell. It is specific for the presence of H_2O_2, but can also identify H_2O_2 as a product of superoxide. Research data on generation of reactive oxygen species show no difference between tottering, leaner or wild type mice (Bawa and Abbott, 2008).

In regards to reactive oxygen species, it was hypothesized that the tg/tg^{la} mouse would show no difference in the amount or rate of change in ROS production compared to age- and gender-matched wild type mice.

EXPERIMENTAL PROCEDURES

Levels of Basal Intracellular Calcium Ion Homeostasis

Calcium homeostasis was assessed by measuring basal levels of free intracellular calcium [Ca^{2+}] in granule cells from the cerebellum and hippocampus of 90-120 day old *tg/tg^{la}* and wild type animals using calcium green-1 fluorescent dye. One *tg/tg^{la}* and one wild type animal of the same gender were assessed for each session of data collection. Each mouse was anesthetized with isoflurane and decapitated, followed by immediate dissection of the cerebellum and hippocampus. Tissue from each brain region was kept separate, sliced into small pieces and placed in Minimum Essential Medium Eagle (MEM; Sigma Aldrich, St. Louis, MO, USA). A series of proteolytic and mechanical disruptions took place, ending with a final centrifugation. The resulting pellet consisted of whole cells (primarily granule cells) from a specific brain region of origin and were reconstituted in MEM and plated on gelatin and poly-d-lysine (Sigma,

St.Louis, MO, USA) coated coverslips to ensure cells adhered securely. Coverslips were incubated in MEM media for 30 minutes in at 37°C, 95% CO_2 to allow the cells to adhere more tightly to the coverslip and to keep the cells viable. After incubation, media was removed and calcium green 1-AM (CaG-1; Invitrogen, Eugene, OR, USA), a dye that fluoresces intensely when bound to calcium, added at a 1uM concentration in Hanks Balanced Salt Solution (HBSS; Sigma Aldrich, St. Louis, MO, USA) for 20 minutes. CG was then removed and replaced with HBSS for imaging.

Ten images per coverslip were captured at 40X on Zeiss Axiovert 200M microscope using SlideBook 4.1.0 software from 3I, FITC Excitation: BP 470/20, dichroic FT 493, emission BP 505-530nm; or Cy3 Excitation: BP 560/40, dichroic FT 585, emission: BP 630/75 nm. Simple PCI and Imaging System Software were used to measure fluorescence from a minimum of 10 individual granule cells per brain region for each animal. Preliminary investigation of cell types adherent to coverslips and stained with DAPI (Invitrogen, Eugene, OR, USA) and NeuN (Chemicon International, Temecula, CA, USA) ensured that granule cells were the predominate cell found in the resulting cultures. A coverslip without adherent cells was imaged in HBSS alone as a negative control. During data collection, granule cells were identified by size and shape. Fluorescence data per cell will be averaged for each animal and percent control was calculated per experiment and statistically analyzed as previously stated.

Levels of Mitochondrial Activity

Mitochondria membrane potential was measured by employing identical cell isolation and imaging techniques as described for the previous experiment with the exception of using tetramethyl rhodamine methylester perchlorate (TMRM; Invitrogen, Eugene, OR, USA), a lipophilic potentiometric mitochondrial dye, at concentrations of 150nM in HBSS as the imaging dye. Fluorescent measurements and data analysis were done in the same manner as presented earlier, except that a minimum of 10 individual mitochondria in each granule cell were measured for fluorescence intensity. Cells not exposed to TMRM and adherent to a coverslip were imaged in HBSS as a negative control.

Data for levels of basal intracellular calcium ion homeostasis and mitochondrial activity were analyzed using SPSS Version 12.0.1 Multivariate Analysis of Variance (ANOVA) at $\alpha = 0.05$ to test gender differences. A Univariate Analysis of Variance (ANOVA) at $\alpha = 0.05$ two way ANOVA was used if the Multivariate ANOVA showed that genders could be combined. Tukey's honest significant difference (HSD) post hoc test was used when significant differences within region and genotypes were assessed.

Amount and Rate of Change in Reactive Oxygen Species Production

Cerebellar and hippocampal cells were isolated as previously described in with adjustments made to plating of cells, dye and imaging procedure. After centrifugation, individual collections of cells from different brain regions and genotypes were reconstituted in 2mL MEM with 0.5mL placed in each of three wells of a 48 well cell

culture plate. Following incubation as described previously, media were removed from wells and replaced with CM-H_2DCFDA (Invitrogen, Eugene, OR, USA) in HBSS. A BioTek Synergy 4 Microplate Reader with Gen5 software read the plate fluorescence with excitation: 485/20, emission 528/20, optics position: top 50% and sensitivity: 75. Readings occured every 2.3 minutes for 45 minutes ending with a total of 19 observations.

After the initial readings were completed, cells entered a process of staining with Janus green (Sigma Aldrich, Milwaukee, WI, USA), a colorimetric dye detecting protein content (Raspotnig et al., 1999). The plate reader was set at absorbance: 630. Fluorescence values given at each time point for each brain region and genotype in their respective three wells were divided by their Janus green value to get an adjusted ROS value. The three adjusted ROS values for each region and genotype at each specific time point were then averaged. Each reading was then divided by the initial reading value from the same brain region from the wild type animal. Data was analyzed using SPSS Version 12.0.1a Mixed Model Analysis of Repeated Measures with $p = 0.05$ to detect any significant changes in amount and rate of ROS production. Preliminary investigation of cell types existing in well plates with staining of DAPI and NeuN ensured that granule cells were highly present in resulting cultures.

The above procedure was also repeated with the addition of 50μM tert-butyl hydrogen peroxide (TBHP; Sigma Aldrich, Milwaukee, WI, USA) to CM-H_2DCFDA as a way to identify if cells from either genotype are reaching a ceiling of ROS production or the cells in both genotypes are able to produce similar rate or amounts of ROS.

Fluorescence reading of cells in a well plate with HBSS dye alone was used as a negative control.

RESULTS

Levels of Basal Intracellular Calcium Ion Homeostasis

Mice with VDCC mutations exhibit abnormal calcium influx and specifically the leaner mouse displayed decreased levels of basal intracellular calcium ion homeostasis in the cerebellar granule cells (Bawa and Abbott, 2008). Therefore, the level of calcium ion homeostasis the *tg/tg*^{la} mouse hippocampal and cerebelar granule cells should be investigated.

Basal intracellular calcium ion homeostasis remained normal in the *tg/tg*^{la} mouse hippocampus as compared to the wild type animal (Figure 4.1; Figure 4.2). As there have been few abnormalities within the mutant hippocampus throughout this study, it comes at no surprise that this region remained normal. Alternatively, the male *tg/tg*^{la} cerebellar granule cells levels of basal intracellular calcium homeostasis were significantly greater than in the wild type animal ($P = 0.028$). This discrepancy is not found in the female mice. Male *tg/tg*^{la} cerebellar granule cell levels of basal intracellular calcium homeostasis were decreased as compared to that of the mutant hippocampus ($P = 0.001$).

While wild type male and female mice could not be compared with each other as the data were presented in percent control, examining raw fluorescent data can suggest whether there are gender differences within either region of the wild type animals.

When the range and standard error of the mean of the wild type animals in both genders were examined, it suggested that there was not a real gender difference between wild type animals (data not shown). It is more likely that the gender difference where the tg/tg^{la} male cerebellum exhibited increased basal intracellular calcium ion levels as compared to the wild type animal is due to the mutation's effect (Figure 4.3).

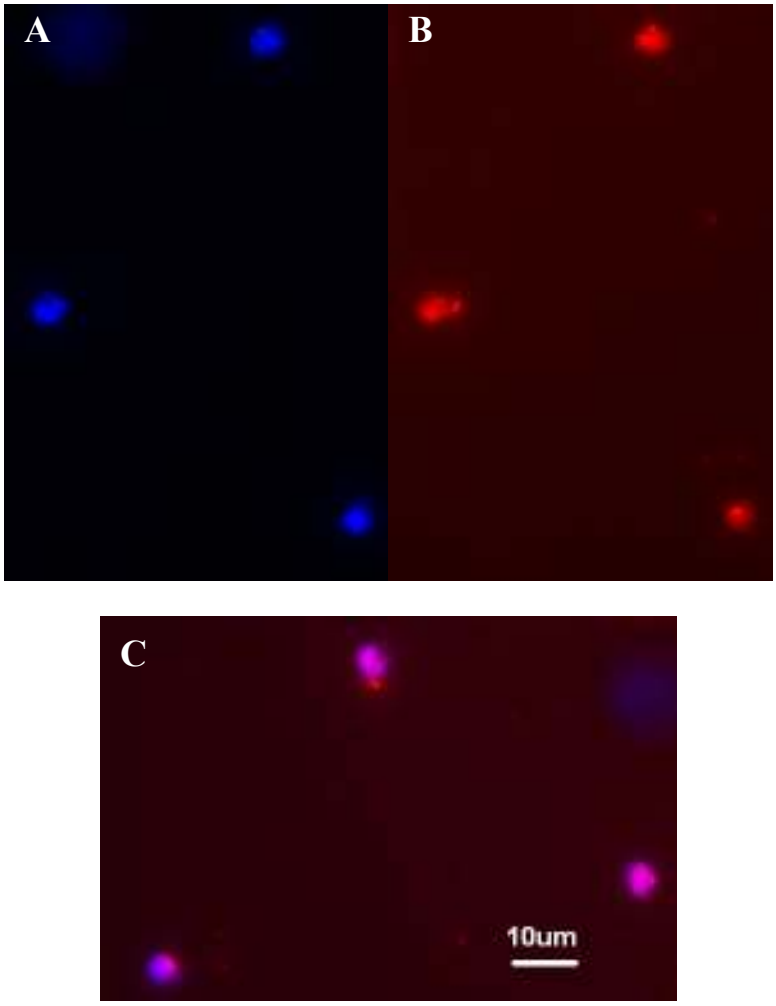

Figure 4.1 Image of DAPI/NeuN labeled granule cells. Representative images of isolated cells stained with DAPI (A), NueN (B), and double labeled with DAPI/NeuN to confirm isolation of granule cells.

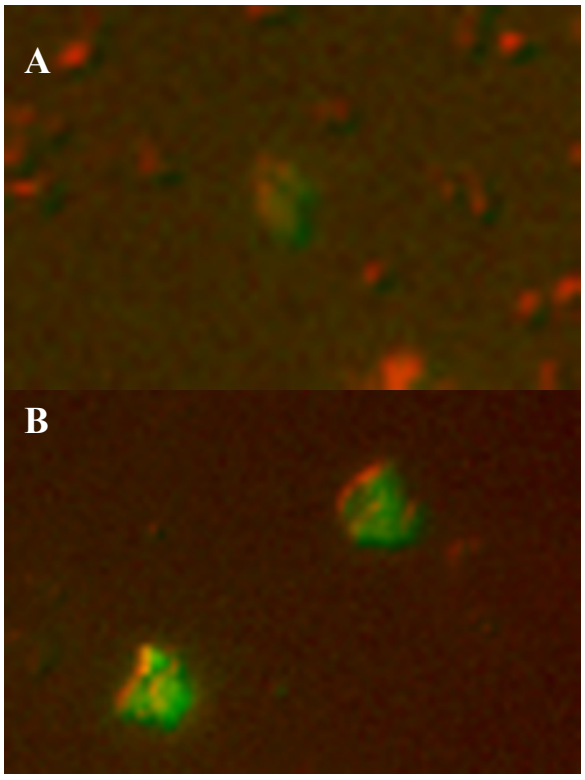

Figure 4.2 Image of CaG-1 and bright field granule cells. Representative images of CAG-1 fluorescent granule cells (green) and bright field (red). 3-month-old male tg/tg^{la} male hippocampus (A) and cerebellum (B).

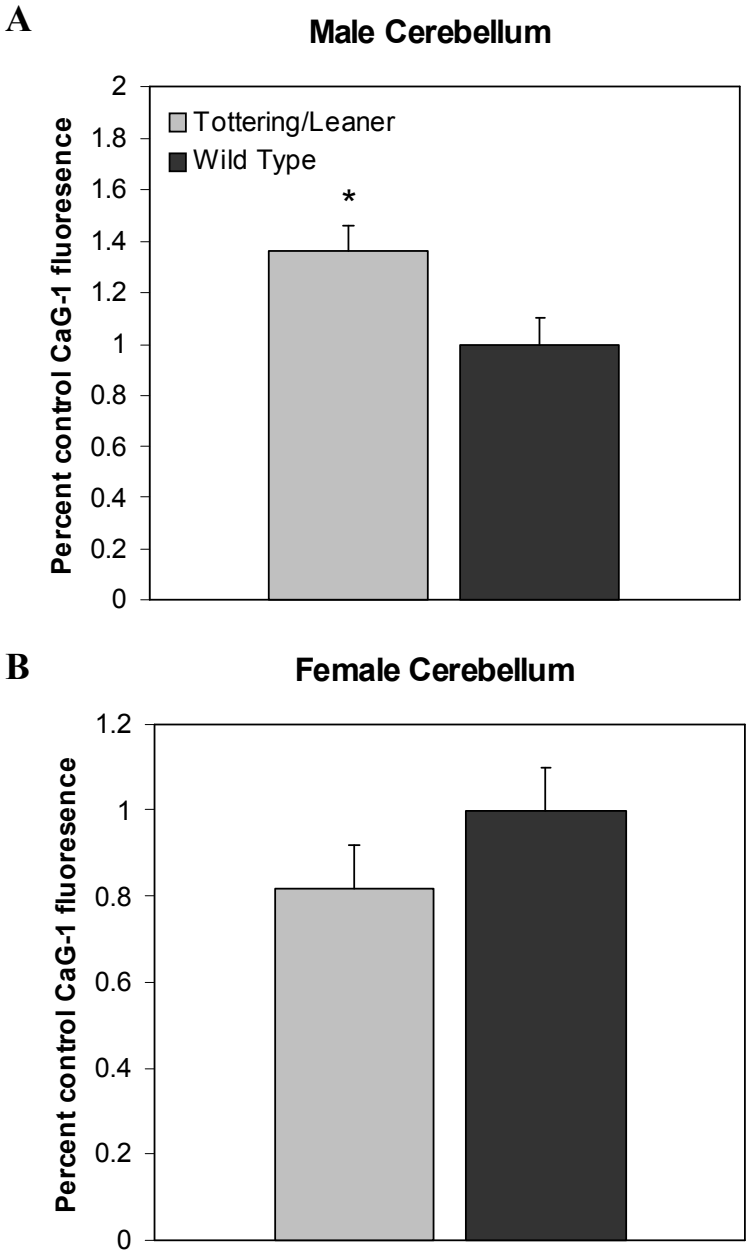

Figure 4.3 Graphs of CaG-1 percent control of fluorescence. Graphs comparing 3-month-old *tg/tg*^{la} and wild type animals percent control of CaG-1 fluorescent granule cells in the male and female cerebellum (A,B), male and female hippocampus (C,D) and as a comparison within the cerebellum and hippocampus of the female (E) and male (F) mutant mouse. (A) Indicates a significant increase of CaG-1 fluorescencein the *tg/tg*^{la} male cerebellar granule cells as compared to the wild type (P = 0.028). (B-E) No significant difference. (F) *tg/tg*^{la} male cerebellar CaG-1 fluorescencein significantly decreased as compared to the hippocampus (P = 0.001).

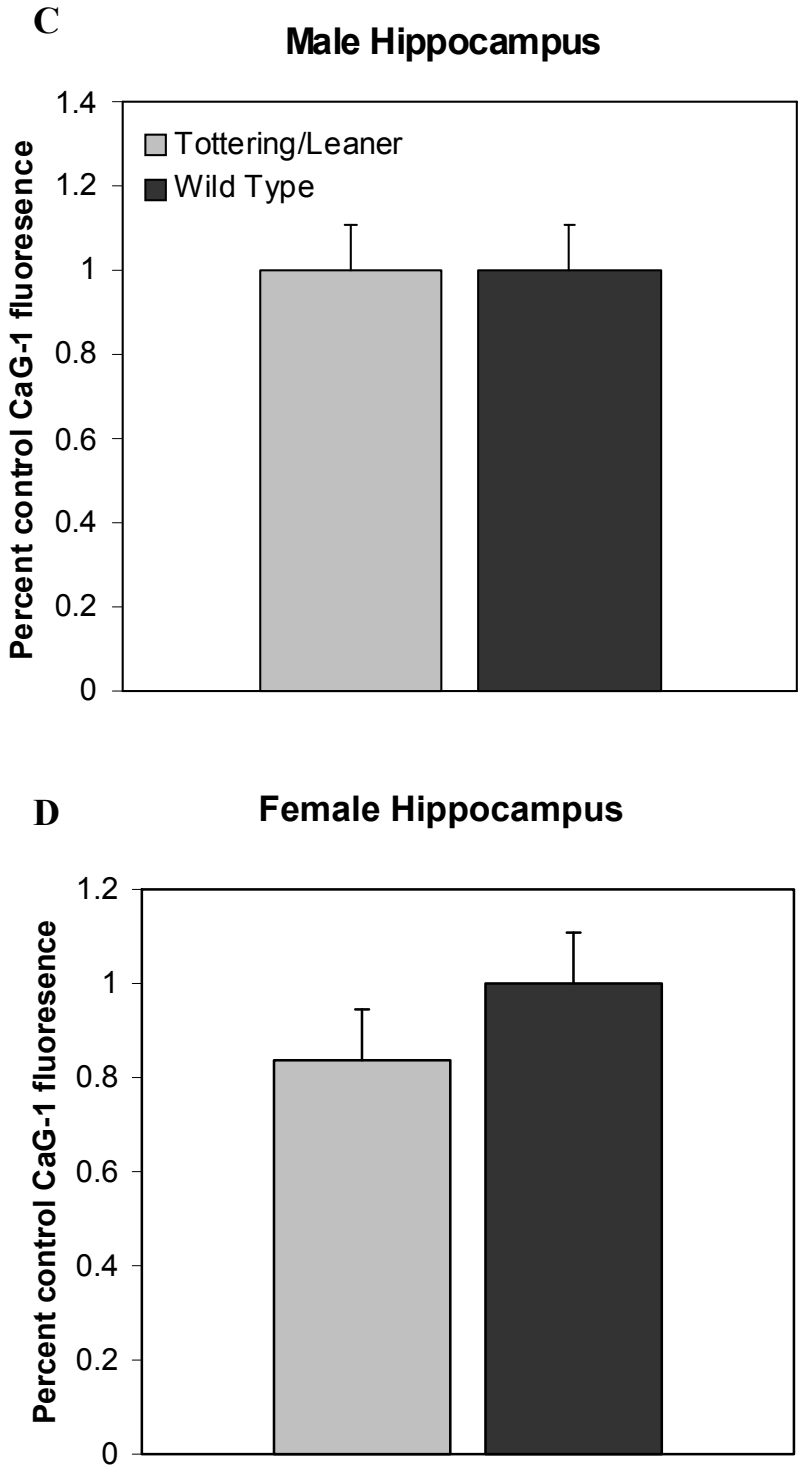

Figure 4.3 continued

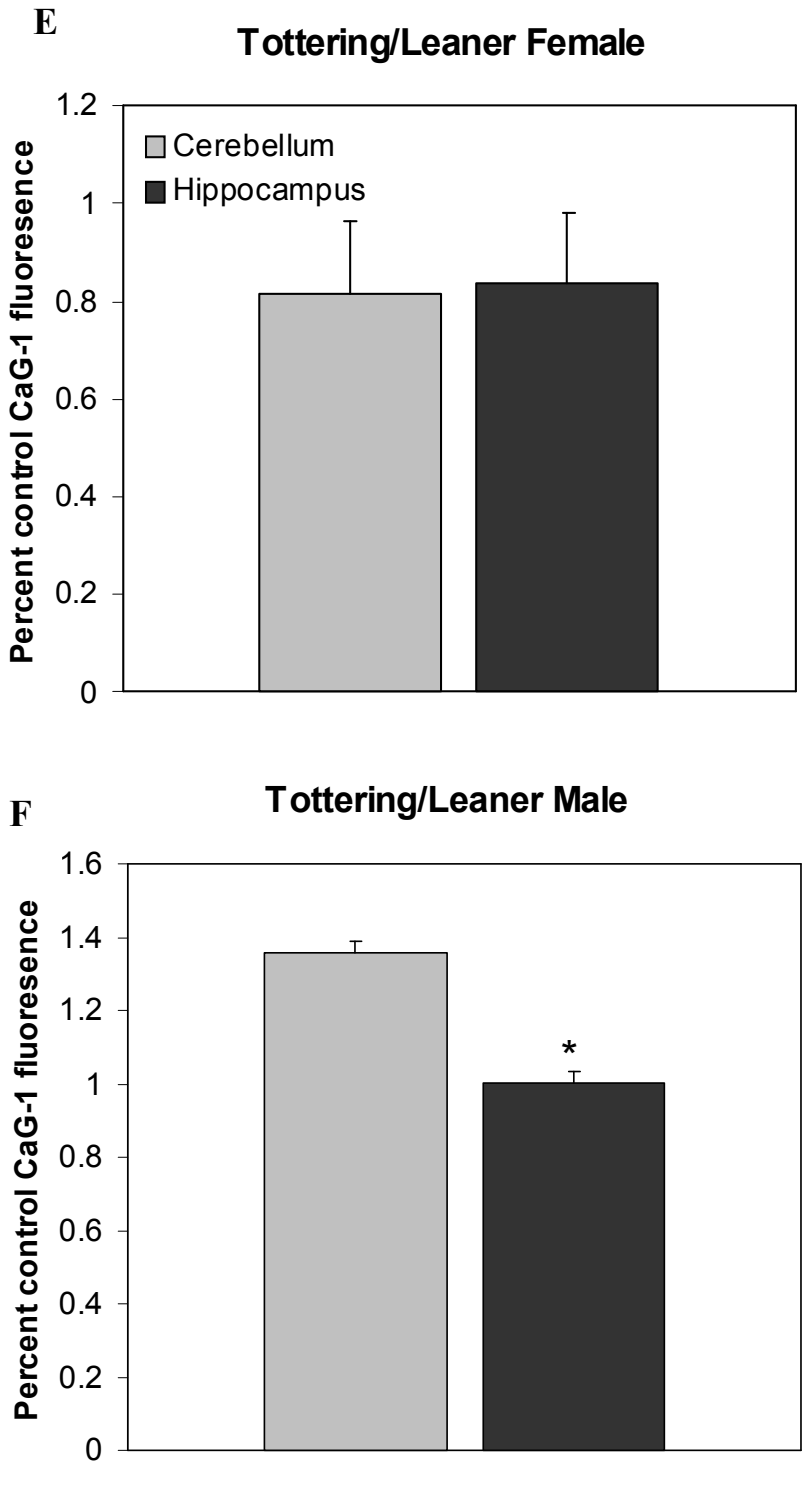

Figure 4.3 continued

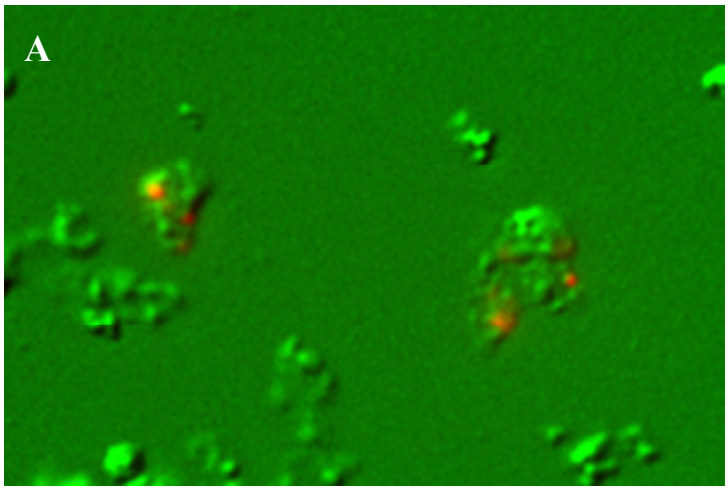

Figure 4.4 Image and graph of TMRM percent control fluorescence. Mitochondrial membrane potential (MMP) in isolated cerebellar granule cells in wild type and tg/tg^{la} mice. (A) Representative image of isolated 3-month-old male *tg/tg^{la}* isolated cerebellar granule cells, bright field (green) and TMRM fluorescence (red). Graphs depict of the percent control of TMRM fluorescence in the wild type and tg/tg^{la} mice with genders combined. B) Hippocampus C) Cerebellum. (A,B) No significant difference between genotypes.

B

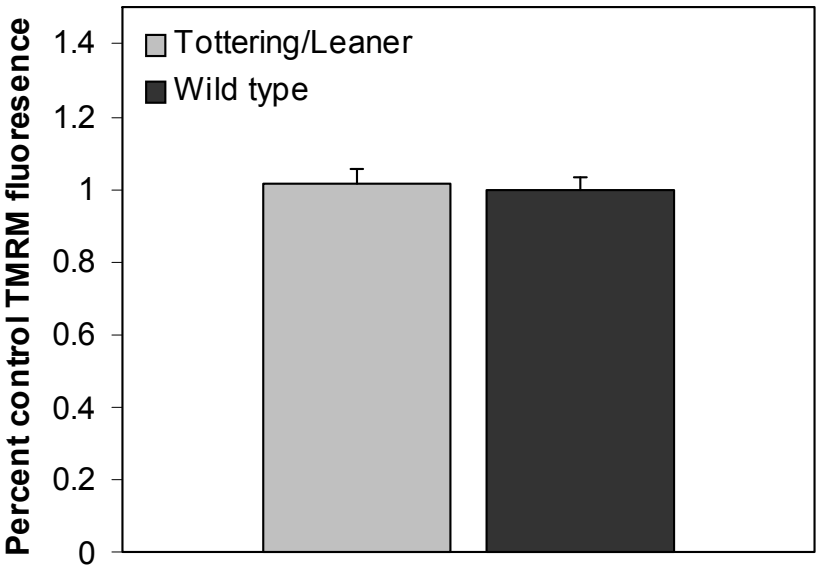

C

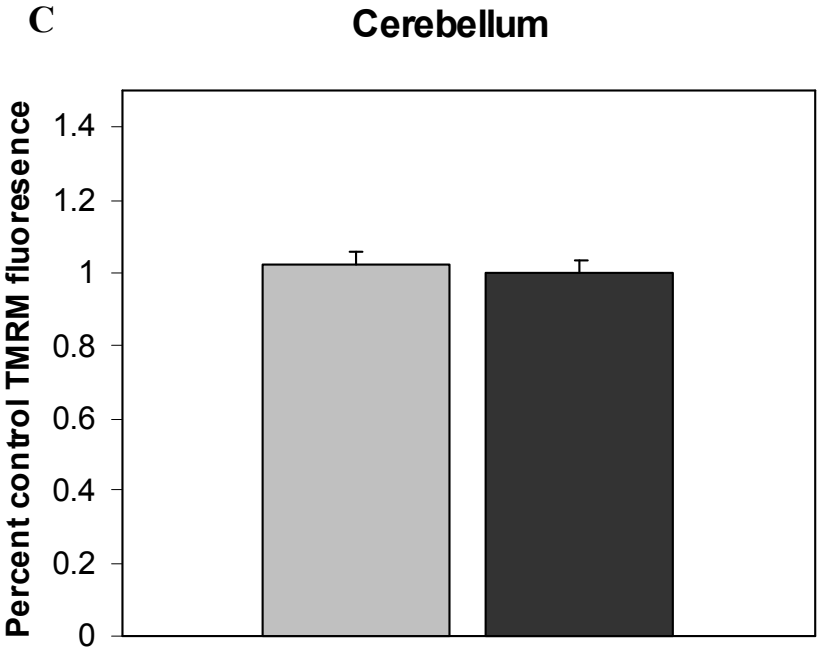

Figure 4.4 continued

Levels of Mitochondrial Memebrane Potential

It was important to investigate the level of mitochondrial functioning in the *tg*/*tg*^{la} mice as alterations in their functioning could be affected by the levels of calcium ions entering into the cells through P/Q type calcium ion channels. Variations in the mutant's MMP could be related to dysfunction in the cell's ability to maintain normal calcium ion levels and could send affected cells into a death cascade such as the apoptosis leaner cerebellar granule cells exhibit. However, both the *tg*/*tg*^{la} male and female mice did not show any evidence of unusual MMP in cerebellar or hippocampal granule cells (Figure 4.4).

Amount and rate of change in reactive oxygen species (ROS) production

The rate and amount of ROS production in the hippocampus remained normal relative to levels observed for wild type mice (Figure 4.5). When ROS production was artificially enhanced by exposure to 50μM TBHP, no variation remained between both genotypes.

The cerebellum revealed more intriguing results as its granule cells show a significant decrease in the amount of ROS produced ($P = 0.000$). The effect of addition of TB on the amount of ROS produced also revealed a ceiling in the *tg*/*tg*^{la} where the wild type animal continued to increase, but the mutant was significantly decreased and unable to reach normal levels despite a slight increase of its own ($P = .002$).

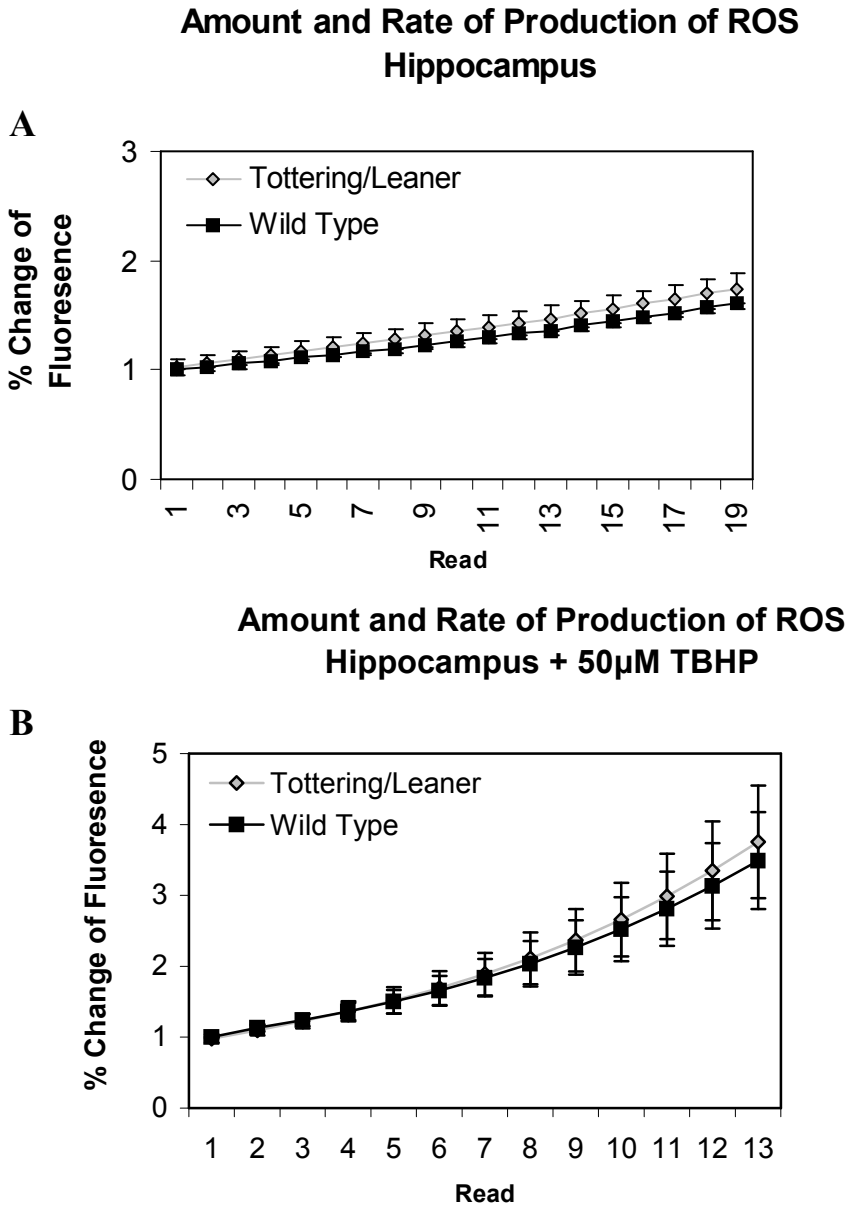

Figure 4.5 Graph of amount and rate of ROS production. The amount and rate of ROS production in the hippocampus (A) and cerebellum (C) of 3-month-old *tg/tg*^{la} and wild type animals. Amount of ROS and rate of ROS production with 50um TBHP in hippocampus (B) and cerebellum (D) of 3-month-old *tg/tg*^{la} and wild type animals. (A, B) No significant difference between genotypes. (C) Significant decrease in amount of ROS production in *tg/tg*^{la} mice as compared to wild type mice (p =.000), no significant difference in rate of ROS production. (D)) Significant decrease in amount of ROS production in *tg/tg*^{la} mice compared to wild type mice (p =.002), no significant difference in rate of ROS production.

C

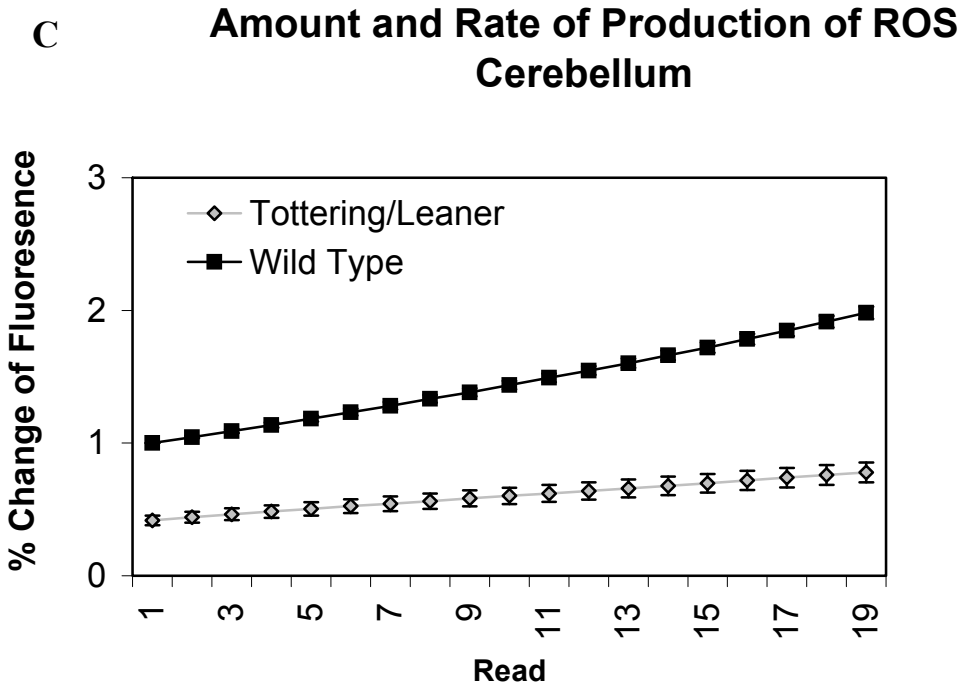

D

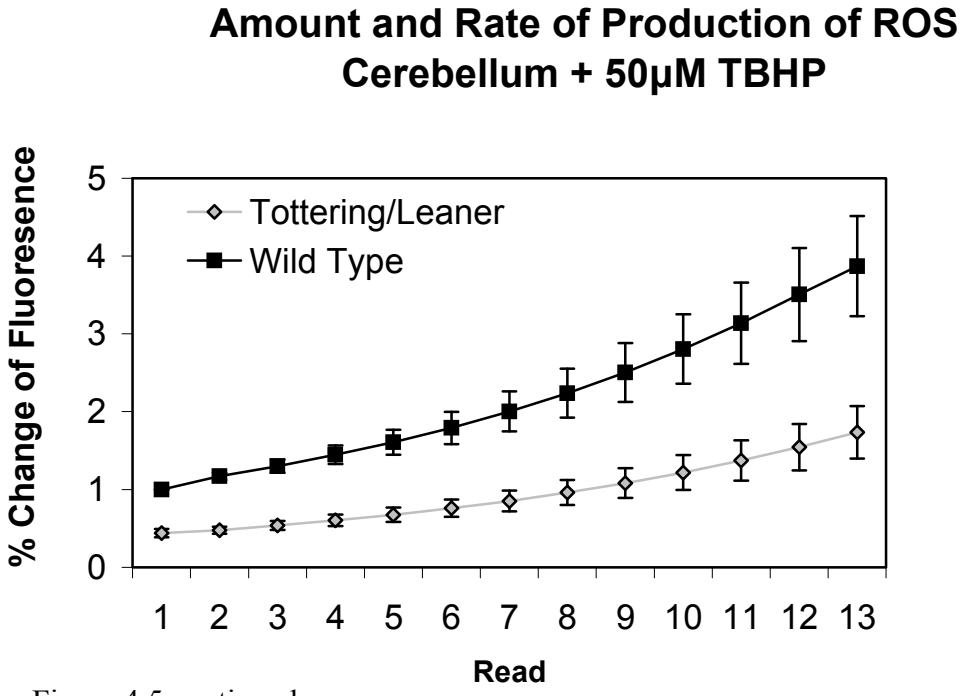

Figure 4.5 continued

DISCUSSION

The gender difference observed in basal intracellular calcium ion homeostasis could be the illustration of the *tg*/*tg*^{la} mouse having abnormal hormone activity as suggested by previous research in the Abbott lab (Serpedin, 2003). Female leaner mice spend a longer amount of time in estrous and nonestrous as compared to age matched wild type females as a result from abnormal hypothalamus activity (Serpedin, 2003). In addition, other reproductive abnormalities exist in the leaner mouse such as diminished reproductive success, along with an increase in plugs and implants as compensation (Serpedin, 2003). Lower amounts of estradiol in the leaner mouse also imply room for a larger gender discrepancy (Serpedin, 2003).

Despite high testosterone levels, estrogen deficiency in males plays a critical role especially in skeletal growth and maturation (Grumbach, 2000). It is possible that while estrogen is less implicated in the male, a decrease in estrogen could have prominent effects on the brain. In light of the alterarions in hormones of the female *tg*^{la}/*tg*^{la} mouse, male *tg*/*tg*^{la} mice may operate with estrogen levels so low that it may greatly affect what normal calcium levels cerebellar cells function at. Estradiol is known to play a significant role in cerebellar development (Gottfried-Blackmore et al., 2007), which could suggest that the *tg*/*tg*^{la} cerebellum is severely affected by hormonal aberrations even prior to the phenotypic onset of abnormalities.

Investigating basal intracellular calcium ion levels does not show the whole picture of calcium in granule cells as this method does not allow for computation of

calcium influx, calcium stores in the endoplasmic reticulum and intracellular stores or calcium binding proteins.

In contrast to the *tg*/*tg*^{la} results, both leaner and tottering mice displayed at least a 20% reduction in basal intracellular calcium ion homeostasis (Bawa and Abbott, 2008). This gives more support to the hypothesis that the *tg*/*tg*^{la} mutation is biologically very different than the homozygous *tg*/*tg* or *tg*^{la}/*tg*^{la} mice.

The decrease in ROS could be a direct result of the mutation or indirectly caused by adjustments in the cellular physiology due to coping with the mutation. A study of postnatal and juvenile animals could shed light on this matter with the absence or presence of altered ROS levels seen prior or during development of the mutant phenotype. It would be interesting to measure the levels of ROS prior to the phenotypic onset of this disorder.

Altered calcium homeostasis likely found in *tg*/*tg*^{la} mice because of the presence of altered calcium homeostasis in *tg*/*tg* and *tg*^{la}/*tg*^{la} mice. Despite no alteration in basal intracellular calcium levels and in mitochondrial membrane potential, the presumed deviation in calcium homeostasis most likely is related to decrease d ROS levels. Other calcium channel mutant mice exhibit abnormal calcium binding proteins, which in turn could lead to decreased ROS. There is not only diminished Ca^{2+} uptake by the endoplasmic reticulum in these mice, but reductions in mRNA levels of Ca^{2+} binding proteins (Dove et al., 2000). In addition, there is a noticeable decrease in the tottering cerebellar granule cell layer mRNA expression of calretinin, calcium binding protein,

which could be correlated with impaired calcium homeostasis and motor coordination (Cicale et al., 2002).

It is possible that the mitochondria, while functional, are not working at levels comparable to the wild type mouse and therefore produce less ROS byproduct. A decrease in amount of ROS could signify increased antioxidants such as scavengers or SODs. This explanation appears less probable as an increase in these antioxidants are linked to positive characteristics not found in these mice such as hippocamal long term potentiation, learning and memory (Hu et al., 2007; Klann, 1998; Levin et al., 1998).

ROS from the mitochondria may be produced in amounts normal to that of the wild type mouse mitochondria, but that the ROS deficits are coming from other areas of production such as the endoplasmic reticulum and nuclear membrane. In light of the ultrastuctural observations, the smooth endoplasmic reticulum is shown to exhibit crystalline-like array in Purkinje cell axons of the three mutant mice, tg^{la}/tg^{la}, *tg*/*tg*, and tg/tg^{la} (Rhyu et al., 1999). In addition, there is diminished Ca^{2+} uptake (Dove et al., 2000) and decrease in the mRNA expression of ryanodine receptor type 1 in the endoplasmic reticulum of granule cells and Purkinje cells, respectively, in the *tg*/*tg* mouse (Cicale et al., 2002).

	tottering	tottering/leaner	leaner
Cerebellum	Decreased volume & weight	Decreased volume & weight	----
Hippocampus	----	No change in volume	----
Cellular Proliferation in the SGZ of the DG	Decreased	No change	Decreased
Calcium Ion Homeostasis in CGC	Decreased	Female: no change Male: increase	Decreased
Mitochondrial Membrane Potential in CGC	No change	No change	Decreased
Amount of ROS	No change	Decrease in normal and TB induced conditions	No change
Rate of ROS Production	No change	No change	No change

Figure 4.6: Comparison of results from thesis experiments for *tg/tg*^{la} mouse as compared to known observations in *tg* and *tg*^{la} mice.

CHAPTER V

CONCLUSIONS

The *tg*/*tg*^{la} mouse is the least understood of the mice carrying mutations at the tottering locus. While somewhat neglected by previous research, this mouse appears to have potential to act as a new model for investigating the critical and delicate role of calcium in the hippocampus and cerebellum.

The studies presented in this thesis shed light on basic morphological and physiological abnormalities in the *tg*/*tg*^{la} mouse which often differ from known phenomena in the *tg*/*tg* and *tg*^{la}/*tg*^{la} mouse (Figure 4.6). While it could be expected that this mouse may mimic both or either of the heterozygous tottering or leaner mouse model, it remains quite unique.

Overall, the *tg*/*tg*^{la} hippocampus shows the least dysfunction. The only hippocampal difference discovered in this study lies in the increase in cellular density in the pyramidal layer of CA3 and the hilus of the dentate gyrus. It is possible that this increased density could highlight abnormal connectivity throughout the hippocampus resulting directly from the mutation or the mutation's effect on estrogen levels or due to the occurrence of epileptiform seizures that occur in these mice. While the cellular architecture and environment in this region show little variation, it suggests that functionality of the hippocampus should be investigated further.

The *tg*/*tg*^{la} cerebellum not only reveals a decrease in volume, but also altered basal intracellular calcium ion homeostasis in male *tg*/*tg*^{la} mice and greatly decreased

amounts of ROS production in *tg*/*tg*^{la} mice of both genders. This calcium channel mutation is able to greatly affect both architecture and physiology in the cerebellum. It could be hypothesized that the cerebellar abnormalities described in this thesis give rise to the *tg*/*tg*^{la} ataxic phenotype. The larger question remains as to whether some of these cerebellar abnormalities are compensations that have occurred in order to maintain life. Future research could investigate the cerebellum morphology at ages prior to the characteristic *tg*/*tg*^{la} phenotypic onset, whether there is any increased incidence of neuronal cell death within the cerebellum, modes of calcium storage and removal and functionality of synaptic connections.

REFERENCES

Abbott, L.C., Isaacs, K.R., Heckroth, J.A., 1996. Co-localization of tyrosine hydroxylase and zebrin II immunoreactivities in Purkinje cells of the mutant mice, tottering and tottering/leaner. Neuroscience. 71**,** 461-75.

Abbott, L.C., Sotelo, C., 2000. Ultrastructural analysis of catecholaminergic innervation in weaver and normal mouse cerebellar cortices. J Comp Neurol. 426**,** 316-29.

Ahmed, M.A., Reid, E., Cooke, A., Arngrimsson, R., Tolmie, J.L., Stephenson, J.B., 1996. Familial hemiplegic migraine in the west of Scotland: a clinical and genetic study of seven families. J Neurol Neurosurg Psychiatry. 61**,** 616-20.

Ahn, A.H., Dziennis, S., Hawkes, R., Herrup, K., 1994. The cloning of zebrin II reveals its identity with aldolase C. Development. 120**,** 2081-90.

Altman, J., 1963. Autoradiographic investigation of cell proliferation in the brains of rats and cats. Anat Rec. 145**,** 573-91.

Altman, J., Das, G.D., 1965a. Post-natal origin of microneurones in the rat brain. Nature. 207**,** 953-6.

Altman, J., Das, G.D., 1965b. Autoradiographic and histological evidence of postnatal hippocampal neurogenesis in rats. J Comp Neurol. 124**,** 319-35.

Altman, J., 1969. Autoradiographic and histological studies of postnatal neurogenesis. IV. Cell proliferation and migration in the anterior forebrain, with special reference to persisting neurogenesis in the olfactory bulb. J Comp Neurol. 137**,** 433-57.

Andreasen, N.C., Paradiso, S., O'Leary, D.S., 1998. "Cognitive dysmetria" as an integrative theory of schizophrenia: a dysfunction in cortical-subcortical-cerebellar circuitry? Schizophr Bull. 24**,** 203-18.

Andres, M., Andre, V.M., Nguyen, S., Salamon, N., Cepeda, C., Levine, M.S., Leite, J.P., Neder, L., Vinters, H.V., Mathern, G.W., 2005. Human cortical dysplasia and epilepsy: an ontogenetic hypothesis based on volumetric MRI and NeuN neuronal density and size measurements. Cereb Cortex. 15**,** 194-210.

Austin, M.C., Schultzberg, M., Abbott, L.C., Montpied, P., Evers, J.R., Paul, S.M., Crawley, J.N., 1992. Expression of tyrosine hydroxylase in cerebellar Purkinje neurons of the mutant tottering and leaner mouse. Brain Res Mol Brain Res. 15**,** 227-40.

Bastian, A.J., 2006. Learning to predict the future: the cerebellum adapts feedforward movement control. Curr Opin Neurobiol. 16**,** 645-9.

Battistini, S., Stenirri, S., Piatti, M., Gelfi, C., Righetti, P.G., Rocchi, R., Giannini, F., Battistini, N., Guazzi, G.C., Ferrari, M., Carrera, P., 1999. A new CACNA1A gene mutation in acetazolamide-responsive familial hemiplegic migraine and ataxia. Neurology. 53**,** 38-43.

Bawa, B., Abbott, L.C., 2008. Analysis of calcium ion homeostasis and mitochondrial function in cerebellar granule cells of adult CaV 2.1 calcium ion channel mutant mice. Neurotox Res. 13**,** 1-18.

Bean, B.P., 1989. Classes of calcium channels in vertebrate cells. Annu Rev Physiol. 51**,** 367-84.

Beutner, G., Sharma, V.K., Giovannucci, D.R., Yule, D.I., Sheu, S.S., 2001. Identification of a ryanodine receptor in rat heart mitochondria. J Biol Chem. 276**,** 21482-8.

Biebl, M., Cooper, C.M., Winkler, J., Kuhn, H.G., 2000. Analysis of neurogenesis and programmed cell death reveals a self-renewing capacity in the adult rat brain. Neurosci Lett. 291**,** 17-20.

Bignami, A., Eng, L.F., Dahl, D., Uyeda, C.T., 1972. Localization of the glial fibrillary acidic protein in astrocytes by immunofluorescence. Brain Res. 43**,** 429-35.

Bignami, A., Dahl, D., 1973. Differentiation of astrocytes in cerebellar cortex and pyramidal tracts of newborn rat - immunofluorescence study with antibodies to a protein specific to astrocytes. Brain Research. 49**,** 393-402.

Blau, J.N., Whitty, C.W., 1955. Familial hemiplegic migraine. Lancet. 269**,** 1115-6.

Bode, V.C., 1984. Ethylnitrosourea mutagenesis and the isolation of mutant alleles for specific genes located in the T region of mouse chromosome 17. Genetics. 108**,** 457-70.

Booth, J.R., Wood, L., Lu, D., Houk, J.C., Bitan, T., 2007. The role of the basal ganglia and cerebellum in language processing. Brain Res. 1133**,** 136-44.

Bothwell, S., Meredith, G.E., Phillips, J., Staunton, H., Doherty, C., Grigorenko, E., Glazier, S., Deadwyler, S.A., O'Donovan, C.A., Farrell, M., 2001. Neuronal hypertrophy in the neocortex of patients with temporal lobe epilepsy. J Neurosci. 21**,** 4789-800.

Bravo, R., Celis, J.E., 1980. A search for differential polypeptide synthesis throughout the cell cycle of HeLa cells. J Cell Biol. 84**,** 795-802.

Bravo, R., Macdonald-Bravo, H., 1987. Existence of two populations of cyclin/proliferating cell nuclear antigen during the cell cycle: association with DNA replication sites. J Cell Biol. 105**,** 1549-54.

Brochu, G., Maler, L., Hawkes, R., 1990. Zebrin II: a polypeptide antigen expressed selectively by Purkinje cells reveals compartments in rat and fish cerebellum. J Comp Neurol. 291**,** 538-52.

Brookes, P.S., Levonen, A.L., Shiva, S., Sarti, P., Darley-Usmar, V.M., 2002. Mitochondria: regulators of signal transduction by reactive oxygen and nitrogen species. Free Radic Biol Med. 33**,** 755-64.

Brown, J., Cooper-Kuhn, C.M., Kempermann, G., Van Praag, H., Winkler, J., Gage, F.H., Kuhn, H.G., 2003. Enriched environment and physical activity stimulate hippocampal but not olfactory bulb neurogenesis. Eur J Neurosci. 17**,** 2042-6.

Bruel-Jungerman, E., Rampon, C., Laroche, S., 2007. Adult hippocampal neurogenesis, synaptic plasticity and memory: facts and hypotheses. Rev Neurosci. 18**,** 93-114.

Calandriello, L., Veneziano, L., Francia, A., Sabbadini, G., Colonnese, C., Mantuano, E., Jodice, C., Trettel, F., Viviani, P., Manfredi, M., Frontali, M., 1997. Acetazolamide-responsive episodic ataxia in an Italian family refines gene mapping on chromosome 19. Brain. 120 (Pt 5)**,** 805-12.

Campbell, D.B., Hess, E.J., 1999. L-type calcium channels contribute to the tottering mouse dystonic episodes. Mol Pharmacol. 55**,** 23-31.

Carbone, E., Lux, H.D., 1984. A low voltage-activated, fully inactivating Ca channel in vertebrate sensory neurones. Nature. 310**,** 501-2.

Cheron, G., 1990. Effect of incisions in the brainstem commissural network on the short-term vestibulo-ocular adaptation of the cat. J Vestib Res. 1**,** 223-39.

Cicale, M., Ambesi-Impiombato, A., Cimini, V., Fiore, G., Muscettola, G., Abbott, L.C., de Bartolomeis, A., 2002. Decreased gene expression of calretinin and ryanodine receptor type 1 in tottering mice. Brain Res Bull. 59**,** 53-8.

Craig, K., Keers, S.M., Archibald, K., Curtis, A., Chinnery, P.F., 2004. Molecular epidemiology of spinocerebellar ataxia type 6. Ann Neurol. 55**,** 752-5.

Cross, C.E., Halliwell, B., Borish, E.T., Pryor, W.A., Ames, B.N., Saul, R.L., McCord, J.M., Harman, D., 1987. Oxygen radicals and human disease. Ann Intern Med. 107**,** 526-45.

De Jongh, K.S., Warner, C., Catterall, W.A., 1990. Subunits of purified calcium channels. Alpha 2 and delta are encoded by the same gene. J Biol Chem. 265**,** 14738-41.

Deluca, H.F., Engstrom, G.W., 1961. Calcium uptake by rat kidney mitochondria. Proc Natl Acad Sci USA. 47**,** 1744-50.

DeMaria, C.D., Soong, T.W., Alseikhan, B.A., Alvania, R.S., Yue, D.T., 2001. Calmodulin bifurcates the local Ca2+ signal that modulates P/Q-type Ca2+ channels. Nature. 411**,** 484-9.

Dobrossy, M.D., Drapeau, E., Aurousseau, C., Le Moal, M., Piazza, P.V., Abrous, D.N., 2003. Differential effects of learning on neurogenesis: learning increases or decreases the number of newly born cells depending on their birth date. Mol Psychiatry. 8**,** 974-82.

Dove, L.S., Abbott, L.C., Griffith, W.H., 1998. Whole-cell and single-channel analysis of P-type calcium currents in cerebellar Purkinje cells of leaner mutant mice. J Neurosci. 18**,** 7687-99.

Dove, L.S., Nahm, S.S., Murchison, D., Abbott, L.C., Griffith, W.H., 2000. Altered calcium homeostasis in cerebellar Purkinje cells of leaner mutant mice. J Neurophysiol. 84**,** 513-24.

Doyle, J., Ren, X., Lennon, G., Stubbs, L., 1997. Mutations in the Cacnl1a4 calcium channel gene are associated with seizures, cerebellar degeneration, and ataxia in tottering and leaner mutant mice. Mamm Genome. 8**,** 113-20.

Droge, W., 2002. Free radicals in the physiological control of cell function. Physiol Rev. 82**,** 47-95.

Ducros, A., 2000. Genetics of migraine. Pathol Biol (Paris). 48**,** 658-62.

Dupret, D., Revest, J.M., Koehl, M., Ichas, F., De Giorgi, F., Costet, P., Abrous, D.N., Piazza, P.V., 2008. Spatial relational memory requires hippocampal adult neurogenesis. PLoS ONE. 3**,** e1959.

Eccles, J.C., Llinas, R., Sasaki, K., 1966. The excitatory synaptic action of climbing fibres on the purinje cells of the cerebellum. J Physiol. 182**,** 268-96.

Ekerot, C.F., Kano, M., 1985. Long-term depression of parallel fibre synapses following stimulation of climbing fibres. Brain Res. 342**,** 357-60.

Elliott, M.A., Peroutka, S.J., Welch, S., May, E.F., 1996. Familial hemiplegic migraine, nystagmus, and cerebellar atrophy. Ann Neurol. 39**,** 100-6.

Ellis, S.B., Williams, M.E., Ways, N.R., Brenner, R., Sharp, A.H., Leung, A.T., Campbell, K.P., McKenna, E., Koch, W.J., Hui, A., et al., 1988. Sequence and expression of mRNAs encoding the alpha 1 and alpha 2 subunits of a DHP-sensitive calcium channel. Science. 241**,** 1661-4.

Encinas, J.M., Vaahtokari, A., Enikolopov, G., 2006. Fluoxetine targets early progenitor cells in the adult brain. Proc Natl Acad Sci U S A. 103**,** 8233-8.

Encinas, J.M., Enikolopov, G., 2008. Identifying and quantitating neural stem and progenitor cells in the adult brain. Methods Cell Biol. 85**,** 243-72.

Erickson, M.A., Haburcak, M., Smukler, L., Dunlap, K., 2007. Altered functional expression of Purkinje cell calcium channels precedes motor dysfunction in tottering mice. Neuroscience. 150**,** 547-55.

Etheredge, J.A., Murchison, D., Abbott, L.C., Griffith, W.H., 2007. Functional compensation by other voltage-gated Ca2+ channels in mouse basal forebrain neurons with Ca(V)2.1 mutations. Brain Res. 1140**,** 105-19.

Fedulova, S.A., Kostyuk, P.G., Veselovsky, N.S., 1985. Two types of calcium channels in the somatic membrane of new-born rat dorsal root ganglion neurones. J Physiol. 359**,** 431-46.

Fletcher, C.F., Lutz, C.M., O'Sullivan, T.N., Shaughnessy, J.D., Jr., Hawkes, R., Frankel, W.N., Copeland, N.G., Jenkins, N.A., 1996. Absence epilepsy in tottering mutant mice is associated with calcium channel defects. Cell. 87**,** 607-17.

Frank, T.C., Nunley, M.C., Sons, H.D., Ramon, R., Abbott, L.C., 2003. Fluoro-jade identification of cerebellar granule cell and purkinje cell death in the alpha1A calcium ion channel mutant mouse, leaner. Neuroscience. 118**,** 667-80.

Frontali, M., 2001. Spinocerebellar ataxia type 6: channelopathy or glutamine repeat disorder? Brain Res Bull. 56**,** 227-31.

Gao, J.H., Parsons, L.M., Bower, J.M., Xiong, J., Li, J., Fox, P.T., 1996. Cerebellum implicated in sensory acquisition and discrimination rather than motor control. Science. 272**,** 545-7.

Gazulla, J., Benavente, I., 2007. Single-blind, placebo-controlled pilot study of pregabalin for ataxia in cortical cerebellar atrophy. Acta Neurol Scand. 116**,** 235-8.

Gazulla, J., Tintore, M., 2007. The P/Q-type voltage-dependent calcium channel: a therapeutic target in spinocerebellar ataxia type 6. Acta Neurol Scand. 115**,** 356-63.

Geschwind, D.H., Perlman, S., Figueroa, K.P., Karrim, J., Baloh, R.W., Pulst, S.M., 1997. Spinocerebellar ataxia type 6. Frequency of the mutation and genotype-phenotype correlations. Neurology. 49**,** 1247-51.

Gordon, N., 2007. The cerebellum and cognition. Eur J Paediatr Neurol. 11**,** 232-4.

Gottfried-Blackmore, A., Croft, G., Clark, J., McEwen, B.S., Jellinck, P.H., Bulloch, K., 2007. Characterization of a cerebellar granule progenitor cell line, EtC.1, and its responsiveness to 17-[beta]-estradiol. Brain Research. 1186**,** 29-40.

Gould, E., Beylin, A., Tanapat, P., Reeves, A., Shors, T.J., 1999. Learning enhances adult neurogenesis in the hippocampal formation. Nat Neurosci. 2**,** 260-5.

Gratzner, H.G., 1982. Monoclonal antibody to 5-bromo- and 5-iododeoxyuridine: a new reagent for detection of DNA replication. Science. 218**,** 474-5.

Green, M.C., Sidman, R.L., 1962. Tottering--a neuromusclar mutation in the mouse. And its linkage with oligosyndacylism. J Hered. 53**,** 233-7.

Grumbach, M.M., 2000. The role of estrogen in the male and female: evidence from mutations in synthesis and action. Horm Res. 53 Suppl 3**,** 23-4.

Gurnett, C.A., De Waard, M., Campbell, K.P., 1996. Dual function of the voltage-dependent Ca2+ channel alpha 2 delta subunit in current stimulation and subunit interaction. Neuron. 16**,** 431-40.

Halliwell, B., Gutteridge, J.M., Cross, C.E., 1992. Free radicals, antioxidants, and human disease: where are we now? J Lab Clin Med. 119**,** 598-620.

Harvey, R.J., Napper, R.M., 1991. Quantitative studies on the mammalian cerebellum. Prog Neurobiol. 36**,** 437-63.

Hawkes, R., Eisenman, L.M., 1997. Stripes and zones: the origins of regionalization of the adult cerebellum. Perspect Dev Neurobiol. 5**,** 95-105.

Heckroth, J.A., Abbott, L.C., 1994. Purkinje cell loss from alternating sagittal zones in the cerebellum of leaner mutant mice. Brain Res. 658**,** 93-104.

Helekar, S.A., Noebels, J.L., 1991. Synchronous hippocampal bursting reveals network excitability defects in an epilepsy gene mutation. Proc Natl Acad Sci USA. 88**,** 4736-40.

Helekar, S.A., Noebels, J.L., 1992. A burst-dependent hippocampal excitability defect elicited by potassium at the developmental onset of spike-wave seizures in the tottering mutant. Brain Res Dev Brain Res. 65**,** 205-10.

Herrup, K., Wilczynski, S.L., 1982. Cerebellar cell degeneration in the leaner mutant mouse. Neuroscience. 7**,** 2185-96.

Hess, E.J., Wilson, M.C., 1991. Tottering and leaner mutations perturb transient developmental expression of tyrosine hydroxylase in embryologically distinct Purkinje cells. Neuron. 6**,** 123-32.

Hess, P., 1990. Calcium channels in vertebrate cells. Annu Rev Neurosci. 13**,** 337-56.

Hillyard, D.R., Monje, V.D., Mintz, I.M., Bean, B.P., Nadasdi, L., Ramachandran, J., Miljanich, G., Azimi-Zoonooz, A., McIntosh, J.M., Cruz, L.J., et al., 1992. A new Conus peptide ligand for mammalian presynaptic Ca2+ channels. Neuron. 9**,** 69-77.

Hoebeek, F.E., Khosrovani, S., Witter, L., De Zeeuw, C.I., 2008. Purkinje cell input to cerebellar nuclei in tottering: ultrastructure and physiology. Cerebellum. 7**,** 547-58.

Hofmann, F., Biel, M., Flockerzi, V., 1994. Molecular basis for Ca2+ channel diversity. Annu Rev Neurosci. 17**,** 399-418.

Hu, D., Cao, P., Thiels, E., Chu, C.T., Wu, G.Y., Oury, T.D., Klann, E., 2007. Hippocampal long-term potentiation, memory, and longevity in mice that overexpress mitochondrial superoxide dismutase. Neurobiol Learn Mem. 87**,** 372-84.

Huang, P., Wills, S., Gomez, F.P, Thuett K.A., Ghandi, D., Abbott, L.C., 2007. Changes in hippocampal volume in calcium ion channel mutant mice, tottering and leaner, as compared to age-matched wild type mice. In: Neuroscience Meeting Planner., Society for Neuroscience, San Diego, CA.

Isaacs, K.R., Abbott, L.C., 1995. Cerebellar volume decreases in the tottering mouse are specific to the molecular layer. Brain Res Bull. 36**,** 309-14.

Ito, M., Kano, M., 1982. Long-lasting depression of parallel fiber-Purkinje cell transmission induced by conjunctive stimulation of parallel fibers and climbing fibers in the cerebellar cortex. Neurosci Lett. 33**,** 253-8.

Ito, M., Sakurai, M., Tongroach, P., 1982. Climbing fibre induced depression of both mossy fibre responsiveness and glutamate sensitivity of cerebellar Purkinje cells. J Physiol. 324**,** 113-34.

Jaarsma, D., Ruigrok, T.J., Caffe, R., Cozzari, C., Levey, A.I., Mugnaini, E., Voogd, J., 1997. Cholinergic innervation and receptors in the cerebellum. Prog Brain Res. 114**,** 67-96.

Jay, S.D., Ellis, S.B., McCue, A.F., Williams, M.E., Vedvick, T.S., Harpold, M.M., Campbell, K.P., 1990. Primary structure of the gamma subunit of the DHP-sensitive calcium channel from skeletal muscle. Science. 248**,** 490-2.

Jay, S.D., Sharp, A.H., Kahl, S.D., Vedvick, T.S., Harpold, M.M., Campbell, K.P., 1991. Structural characterization of the dihydropyridine-sensitive calcium channel alpha 2-subunit and the associated delta peptides. J Biol Chem. 266**,** 3287-93.

Jodice, C., Mantuano, E., Veneziano, L., Trettel, F., Sabbadini, G., Calandriello, L., Francia, A., Spadaro, M., Pierelli, F., Salvi, F., Ophoff, R.A., Frants, R.R., Frontali, M., 1997. Episodic ataxia type 2 (EA2) and spinocerebellar ataxia type 6 (SCA6) due to CAG repeat expansion in the CACNA1A gene on chromosome 19p. Hum Mol Genet. 6**,** 1973-8.

Joutel, A., Bousser, M.G., Biousse, V., Labauge, P., Chabriat, H., Nibbio, A., Maciazek, J., Meyer, B., Bach, M.A., Weissenbach, J., et al., 1993. A gene for familial hemiplegic migraine maps to chromosome 19. Nat Genet. 5**,** 40-5.

Kato, M., Hosokawa, S., Tobimatsu, S., Kuroiwa, Y., 1982. Increased local cerebral glucose utilization in the basal ganglia of the rolling mouse Nagoya. J Cereb Blood Flow Metab. 2**,** 385-93.

Kaube, H., Herzog, J., Kaufer, T., Dichgans, M., Diener, H.C., 2000. Aura in some patients with familial hemiplegic migraine can be stopped by intranasal ketamine. Neurology. 55**,** 139-41.

Kempermann, G., Kuhn, H.G., Gage, F.H., 1997. More hippocampal neurons in adult mice living in an enriched environment. Nature. 386**,** 493-5.

Kempermann, G., 2005. Adult Neurogenesis: Stem Cells and Neuronal Development in the Adult Brain., Oxford University Press, New York.

Kinoshita, K., Watanabe, Y., Asai, H., Yamamura, M., Matsuoka, Y., 1995. Anti-ataxic effects of TRH and its analogue, TA-0910, in Rolling mouse Nagoya by metabolic normalization of the ventral tegmental area. Br J Pharmacol. 116**,** 3274-8.

Kinoshita, K., Yamamura, M., Sugihara, J., 1997. Distribution of thyrotropin-releasing hormone (TRH) receptors in the brain of the ataxic mutant mouse, rolling mouse Nagoya. Biol Pharm Bull. 20**,** 86-7.

Kirichok, Y., Krapivinsky, G., Clapham, D.E., 2004. The mitochondrial calcium uniporter is a highly selective ion channel. Nature. 427**,** 360-4.

Klann, E., 1998. Cell-permeable scavengers of superoxide prevent long-term potentiation in hippocampal area CA1. J Neurophysiol. 80**,** 452-7.

Kodama, T., Itsukaichi-Nishida, Y., Fukazawa, Y., Wakamori, M., Miyata, M., Molnar, E., Mori, Y., Shigemoto, R., Imoto, K., 2006. A CaV2.1 calcium channel mutation rocker reduces the number of postsynaptic AMPA receptors in parallel fiber-Purkinje cell synapses. Eur J Neurosci. 24**,** 2993-3007.

Kramer, P.L., Yue, Q., Gancher, S.T., Nutt, J.G., Baloh, R., Smith, E., Browne, D., Bussey, K., Lovrien, E., Nelson, S., et al., 1995. A locus for the nystagmus-associated form of episodic ataxia maps to an 11-cM region on chromosome 19p. Am J Hum Genet. 57**,** 182-5.

Kroemer, G., Zamzami, N., Susin, S.A., 1997. Mitochondrial control of apoptosis. Immunol Today. 18**,** 44-51.

Kroemer, G., 1999. Mitochondrial control of apoptosis: an overview. Biochem Soc Symp. 66**,** 1-15.

Laine, J., Axelrad, H., 1994. The candelabrum cell: a new interneuron in the cerebellar cortex. J Comp Neurol. 339**,** 159-73.

Larsell, O., 1970. The Comparative Anatomy and Histology of the Cerebellum from Monotremes through Apes, Vol. 3, Univ. Minnesota Press, Minneapolis, MN.

Lau, F.C., Abbott, L.C., Rhyu, I.J., Kim, D.S., Chin, H., 1998. Expression of calcium channel alpha1A mRNA and protein in the leaner mouse (tgla/tgla) cerebellum. Brain Res Mol Brain Res. 59**,** 93-9.

Lau, F.C., Frank, T.C., Nahm, S.S., Stoica, G., Abbott, L.C., 2004. Postnatal apoptosis in cerebellar granule cells of homozygous leaner (tg1a/tg1a) mice. Neurotox Res. 6**,** 267-80.

Lee, A., Westenbroek, R.E., Haeseleer, F., Palczewski, K., Scheuer, T., Catterall, W.A., 2002. Differential modulation of Ca(v)2.1 channels by calmodulin and Ca2+-binding protein 1. Nat Neurosci. 5**,** 210-7.

Lee, A., Zhou, H., Scheuer, T., Catterall, W.A., 2003. Molecular determinants of Ca(2+)/calmodulin-dependent regulation of Ca(v)2.1 channels. Proc Natl Acad Sci USA. 100**,** 16059-64.

Lehninger, A.L., 1970. Biochemistry, Vol. 2, Worth Publishers Inc, New York.

Lemaire, V., Koehl, M., Le Moal, M., Abrous, D.N., 2000. Prenatal stress produces learning deficits associated with an inhibition of neurogenesis in the hippocampus. Proc Natl Acad Sci USA. 97**,** 11032-7.

Leuner, B., Kozorovitskiy, Y., Gross, C.G., Gould, E., 2007. Diminished adult neurogenesis in the marmoset brain precedes old age. Proc Natl Acad Sci USA. 104**,** 17169-73.

Levin, E.D., Brady, T.C., Hochrein, E.C., Oury, T.D., Jonsson, L.M., Marklund, S.L., Crapo, J.D., 1998. Molecular manipulations of extracellular superoxide dismutase: functional importance for learning. Behav Genet. 28**,** 381-90.

Lin, S.C., Huck, J.H., Roberts, J.D., Macklin, W.B., Somogyi, P., Bergles, D.E., 2005. Climbing fiber innervation of NG2-expressing glia in the mammalian cerebellum. Neuron. 46**,** 773-85.

Llinas, R., Sugimori, M., Hillman, D.E., Cherksey, B., 1992. Distribution and functional significance of the P-type, voltage-dependent Ca2+ channels in the mammalian central nervous system. Trends Neurosci. 15**,** 351-5.

Llinas, R.R., Sugimori, M., Cherksey, B., 1989. Voltage-dependent calcium conductances in mammalian neurons. The P channel. Ann NY Acad Sci. 560**,** 103-11.

Lorenzon, N.M., Lutz, C.M., Frankel, W.N., Beam, K.G., 1998. Altered calcium channel currents in Purkinje cells of the neurological mutant mouse leaner. J Neurosci. 18**,** 4482-9.

Mandyam, C.D., Harburg, G.C., Eisch, A.J., 2007. Determination of key aspects of precursor cell proliferation, cell cycle length and kinetics in the adult mouse subgranular zone. Neuroscience. 146**,** 108-22.

Markakis, E.A., Gage, F.H., 1999. Adult-generated neurons in the dentate gyrus send axonal projections to field CA3 and are surrounded by synaptic vesicles. J Comp Neurol. 406**,** 449-60.

McCleskey, E.W., Fox, A.P., Feldman, D.H., Cruz, L.J., Olivera, B.M., Tsien, R.W., Yoshikami, D., 1987. Omega-conotoxin: direct and persistent blockade of specific types of calcium channels in neurons but not muscle. Proc Natl Acad Sci USA. 84**,** 4327-31.

McCormick, D.A., 1989. Cholinergic and noradrenergic modulation of thalamocortical processing. Trends Neurosci. 12**,** 215-21.

McDonough, S.I., Mintz, I.M., Bean, B.P., 1997. Alteration of P-type calcium channel gating by the spider toxin omega-Aga-IVA. Biophys J. 72**,** 2117-28.

Melov, S., 2000. Mitochondrial oxidative stress. Physiologic consequences and potential for a role in aging. Ann NY Acad Sci. 908**,** 219-25.

Miles, F.A., Lisberger, S.G., 1981. Plasticity in the vestibulo-ocular reflex: a new hypothesis. Annu Rev Neurosci. 4**,** 273-99.

Miller, M.W., Nowakowski, R.S., 1988. Use of bromodeoxyuridine-immunohistochemistry to examine the proliferation, migration and time of origin of cells in the central nervous system. Brain Res. 457**,** 44-52.

Miller, M.W., Nowakowski, R.S., 1991. Effect of prenatal exposure to ethanol on the cell cycle kinetics and growth fraction in the proliferative zones of fetal rat cerebral cortex. Alcohol Clin Exp Res. 15**,** 229-32.

Mintz, I.M., Venema, V.J., Swiderek, K.M., Lee, T.D., Bean, B.P., Adams, M.E., 1992. P-type calcium channels blocked by the spider toxin omega-Aga-IVA. Nature. 355**,** 827-9.

Mintz, I.M., Sabatini, B.L., Regehr, W.G., 1995. Calcium control of transmitter release at a cerebellar synapse. Neuron. 15**,** 675-88.

Mori, Y., Friedrich, T., Kim, M.S., Mikami, A., Nakai, J., Ruth, P., Bosse, E., Hofmann, F., Flockerzi, V., Furuichi, T., et al., 1991. Primary structure and functional expression from complementary DNA of a brain calcium channel. Nature. 350**,** 398-402.

Mugnaini, E., Dino, M.R., Jaarsma, D., 1997. The unipolar brush cells of the mammalian cerebellum and cochlear nucleus: cytology and microcircuitry. Prog Brain Res. 114**,** 131-50.

Mullen, R.J., Buck, C.R., Smith, A.M., 1992. NeuN, a neuronal specific nuclear protein in vertebrates. Development. 116**,** 201-11.

Muramoto, O., Kanazawa, I., Ando, K., 1981. Neurotransmitter abnormality in Rolling mouse Nagoya, an ataxic mutant mouse. Brain Res. 215**,** 295-304.

Nahm, S.S., Tomlinson, D.J., Abbott, L.C., 2002. Decreased calretinin expression in cerebellar granule cells in the leaner mouse. J Neurobiol. 51**,** 313-22.

Nahm, S.S., Frank, T.C., Browning, M.D., Sepulvado, J.M., Hiney, J.K., Abbott, L.C., 2003. Insulin-like growth factor-I improves cerebellar dysfunction but does not prevent cerebellar neurodegeneration in the calcium channel mutant mouse, leaner. Neurobiol Dis. 14**,** 157-65.

Nicholls, D.G., Ward, M.W., 2000. Mitochondrial membrane potential and neuronal glutamate excitotoxicity: mortality and millivolts. Trends Neurosci. 23**,** 166-74.

Nishimura, Y., 1975. The cerebellum of rolling mice, Nagoya (Japanese). Adv. Neurol. Sci. 19**,** 670-672.

Noebels, J.L., Sidman, R.L., 1979. Inherited epilepsy: spike-wave and focal motor seizures in the mutant mouse tottering. Science. 204**,** 1334-6.

Nowakowski, R.S., Lewin, S.B., Miller, M.W., 1989. Bromodeoxyuridine immunohistochemical determination of the lengths of the cell cycle and the DNA-synthetic phase for an anatomically defined population. J Neurocytol. 18**,** 311-8.

Nowycky, M.C., Fox, A.P., Tsien, R.W., 1985. Three types of neuronal calcium channel with different calcium agonist sensitivity. Nature. 316**,** 440-3.

Nunzi, M.G., Grillo, M., Margolis, F.L., Mugnaini, E., 1999. Compartmental organization of Purkinje cells in the mature and developing mouse cerebellum as revealed by an olfactory marker protein-lacZ transgene. J Comp Neurol. 404**,** 97-113.

Oda, S., 1981. A new allele of the tottering locus, rolling mouse Nagoya, on chromosome No.8 in the mouse. Jpn J Genet. 56**,** 295-299.

Ophoff, R.A., Terwindt, G.M., Vergouwe, M.N., van Eijk, R., Oefner, P.J., Hoffman, S.M., Lamerdin, J.E., Mohrenweiser, H.W., Bulman, D.E., Ferrari, M., Haan, J., Lindhout, D., van Ommen, G.J., Hofker, M.H., Ferrari, M.D., Frants, R.R., 1996.

Familial hemiplegic migraine and episodic ataxia type-2 are caused by mutations in the Ca2+ channel gene CACNL1A4. Cell. 87**,** 543-52.

Ozol, K., Hayden, J.M., Oberdick, J., Hawkes, R., 1999. Transverse zones in the vermis of the mouse cerebellum. J Comp Neurol. 412**,** 95-111.

Patestas, M.A., Gartner, L.P, 2006. A Textbook of Neuroanatomy, Vol. 5, Blackwell Publishing, Malden, MA.

Piedras-Renteria, E.S., Watase, K., Harata, N., Zhuchenko, O., Zoghbi, H.Y., Lee, C.C., Tsien, R.W., 2001. Increased expression of alpha 1A Ca2+ channel currents arising from expanded trinucleotide repeats in spinocerebellar ataxia type 6. J Neurosci. 21**,** 9185-93.

Puskin, J.S., Gunter, T.E., Gunter, K.K., Russell, P.R., 1976. Evidence for more than one Ca2+ transport mechanism in mitochondria. Biochemistry. 15**,** 3834-42.

Qian, J., Noebels, J.L., 2000. Presynaptic Ca(2+) influx at a mouse central synapse with Ca(2+) channel subunit mutations. J Neurosci. 20**,** 163-70.

Randall, A., Tsien, R.W., 1995. Pharmacological dissection of multiple types of Ca2+ channel currents in rat cerebellar granule neurons. J Neurosci. 15**,** 2995-3012.

Rao, M.S., Shetty, A.K., 2004. Efficacy of doublecortin as a marker to analyse the absolute number and dendritic growth of newly generated neurons in the adult dentate gyrus. Eur J Neurosci. 19**,** 234-46.

Rasband, W.S., 1997-2008. ImageJ. Bethesda, MD: US National Institute of Health.

Raspotnig, G., Fauler, G., Jantscher, A., Windischhofer, W., Schachl, K., Leis, H.J., 1999. Colorimetric determination of cell numbers by Janus green staining. Anal Biochem. 275**,** 74-83.

Raymond, J.L., Lisberger, S.G., Mauk, M.D., 1996. The cerebellum: a neuronal learning machine? Science. 272**,** 1126-31.

Regan, L.J., 1991. Voltage-dependent calcium currents in Purkinje cells from rat cerebellar vermis. J Neurosci. 11**,** 2259-69.

Rhyu, I.J., Abbott, L.C., Walker, D.B., Sotelo, C., 1999. An ultrastructural study of granule cell/Purkinje cell synapses in tottering (tg/tg), leaner (tg(la)/tg(la)) and compound heterozygous tottering/leaner (tg/tg(la)) mice. Neuroscience. 90**,** 717-28.

Rhyu, I.J., Nahm, S.S., Hwang, S.J., Kim, H., Suh, Y.S., Oda, S.I., Frank, T.C., Abbott, L.C., 2003. Altered neuronal nitric oxide synthase expression in the cerebellum of calcium channel mutant mice. Brain Res. 977**,** 129-40.

Ruth, P., Rohrkasten, A., Biel, M., Bosse, E., Regulla, S., Meyer, H.E., Flockerzi, V., Hofmann, F., 1989. Primary structure of the beta subunit of the DHP-sensitive calcium channel from skeletal muscle. Science. 245**,** 1115-8.

Sarna, J.R., Hawkes, R., 2003. Patterned Purkinje cell death in the cerebellum. Prog Neurobiol. 70**,** 473-507.

Sather, W.A., Tanabe, T., Zhang, J.F., Mori, Y., Adams, M.E., Tsien, R.W., 1993. Distinctive biophysical and pharmacological properties of class A (BI) calcium channel alpha 1 subunits. Neuron. 11**,** 291-303.

Sawada, K., Sakata-Haga, H., Hisano, S., Fukui, Y., 2001. Topological relationship between corticotropin-releasing factor-immunoreactive cerebellar afferents and

tyrosine hydroxylase-immunoreactive Purkinje cells in a hereditary ataxic mutant, rolling mouse Nagoya. Neuroscience. 102**,** 925-35.

Sawada, K., Hosoi, E., Bando, M., Sakata-Haga, H., Lee, N.S., Jeong, Y.G., Fukui, Y., 2008. Differential alterations in expressions of ryanodine receptor subtypes in cerebellar cortical neurons of an ataxic mutant, rolling mouse Nagoya. Neuroscience. 152**,** 609-17.

Schmahmann, J.D., Sherman, J.C., 1998. The cerebellar cognitive affective syndrome. Brain. 121 (Pt 4)**,** 561-79.

Schmahmann, J.D., 2004. Disorders of the cerebellum: ataxia, dysmetria of thought, and the cerebellar cognitive affective syndrome. J Neuropsychiatry Clin Neurosci. 16**,** 367-78.

Schmahmann, J.D., Caplan, D., 2006. Cognition, emotion and the cerebellum. Brain. 129**,** 290-2.

Schmued, L.C., Albertson, C., Slikker, W., Jr., 1997. Fluoro-Jade: a novel fluorochrome for the sensitive and reliable histochemical localization of neuronal degeneration. Brain Res. 751**,** 37-46.

Seki, T., Arai, Y., 1993. Highly polysialylated neural cell adhesion molecule (NCAM-H) is expressed by newly generated granule cells in the dentate gyrus of the adult rat. J Neurosci. 13**,** 2351-8.

Seri, B., Garcia-Verdugo, J.M., Collado-Morente, L., McEwen, B.S., Alvarez-Buylla, A., 2004. Cell types, lineage, and architecture of the germinal zone in the adult dentate gyrus. J Comp Neurol. 478**,** 359-78.

Serpedin, N., 2003. Abnormal Reproductive Function in Female Homozygous Leaner Mice. In: Toxicology. Texas A&M University, College Station, pp. 41.

Shors, T.J., Miesegaes, G., Beylin, A., Zhao, M., Rydel, T., Gould, E., 2001. Neurogenesis in the adult is involved in the formation of trace memories. Nature. 410**,** 372-6.

Smith, L.A., Wang, X., Peixoto, A.A., Neumann, E.K., Hall, L.M., Hall, J.C., 1996. A Drosophila calcium channel alpha1 subunit gene maps to a genetic locus associated with behavioral and visual defects. J Neurosci. 16**,** 7868-79.

Snyder, J.S., Hong, N.S., McDonald, R.J., Wojtowicz, J.M., 2005. A role for adult neurogenesis in spatial long-term memory. Neuroscience. 130**,** 843-52.

Sokoloff, L., Reivich, M., Kennedy, C., Des Rosiers, M.H., Patlak, C.S., Pettigrew, K.D., Sakurada, O., Shinohara, M., 1977. The [14C]deoxyglucose method for the measurement of local cerebral glucose utilization: theory, procedure, and normal values in the conscious and anesthetized albino rat. J Neurochem. 28**,** 897-916.

Sokoloff, L., 1981. Relationships among local functional activity, energy metabolism, and blood flow in the central nervous system. Fed Proc. 40**,** 2311-6.

Spranger, M., Spranger, S., Schwab, S., Benninger, C., Dichgans, M., 1999. Familial hemiplegic migraine with cerebellar ataxia and paroxysmal psychosis. Eur Neurol. 41**,** 150-2.

Stadtman, E.R., Levine, R.L., 2000. Protein oxidation. Ann NY Acad Sci. 899**,** 191-208.

Stea, A., Tomlinson, W.J., Soong, T.W., Bourinet, E., Dubel, S.J., Vincent, S.R., Snutch, T.P., 1994. Localization and functional properties of a rat brain alpha 1A calcium

channel reflect similarities to neuronal Q- and P-type channels. Proc Natl Acad Sci USA. 91**,** 10576-80.

Stephens, G.J., Morris, N.P., Fyffe, R.E., Robertson, B., 2001. The Cav2.1/alpha1A (P/Q-type) voltage-dependent calcium channel mediates inhibitory neurotransmission onto mouse cerebellar Purkinje cells. Eur J Neurosci. 13**,** 1902-12.

Strahlendorf, J.C., Hubbard, G.D., 1983. Serotonergic interactions with rat cerebellar Purkinje cells. Brain Res Bull. 11**,** 265-9.

Suh, Y.S., Oda, S., Kang, Y.H., Kim, H., Rhyu, I.J., 2002. Apoptotic cell death of cerebellar granule cells in rolling mouse Nagoya. Neurosci Lett. 325**,** 1-4.

Takahashi, T., Momiyama, A., 1993. Different types of calcium channels mediate central synaptic transmission. Nature. 366**,** 156-8.

Takasaki, Y., Deng, J.S., Tan, E.M., 1981. A nuclear antigen associated with cell proliferation and blast transformation. J Exp Med. 154**,** 1899-909.

Taniwaki, T., Shinoda, H., Kaseda, Y., Kato, M., Goto, I., 1996. Increased preproenkephalin mRNA and preprotachykinin mRNA in the striatum of Rolling mouse Nagoya. Brain Res. 714**,** 231-4.

Teh, B.T., Silburn, P., Lindblad, K., Betz, R., Boyle, R., Schalling, M., Larsson, C., 1995. Familial periodic cerebellar ataxia without myokymia maps to a 19-cM region on 19p13. Am J Hum Genet. 56**,** 1443-9.

Terwindt, G.M., Ophoff, R.A., Haan, J., Frants, R.R., Ferrari, M.D., 1996. Familial hemiplegic migraine: a clinical comparison of families linked and unlinked to chromosome 19. DMG RG. Cephalalgia. 16**,** 153-5.

Thach, W.T., 1968. Discharge of Purkinje and cerebellar nuclear neurons during rapidly alternating arm movements in the monkey. J Neurophysiol. 31**,** 785-97.

Thach, W.T., Goodkin, H.P., Keating, J.G., 1992. The cerebellum and the adaptive coordination of movement. Annu Rev Neurosci. 15**,** 403-42.

Thach, W.T., 2007. On the mechanism of cerebellar contributions to cognition. Cerebellum. 6**,** 163-7.

Thannickal, V.J., Fanburg, B.L., 2000. Reactive oxygen species in cell signaling. Am J Physiol Lung Cell Mol Physiol. 279**,** L1005-28.

Tottene, A., Moretti, A., Pietrobon, D., 1996. Functional diversity of P-type and R-type calcium channels in rat cerebellar neurons. J Neurosci. 16**,** 6353-63.

Tsien, R.W., Lipscombe, D., Madison, D.V., Bley, K.R., Fox, A.P., 1988. Multiple types of neuronal calcium channels and their selective modulation. Trends Neurosci. 11**,** 431-8.

Tsuji, S., Meier, H., 1971. Evidence for allelism of leaner and tottering in the mouse. Genet Res. 17**,** 83-8.

Tsujimoto, T., Jeromin, A., Saitoh, N., Roder, J.C., Takahashi, T., 2002. Neuronal calcium sensor 1 and activity-dependent facilitation of P/Q-type calcium currents at presynaptic nerve terminals. Science. 295**,** 2276-9.

Usowicz, M.M., Sugimori, M., Cherksey, B., Llinas, R., 1992. P-type calcium channels in the somata and dendrites of adult cerebellar Purkinje cells. Neuron. 9**,** 1185-99.

van de Nes, J.A., Nafe, R., Schlote, W., 2008. Non-tau based neuronal degeneration in Alzheimer's disease -- an immunocytochemical and quantitative study in the supragranular layers of the middle temporal neocortex. Brain Res. 1213**,** 152-65.

van Praag, H., Kempermann, G., Gage, F.H., 1999. Running increases cell proliferation and neurogenesis in the adult mouse dentate gyrus. Nat Neurosci. 2**,** 266-70.

Voogd, J., Glickstein, M., 1998. The anatomy of the cerebellum. Trends Neurosci. 21**,** 370-5.

Wakamori, M., Yamazaki, K., Matsunodaira, H., Teramoto, T., Tanaka, I., Niidome, T., Sawada, K., Nishizawa, Y., Sekiguchi, N., Mori, E., Mori, Y., Imoto, K., 1998. Single tottering mutations responsible for the neuropathic phenotype of the P-type calcium channel. J Biol Chem. 273**,** 34857-67.

Westenbroek, R.E., Sakurai, T., Elliott, E.M., Hell, J.W., Starr, T.V., Snutch, T.P., Catterall, W.A., 1995. Immunochemical identification and subcellular distribution of the alpha 1A subunits of brain calcium channels. J Neurosci. 15**,** 6403-18.

Whitty, C.W., 1953. Familial hemiplegic migraine. J Neurol Neurosurg Psychiatry. 16**,** 172-7.

Wills, S., 2006. Neurogenesis in the Dentate Gyrus of Age-matched Calcium Ion Channel Mutant Mice, Leaner and Tottering. Texas A&M University, College Station, pp. 94.

Yamaguchi, T., Kato, M., Fukui, M., Akazawa, K., 1992. Rolling mouse Nagoya as a mutant animal model of basal ganglia dysfunction: determination of absolute rates of local cerebral glucose utilization. Brain Res. 598**,** 38-44.

Zhang, J.F., Randall, A.D., Ellinor, P.T., Horne, W.A., Sather, W.A., Tanabe, T., Schwarz, T.L., Tsien, R.W., 1993. Distinctive pharmacology and kinetics of cloned neuronal Ca2+ channels and their possible counterparts in mammalian CNS neurons. Neuropharmacology. 32**,** 1075-88.

Zhuchenko, O., Bailey, J., Bonnen, P., Ashizawa, T., Stockton, D.W., Amos, C., Dobyns, W.B., Subramony, S.H., Zoghbi, H.Y., Lee, C.C., 1997. Autosomal dominant cerebellar ataxia (SCA6) associated with small polyglutamine expansions in the alpha 1A-voltage-dependent calcium channel. Nat Genet. 15**,** 62-9.

Zwingman, T.A., Neumann, P.E., Noebels, J.L., Herrup, K., 2001. Rocker is a new variant of the voltage-dependent calcium channel gene Cacna1a. J Neurosci. 21**,** 1169-78.

APPENDIX

Volume of the Cerebellum

genotype	Mean	Std. Error	95% Confidence Interval	
			Lower Bound	Upper Bound
Wild type	50.396	2.165	45.499	55.293
tg/tg^{la}	40.711	2.314	35.476	45.946

Volume of the Hippocampus

genotype	Mean	Std. Error	95% Confidence Interval	
			Lower Bound	Upper Bound
Wild type	13.100	.843	11.403	15.290
tg/tg^{la}	13.347	.843	11.157	15.044

Hippocampal Density

Pyramidal Cell Layer of CA1

genotype	Mean	Std. Error	95% Confidence Interval	
			Lower Bound	Upper Bound
Wild type	21.318	.659	19.947	22.698
tg/tg^{la}	22.594	.631	21.281	23.906

Pyramidal Cell Layer of CA3

genotype	Mean	Std. Error	95% Confidence Interval	
			Lower Bound	Upper Bound
Wild type	14.020	.336	13.321	14.720
tg/tg^{la}	12.175	.322	11.506	12.844

Granule Cell Layer of the Dentate Gyrus

genotype	Mean	Std. Error	95% Confidence Interval	
			Lower Bound	Upper Bound
Wild type	46.580	.608	45.315	47.844
tg/tg^{la}	47.896	.582	46.685	49.107

Hilus of the Dentate Gyrus

genotype	Mean	Std. Error	95% Confidence Interval	
			Lower Bound	Upper Bound
Wild type	10.273	.341	9.563	10.982
tg/tg^{la}	8.917	.327	8.237	9.596

Lacunosum Molecular Layer

genotype	Mean	Std. Error	95% Confidence Interval	
			Lower Bound	Upper Bound
Wild type	1.413	.145	1.110	1.715
tg/tg^{la}	1.708	.132	1.432	1.984

Oriens Layer

genotype	Mean	Std. Error	95% Confidence Interval	
			Lower Bound	Upper Bound
Wild type	2.670	.147	2.365	2.976
tg/tg^{la}	2.469	.141	2.167	2.761

Cerebellar Density

Anterior and Posterior Lobes and Layers Combined

genotype	Mean	Std. Error	95% Confidence Interval	
			Lower Bound	Upper Bound
Wild type	28.113	.827	26.444	29.781
tg/tg^{la}	25.815	.806	24.190	27.439

Molecular Layer, Anterior and Posterior Lobes Combined

genotype	Mean	Std. Error	95% Confidence Interval	
			Lower Bound	Upper Bound
Wild type	65.519	3.878	57.516	73.523
tg/tg^{la}	57.538	3.878	49.535	65.542

Granule Cell Layer, Anterior and Posterior Lobes Combined

genotype	Mean	Std. Error	95% Confidence Interval	
			Lower Bound	Upper Bound
Wild type	11.695	1.302	9.070	14.321
tg/tg^{la}	10.713	1.268	8.156	13.270

Purkinje Cell Layer, Anterior and Posterior Lobes Combined

genotype	Mean	Std. Error	95% Confidence Interval	
			Lower Bound	Upper Bound
Wild type	5.830	1.065	3.683	7.978
tg/tg^{la}	4.802	1.065	2.655	6.950

Granule Cell Layer, Anterior vs. Posterior Lobe

Genotype	Lobe	Mean	Std. Error	95% Confidence Interval	
				Lower Bound	Upper Bound
Wild type	anterior	65.519	3.560	58.334	72.705
	posterior	74.889	4.279	66.253	83.525
tg/tg^{la}	anterior	57.538	3.560	50.353	64.724
	posterior	66.318	3.871	58.507	74.129

Lobule 10, Layers Combined

genotype	Mean	Std. Error	95% Confidence Interval	
			Lower Bound	Upper Bound
Wild type	28.075	1.666	24.574	31.576
tg/tg^{la}	26.533	1.666	23.032	30.034

Molecular Layer, Lobule 10

genotype	Mean	Std. Error	95% Confidence Interval	
			Lower Bound	Upper Bound
Wild type	10.750	.970	8.712	12.863
tg/tg^{la}	10.825	.970	8.787	12.788

Purkinje Cell Layer, Lobule 10

genotype	Mean	Std. Error	95% Confidence Interval	
			Lower Bound	Upper Bound
Wild type	3.625	.365	2.858	4.392
tg/tg^{la}	4.200	.365	3.433	4.967

Granule Cell Layer, Lobule 10

genotype	Mean	Std. Error	95% Confidence Interval	
			Lower Bound	Upper Bound
Wild type	69.175	4.421	59.887	78.463
tg/tg^{la}	64.575	4.421	55.287	73.863

Hippocampal Cell Size

Pyramidal Cell Layer of CA3

genotype	Mean	Std. Error	95% Confidence Interval	
			Lower Bound	Upper Bound
Wild type	109.229	.949	107.281	111.148
tg/tg^{la}	109.494	1.007	107.443	111.545

Hilus of the Dentate Gyrus

Genotype	gender	Mean	Std. Error	95% Confidence Interval	
				Lower Bound	Upper Bound
Wild type	female	70.109	.664	68.753	71.465
	male	65.615	.742	64.099	67.131
tg/tg^{la}	female	64.291	.742	62.775	65.807
	male	65.549	.742	64.033	67.065

Fluoro-Jade

genotype	Mean	Std. Error	95% Confidence Interval	
			Lower Bound	Upper Bound
Wild type	1.655	.312	.960	2.350
tg/tg^{la}	.605	.312	-.090	1.300

BrdU

genotype	Mean	Std. Error	95% Confidence Interval	
			Lower Bound	Upper Bound
Wild type	3.462	.776	1.733	5.191
tg/tg^{la}	5.101	.776	3.372	6.830

PCNA

Granular Cell Layer of the Dentate Gyrus

genotype	Mean	Std. Error	95% Confidence Interval	
			Lower Bound	Upper Bound
Wild type	1.682	.360	.934	2.430
tg/tg^{la}	1.708	.344	.992	2.424

Hilus of the Dentate Gyrus

genotype	Mean	Std. Error	95% Confidence Interval	
			Lower Bound	Upper Bound
Wild type	1.795	.294	1.184	2.407
tg/tg^{la}	2.542	.281	1.956	3.127

Subgranular Zone of the Dentate Gyrus

genotype	Mean	Std. Error	95% Confidence Interval	
			Lower Bound	Upper Bound
Wild type	3.750	.461	2.792	4.708
tg/tg^{la}	4.896	.441	3.978	5.813

GFAP/BrdU Double Labeling

genotype	Mean	Std. Error	95% Confidence Interval	
			Lower Bound	Upper Bound
Wild type	20.417	7.392	4.148	36.686
tg/tg^{la}	24.312	6.843	9.250	39.374

NeuN/BrdU Double Labelimg

genotype	Mean	Std. Error	95% Confidence Interval	
			Lower Bound	Upper Bound
Wild type	77.746	4.929	66.762	88.729
tg/tg^{la}	79.817	4.929	68.834	90.801

Basal Intracellular Calcium Ion Homeostasis

Cerebellum

genotype		Mean	Std. Error	95% Confidence Interval	
				Lower Bound	Upper Bound
Wild type	male	1.000	.070	.838	1.162
	female	1.000	.070	.838	1.162
tg/tg^{la}	male	.818	.070	1.196	1.520
	female	1.358	.070	.656	.980

Hippocampus

genotype		Mean	Std. Error	95% Confidence Interval	
				Lower Bound	Upper Bound
Wild type	male	1.000	.076	.824	1.176
	female	1.000	.076	.824	1.176
tg/tg^{la}	male	1.003	.076	.826	1.179
	female	.837	.076	.660	1.013

Mitochondrial Membrane Potential

genotype	Mean	Std. Error	95% Confidence Interval	
			Lower Bound	Upper Bound
Wild type				
hippocampus	1.000	.033	.930	1.070
cerebellum	1.000	.033	.930	1.070
tg/tg^{la}				
hippocampus	1.019	.033	.950	1.089
cerebellum	1.024	.033	.954	1.093

Amount and Rate of ROS Production

Cerebellum

genotype	Mean	Std. Error	df	95% Confidence Interval	
				Lower Bound	Upper Bound
Wild type	1.456	.047	10	1.353	1.560
tg/tg^{la}	.601	.047	10	.497	.705

Cerebellum + 50um TB

genotype	Mean	Std. Error	df	95% Confidence Interval	
				Lower Bound	Upper Bound
Wild type	2.880	.275	6.390	2.217	3.543
tg/tg^{la}	1.140	.181	5.247	.681	1.598

Hippocampus

genotype	Mean	Std. Error	df	95% Confidence Interval	
				Lower Bound	Upper Bound
Wild type	23.000	.000	21243.482	23.000	23.000
tg/tg^{la}	23.000	.000	13796.967	23.000	23.000

Hippocampus + 50uM TB

genotype	Mean	Std. Error	df	95% Confidence Interval	
				Lower Bound	Upper Bound
Wild type	2.696	.384	7.480	1.799	3.592
tg/tg^{la}	1.859	.255	6.223	1.241	2.476

VITA

Emily Mary Murawski received her Bachelor of Science degree in psychology from Texas A&M University in 2007. She entered into the Biomedical Science program with an emphasis in neuroscience research at Texas A&M University College of Veterinary Medicine in August 2007 and received her Master of Science degree in December 2009. Her research interests include neurodegeneration in the hippocampus and cerebellum. She entered the College of Veterinary Medicine at Texas A&M University in August of 2009 in pursuit of a DVM degree. She anticipates practicing with her DVM in a mixed animal clinic.

Ms. Murawski may be reached at 4458 TAMU, Texas A&M University College of Veterinary Medicine, College Station, TX 77843-4458

Her email is Emurawski@cvm.tamu.edu